Random matrices and chaos in nuclear physics: Nuclear reactions

G. E. Mitchell*

North Carolina State University, Raleigh, North Carolina 27695, USA
and Triangle Universities Nuclear Laboratory, Durham, North Carolina 27706, USA

A. Richter†

Institut für Kernphysik, Technische Universität Darmstadt, D-64289 Darmstadt, Germany
and ECT, Villa Tambosi, I-38123 Villazzano (Trento), Italy*

H. A. Weidenmüller‡

Max-Planck-Institut für Kernphysik, D-69029 Heidelberg, Germany

(Published 5 October 2010)

The application of random-matrix theory (RMT) to compound-nucleus (CN) reactions is reviewed. An introduction into the basic concepts of nuclear scattering theory is followed by a survey of phenomenological approaches to CN scattering. The implementation of a random-matrix approach into scattering theory leads to a statistical theory of CN reactions. Since RMT applies generically to chaotic quantum systems, that theory is, at the same time, a generic theory of quantum chaotic scattering. It uses a minimum of input parameters (average S matrix and mean level spacing of the CN). Predictions of the theory are derived with the help of field-theoretical methods adapted from condensed-matter physics and compared with those of phenomenological approaches. Thorough tests of the theory are reviewed, as are applications in nuclear physics, with special attention given to violation of symmetries (isospin and parity) and time-reversal invariance.

DOI: 10.1103/RevModPhys.82.2845 PACS number(s): 24.60.Lz, 24.80.+y, 25.40.Ny

CONTENTS

I. Introduction 2846
II. Basic Facts and Concepts 2847
A. Resonances 2847
1. Dynamic origin of resonances 2848
B. S matrix 2848
III. Statistical Models 2850
A. Bohr assumption and Weisskopf estimate 2850
B. Ericson fluctuations 2851
C. Direct reactions 2853
D. Limitations of the compound-nucleus picture 2854
IV. Random-Matrix Approach to Quantum Chaotic Scattering 2855
A. Resonance reactions 2855
1. Single resonance 2855
2. N resonances 2857
B. Stochastic scattering matrix 2858
C. History 2861
V. Average S Matrix 2863
A. Calculation of $\langle S^{CN}(E)\rangle$ 2863
B. Physical interpretation of $\langle S\rangle$ 2864
C. Satchler's transmission matrix 2865
D. Optical model and strength function. Direct reactions 2866
VI. Results of the Statistical Theory 2867
A. Isolated resonances ($\Gamma \ll d$) 2867
B. Ericson regime ($\Gamma \gg d$) 2868
1. Diagrammatic expansion 2868
2. Replica trick 2869
3. Summary 2870
C. S-matrix correlation function 2870
1. Decay in time of the compound nucleus 2872
D. Distribution of S-matrix elements 2873
1. Fit formulas 2873
2. Many open channels 2874
3. Exact results for low moments 2874
4. Maximum-entropy approach 2874
E. Cross-section fluctuations 2875
F. Poles of the S matrix 2876
G. Correlations of S-matrix elements carrying different quantum numbers 2878
VII. Tests and Applications of the Statistical Theory 2878
A. Isolated and weakly overlapping CN resonances 2878
B. Strongly overlapping CN resonances: Ericson fluctuations 2883
VIII. Violation of Symmetry or Invariance 2886
A. Isospin 2886
1. Ericson regime 2886
2. Fine structure of isobaric analog resonances 2888
B. Parity 2892
C. Time reversal 2894
IX. Summary and Conclusions 2896
Acknowledgments 2897
References 2897

*mitchell@tunl.duke.edu
†richter@ikp.tu-darmstadt.de
‡Hans.Weidenmueller@mpi-hd.mpg.de

I. INTRODUCTION

Random-matrix theory (RMT) as developed in the 1950s by Wigner and Dyson [see Wigner (1955a, 1957), Dyson (1962a, 1962b, 1962c), and the reprint collection of Porter (1965)] plays an important role not only in the analysis of nuclear spectra. Random matrices and chaos play perhaps an even bigger role in the theory of nuclear reactions. The resulting "Statistical Theory of Nuclear Reactions" is the topic of the present review. It completes the review by two of the present authors of random matrices and chaos in nuclear structure (Weidenmüller and Mitchell, 2009).

In proposing RMT, Wigner was probably inspired by Bohr's idea (Bohr, 1936) of the compound nucleus (CN). After the early experimental confirmation of Bohr's idea as implemented in the Hauser-Feshbach formula (Hauser and Feshbach, 1952), the field received a boost in 1960 by Ericson's prediction (Ericson, 1960) of statistical fluctuations in nuclear cross sections. Subsequent intense experimental work on a number of topics in CN reactions (Ericson fluctuations, isobaric analog resonances, isospin mixing in nuclear reactions, and tests of time-reversal symmetry) reached saturation at the end of the 1970s, to be followed later only by studies of parity violation in nuclear reactions. Theoretical work extended the Hauser-Feshbach formula to the case of direct reactions (Kawai *et al.*, 1973). At the same time, theorists set out to connect the statistical models of CN scattering with RMT. That turned out to be a very challenging problem. Motivated by the fundamental interest in CN scattering and by the need in other fields of physics (neutron physics, shielding problems, nuclear astrophysics, etc.) to have a viable theory of CN reactions with predictive power, that work was carried on for a number of years and led to partial insights into the connection between RMT and CN scattering.

Theoretical efforts at constructing a comprehensive theory of CN reactions received a strong stimulus in the beginning of the 1980s by developments in the theory of chaotic motion, i.e., the theory of nonintegrable classical systems and their quantum counterparts. It is not a coincidence that the Bohigas-Giannoni-Schmit conjecture (Bohigas *et al.*, 1984; Heusler *et al.*, 2007), which connects properties of quantum spectra of classically chaotic systems with RMT, and the first papers (Verbaarschot *et al.*, 1984a, 1985; Weidenmüller, 1984), establishing a firm connection between RMT, CN scattering theory, and chaotic quantum scattering, appeared almost simultaneously. Technically, progress became possible by combining scattering theory based on the shell model with novel techniques using a supersymmetric generating functional borrowed from condensed-matter physics (Efetov, 1983). Physically, CN scattering was recognized as a paradigmatic case of chaotic quantum scattering, and the theory of CN scattering was seen to apply to chaotic scattering processes in general. Actually the theory of CN scattering is richer than that for most other cases of chaotic scattering for two reasons. First, there exist conserved quantum numbers (spin and parity). The nuclear cross section is the square of a sum of resonance contributions each carrying these quantum numbers. Chaotic motion only affects resonances carrying the same quantum numbers. Second, the nucleus has internal structure. This leads to a strong increase of the number of open channels with excitation energy. Inelastic processes (where the masses, charges, and/or excitation energies of the reaction products differ from those of target and projectile) add complexity and richness to the theory: Nuclear reactions can be studied versus scattering angle and versus bombarding energy and for different final fragment configurations.

The statistical theory of CN reactions is generic and applies likewise to many other cases of chaotic scattering. That fact is borne out by applications to electron transport through disordered mesoscopic samples (Beenakker, 1997; Alhassid, 2000; Imry, 2002) and to the passage of electromagnetic waves through microwave cavities (Fyodorov *et al.*, 2005). Some of these cases are treated below. However, the theoretical developments reviewed in this paper do not cover all aspects of the theory of chaotic scattering. In systems with few degrees of freedom, semiclassical periodic-orbit theory (Gutzwiller, 1990; Gaspard, 1991; Smilansky, 1991) plays a prominent role. That branch of scattering theory has not been much used in nuclear many-body physics. (It has found applications, for instance, in the scattering of two heavy ions where it applies to relative motion.) This is the reason why it is not dealt with here. The connection between the RMT approach and periodic-orbit theory is discussed, for instance, in Lewenkopf and Weidenmüller (1991).

In view of the very general applicability of the statistical theory to chaotic scattering processes governed by RMT, we aim at a presentation which is accessible to readers not familiar with the topic. We have in mind, for instance, physicists working in other areas of nuclear physics or in chaotic scattering. Therefore, we begin this review in Sec. II with a summary of some basic facts and concepts of nuclear reaction theory. We also present the central ideas and models that were developed with the help of plausible albeit intuitive arguments and that were used to treat CN scattering before the connection to RMT was established. These are the Hauser-Feshbach formula, the Weisskopf estimate for the average total width of CN resonances, Ericson fluctuations, and modifications of the Hauser-Feshbach formula due to direct reactions. In order to avoid repeating our arguments later in slightly different form, we present the arguments in modern terminology.

Current access to the statistical theory of CN reactions is based on RMT and presented in Secs. IV–VI. While the aforementioned models do not all survive close scrutiny, at least their results are vindicated and their ranges of validity are established. Needless to say, additional results are also obtained. Tests of the theory and applications to a number of topics are reviewed in later sections.

The field has not been reviewed comprehensively for many years. A review of RMT in nuclear physics (Brody

et al., 1981) contains sections on the statistical theory of nuclear reactions. Shorter reviews may be found in Mahaux and Weidenmüller (1979), Bohigas and Weidenmüller (1988), Weidenmüller (2002), and Fyodorov and Savin (2010). We refer to part I of this review (Weidenmüller and Mitchell, 2009) with the letter I so that equations, figures, or sections in that paper are referred to, for instance, as Eq. (I.34), as Fig. I.16, or as Sec. I.II.A. As in part I, we have preferred citing a review over giving a large number of references: Readability of the paper was our primary concern.

The paper is organized as follows. In Sec. II we collect some basic facts and formulas of nuclear reaction theory that are needed to make our review self-contained. Our treatment of the subject proper begins with Sec. III. We divide the material into three parts: models that motivate the statistical theory, the development of that theory, and tests and applications of the theory. In Sec. III we introduce the Bohr assumption and the statistical models that were developed in its wake. These date back several decades but motivate the statistical theory and define its scope. Are the Bohr assumption and the statistical models consistent with a random-matrix description of nuclear resonances? Can they be derived from such a description? What is the range of validity of the models? Which are the relevant parameters? These questions are answered in Secs. IV–VI. Section IV defines the theoretical framework of the statistical theory by establishing the connection between the scattering matrix and a statistical description of CN resonances. Properties of the average S matrix are described in Sec. V. Results of the theory are collected and compared with the Bohr assumption and the statistical models in Sec. VI. Recent experimental tests of the theory form the content of Sec. VII. Applications of the theory to violation of symmetry or invariance are reviewed in Sec. VIII. As a consequence of that arrangement, individual topics of CN reaction theory such as Ericson fluctuations are dealt with more than once in several parts of the review.

II. BASIC FACTS AND CONCEPTS

A stable nucleus with mass number A possesses a discrete spectrum of levels that extends from the ground state up to the lowest energy where decay by particle emission is possible (the first "particle threshold"). (Here we disregard the small widths of levels due to beta or gamma decay.) In most cases the first particle threshold corresponds to nucleon emission $[A \rightarrow (A-1)+n]$ and typically has an excitation energy of 6 or 8 MeV in nucleus A. The levels above that threshold have finite widths for particle decay and appear as resonances in the scattering of a nucleon by the nucleus with mass number $(A-1)$. The density $\rho(E)$ of nuclear levels increases roughly exponentially with excitation energy E [more precisely, $\rho(E) \propto \exp\sqrt{aE}$, where a is a mass-dependent constant] and the average spacing $d=\rho^{-1}$ of resonances decreases accordingly. The number of decay channels also grows with E since the density of states available for decay in neighboring nuclei likewise grows nearly exponentially. As a result, the average total decay width Γ of the resonances grows strongly with excitation energy. The Weisskopf estimate given in Eq. (11) below shows that Γ/d is roughly given by the number of decay channels over 2π. Thus, we deal with isolated resonances ($\Gamma \ll d$) at the first particle threshold and with strongly overlapping resonances ($\Gamma \gg d$) several MeV higher. A comprehensive theory of nuclear reactions should cover the entire range from $\Gamma \ll d$ to $\Gamma \gg d$.

A. Resonances

Resonances in the cross section play a central role in the theory. In part I, the empirical evidence was discussed showing that isolated resonances measured near neutron threshold or near the Coulomb barrier for protons display stochastic behavior: Spacings and widths of resonances with identical quantum numbers (spin and parity) are in agreement with predictions of RMT, more precisely, with the predictions of the Gaussian orthogonal ensemble (GOE) of random matrices. That evidence is here taken for granted and not reviewed again. The connection between RMT and chaotic motion was also reviewed in part I. We use the term "chaos" as synonymous with spectral fluctuation properties of the GOE type. The theory of nuclear reactions makes use of the GOE properties of nuclear resonances. It is postulated that the stochastic features found for isolated resonances also prevail at higher bombarding energies where resonances overlap. The stochastic description of resonances then applies for all bombarding energies where resonance scattering is relevant. Actually, statistical concepts are used in one form or another to describe all collision processes between atomic nuclei with center-of-mass energies between 0 and about 100 MeV, except for reactions between pairs of very light nuclei (where the density of resonances is too small for a statistical approach).

A stochastic description of CN resonances is not only physically motivated but a practical necessity. While typical spacings of neighboring levels near the ground state are of the order of 100 keV, the resonances seen in the scattering of slow neutrons have typical spacings of 10 eV (see Fig. I.1). This is a consequence of the nearly exponential growth of the average level density with E mentioned above. Stated differently, there are about 10^5–10^6 levels between the ground state of the CN and the isolated resonances seen in the scattering of a slow neutron. There is no viable theoretical approach that would allow the prediction of spectroscopic properties of such highly excited states. Needless to say, the situation becomes worse as the excitation energy increases further.

Within the framework of a statistical approach, one does not predict positions and widths of individual resonances. Rather, the GOE predicts the distribution of spacings between resonances and the distribution of partial and total widths for decay into the available chan-

nels. By the same token, the statistical theory of nuclear reactions does not aim at predicting the precise form of some reaction cross section versus energy or scattering angle. Rather, it aims at predicting the average values, higher moments, and correlation functions of cross sections obtained by averaging over some energy interval. The energy interval must encompass a large number N of resonances. For isolated resonances, the resulting finite-range-of-data error is expected to be inversely proportional to N. For overlapping resonances, N is replaced by the length of the averaging interval divided by the average width of the resonances. With the exception of the lightest nuclei, such averages are the only theoretical predictions presently available for nuclear reactions in the regime of resonance scattering.

1. Dynamic origin of resonances

It is useful to have an idea how the numerous resonances dominating CN reactions come about dynamically. Subsequent theoretical developments then do not appear as purely formal exercises. We use the nuclear shell model reviewed in Sec. I.IV.A as the fundamental dynamical nuclear model. In the shell model, two mechanisms lead to resonances. The dominant mechanism is that of formation of bound single-particle shell-model configurations with energies above the first particle threshold. These states become particle unstable when the residual two-body interaction is taken into account. We refer to such states as to quasibound states. Mahaux and Weidenmüller (1969) used the term "bound states embedded in the continuum." Details follow in the next paragraph. A second and less important mechanism is due to barrier effects of the shell-model potential. The angular-momentum and Coulomb barriers cause the occurrence of more or less narrow single-particle resonances. These occur typically within the first MeV or so of the continuous spectrum of the single-particle Hamiltonian. There is at most one such narrow single-particle resonance for each angular-momentum value; resonances at higher energies are too wide to matter in our context. It is clear that with only one single-particle resonance for each value of angular momentum we cannot account for the numerous CN resonances with equal spins and average spacings of about 10 eV observed at neutron threshold. Therefore, the quasibound states are the main contributor to the large number of resonances in CN scattering. Single-particle resonances can be incorporated in the description of CN resonances as quasibound states (Mahaux and Weidenmüller, 1969) and are not mentioned explicitly again.

To describe the quasibound states in more detail, we consider nuclei in the middle of the *sd* shell, i.e., nuclei with mass number 28 and with 12 valence nucleons. This same example was extensively discussed in part I. Our considerations apply likewise to other nuclei. The spacings of the energies of the single-particle states $d_{5/2}$, $s_{1/2}$, and $d_{3/2}$ (in spectroscopic notation) in the *sd* shell are of the order of 1 MeV. In ^{17}O, for instance, the spacing between the lowest ($d_{5/2}$) and highest ($d_{3/2}$) single-particle states is 5.08 MeV (Zelevinsky *et al.*, 1996). Thus, the spectrum of the bound *sd*-shell-model configurations of 12 nucleons (which typically comprises 10^3 states for low values of total spin J) extends over several tens of MeV while the first particle threshold in these nuclei has a typical energy of only several MeV. Inclusion of the residual interaction within this set of bound states spreads the spectrum further and produces chaos. But the two-body interaction also connects the resulting bound many-body states with other shell-model states defining the open channels. Such states are obtained, for instance, by lifting one nucleon into the *s*-wave continuum of the shell model and diagonalizing the residual interaction among the remaining 11 nucleons in the *sd* shell. The antisymmetrized product of the ground state or of the nth excited state containing 11 nucleons with the single-particle *s*-wave continuum state would define channels with different threshold energies. The coupling of the diagonalized quasibound 12-nucleon states to the channels causes the states above the first particle threshold to turn into CN resonances. Lifting one or several nucleons out of the *sd* shell into bound states of the *pf* shell increases the number of bound single-particle configurations and, thus, of CN resonances. This shows how the (nearly exponential) increase of the nuclear level density leads to a corresponding increase of the density of CN resonances.

Resonance formation in the continuum shell model remains a topic of current interest [see Okolowicz *et al.* (2003), Michel *et al.* (2004), Volya and Zelevinsky (2006), and references therein].

B. S matrix

We now introduce some elements of nuclear reaction theory. We assume throughout that two-body fragmentation dominates the reaction. (Three-body fragmentation is a rare event in the energy range under consideration.) Mass, charge, and the internal states of both fragments are jointly referred to by greek letters $\alpha, \beta, \ldots$. The energy of relative motion of the fragmentation α at asymptotic distance is denoted by E_α while E denotes the excitation energy of the CN. By energy conservation, E_α is trivially related to E and to the energy E_β of relative motion of any other fragmentation β via the binding energies of the fragments. Channels $a, b, \ldots$ are specified by the fragmentation α, by the angular momentum ℓ of relative motion, by total spin J, and by parity Π. A channel a "opens" when $E_\alpha = 0$; the corresponding value of E is called the threshold energy for fragmentation α. A channel is said to be open (closed) when $E_\alpha > 0$ ($E_\alpha < 0$). We speak of elastic scattering when incident and outgoing fragments are equal ($\alpha = \beta$) because $E_\alpha = E_\beta$. But elastic scattering does not imply $a = b$ (while J is conserved, ℓ is not when the fragments carry spin). We use the term "strictly elastic" for $a = b$. Some of these concepts are shown in Fig. 1.

The central object in the theory of nuclear reactions is the scattering matrix $S(E)$. It is a matrix in the space of

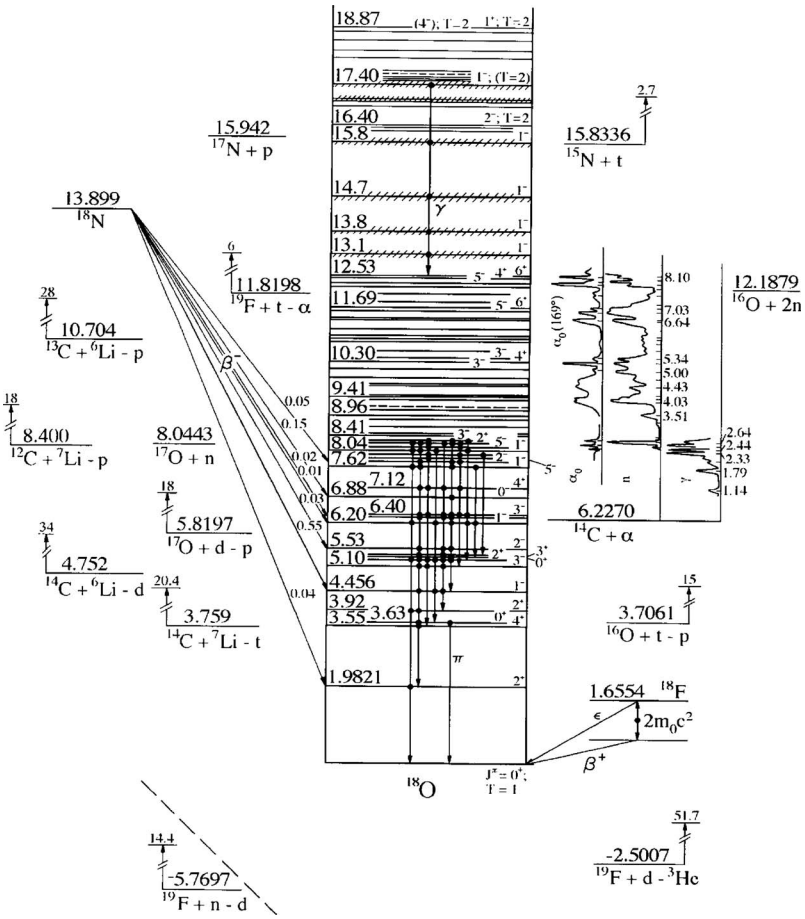

FIG. 1. Level scheme of ^{18}O. The center part shows the low-lying levels, beginning with the ground state. On the left and right, various thresholds are indicated plus the energy dependence of some reaction cross sections. From Tilley *et al.*, 1995.

open channels and carries fixed quantum numbers J, Π, and, if applicable, isospin T. It is defined in terms of the asymptotic behavior of the scattering wave functions $|\Psi_a^+\rangle$. These are solutions of the Schrödinger equation subject to the boundary condition that there is an incoming wave only in channel a. We simplify the notation by considering only channels with neutral fragments. With ℓ_c the angular momentum of relative motion in channel c, r_c the radial coordinate of relative motion, k_c the wave number, m_c the reduced mass, and $h_\ell^\pm$ the spherical Hankel functions, the radial part of $|\Psi_a^+\rangle$ in channel b has the form $\delta_{ab}(m_a/k_a^{1/2})h_{\ell_a}^-(k_a r_a)-(m_b/k_b^{1/2})S_{ba}(E)h_{\ell_b}^+(k_b r_b)$. Thus, the element $S_{ba}(E)$ of S gives the amplitude of the asymptotic flux in channel b for unit incident flux in channel a at energy E. The straightforward generalization to charged fragments is obtained by replacing the spherical Hankel functions by the Coulomb wave functions. The definition of a channel includes the quantum numbers J and Π. In writing $S_{ab}(E)$ we omit J and Π (which must be identical for a and b). In general, channels a and b will belong to different fragmentations α and β, respectively.

The nuclear Hamiltonian is invariant under time reversal. Therefore, the amplitude of the asymptotic flux in channel b for unit incident flux in channel a is equal to the amplitude of the asymptotic flux in channel a for unit incident flux in channel b, and S is symmetric, $S_{ab}(E)=S_{ba}(E)$. The conservation of total flux implies the unitarity relation

$$\sum_c S_{ac}(E)S_{bc}^*(E) = \delta_{ab}. \tag{1}$$

The dimension of S is equal to the number Λ of open channels. With increasing E that number grows nearly exponentially and so does the number of states in the residual nuclei into which the CN may decay. We can work with a matrix S of fixed dimension Λ only for E in an energy window with end points given by two nearest threshold energies. The size of that window decreases nearly exponentially with E. The size constraint is usually neglected in applications of the theory because the flux into channels that have just opened is typically small due to angular-momentum and Coulomb-barrier effects. Moreover, because of the nearly exponential increase of the level density the number $\mathcal{N}$ of resonances within each window changes only algebraically (and not exponentially) with energy E in spite of the exponentially decreasing size of the window. At neutron threshold, where d is of the order of 10 eV and the spacing of thresholds is of the order of several hundreds of keV, we have $\mathcal{N}\approx 10^4$. At 15 MeV above neutron threshold [the Ericson regime (see Sec. III.B)] $\mathcal{N}$ is estimated to be one or two orders of magnitude smaller.

Given S, the differential cross section of any nuclear reaction is obtained as a bilinear form in the elements

$S_{ab}(E)$ of the S matrix and similarly for other observables such as fragment polarization. In addition to the elements of the S matrix, the formulas involve kinematical factors and angular-momentum coupling coefficients (Blatt and Biedenharn, 1952) and are not reproduced here. The statistical theory of nuclear reactions focuses on the calculation of the statistical properties of the S matrix.

For later use we introduce the eigenvalues of the unitary and symmetric matrix S. These have unit magnitude and are written as $\exp[2i\delta_c(E)]$. The real phase shifts $\delta_c(E)$ are called the eigenphase shifts of S. A theorem analogous to the Wigner–von Neumann noncrossing theorem for the eigenvalues of a Hermitian matrix also applies in the present case (Weidenmüller, 1967). Therefore, generically no two eigenphase shifts coincide, and the matrix S can be written as

$$S_{ab}(E) = \sum_c \mathcal{O}_{ac}(E)\exp[2i\delta_c(E)]\mathcal{O}_{bc}(E). \tag{2}$$

Here the real orthogonal matrix $\mathcal{O}(E)$ induces a transformation from the physical channels to the "eigenchannels" of S. The scattering wave functions in the eigenchannel representation are given by $|\Omega_c(E)\rangle = \Sigma_a \mathcal{O}_{ca}|\Psi_a^+(E)\rangle$. The radial part of $|\Omega_c(E)\rangle$ in the physical channel a has the form $\mathcal{O}_{ca}[h_{\ell_a}^-(k_a r_a) - \exp(2i\delta_c)h_{\ell_a}^+(k_a r_a)]$, in keeping with the fact that S is diagonal in the eigenchannel basis. The eigenchannels are unphysical because there is an incident wave in every physical channel. Nevertheless, the eigenchannels are helpful theoretical constructs.

III. STATISTICAL MODELS

A. Bohr assumption and Weisskopf estimate

Statistical concepts have governed the theory of CN scattering from its inception. Bohr (1936) introduced the idea of the CN as an equilibrated system of strongly interacting nucleons. The incident nucleon shares its energy with the nucleons in the target. The system equilibrates and "forgets" its mode of formation. It takes a long time (long in comparison with the time it takes a nucleon with the Fermi velocity to traverse the nucleus) for the CN to accidentally concentrate the available energy back onto a single nucleon which can then be reemitted. Therefore, formation and decay of the CN are independent processes ("Bohr assumption"). The decay of the CN is assumed to be governed by statistical laws (with the proviso that energy, spin, and parity are conserved).

Bohr's intuitive picture found its first quantitative formulation in the "Hauser-Feshbach formula" (Wolfenstein, 1951; Hauser and Feshbach, 1952) for the average differential cross section. The average is taken over an energy interval containing a large number of resonances. We list the assumptions that were used and defer a discussion of their validity to Sec. VI. Because of the presence of resonances (which behave stochastically) the scattering matrix S fluctuates randomly in energy and is accordingly decomposed into an average part and a fluctuating part (Feshbach *et al.*, 1954),

$$S_{ab}(E) = \langle S_{ab}(E)\rangle + S_{ab}^{\mathrm{fl}}(E). \tag{3}$$

The average over energy is indicated by angular brackets. By definition, we have $\langle S_{ab}^{\mathrm{fl}}(E)\rangle = 0$. The standard assumption (Feshbach *et al.*, 1954) on the average part is that it vanishes for $a \neq b$,

$$\langle S_{ab}(E)\rangle = \delta_{ab}\langle S_{aa}(E)\rangle. \tag{4}$$

It is also assumed that in the CN, S-matrix elements pertaining to different conserved quantum numbers are uncorrelated,

$$\langle S_{ab}^{\mathrm{fl}}(E)(S_{cd}^{\mathrm{fl}}(E))^*\rangle = 0 \quad \text{for } J \neq J' \text{ and/or } \Pi \neq \Pi', \tag{5}$$

and that even when the quantum numbers are equal we have

$$\langle S_{ab}^{\mathrm{fl}}(E)(S_{cd}^{\mathrm{fl}}(E))^*\rangle = 0 \quad \text{unless } a = c,\ b = d \text{ or } a = d,\ b = c, \tag{6}$$

where we have used the symmetry of S. Intuitively, assumptions (5) and (6) are related to random phases for the contributing resonances (only absolute squares survive the averaging process). The decomposition (3) of the scattering matrix implies a corresponding decomposition of the average cross section. The average consists of a sum over terms of the form $\langle S_{ab}(E)S_{cd}^*(E)\rangle$. We use Eq. (3) and focus our attention on the part which is bilinear in the elements S^{fl}. It is that part which contributes to the average CN cross section $\langle\sigma^{\mathrm{CN}}\rangle$. With assumption (5), $\langle\sigma^{\mathrm{CN}}\rangle$ contains only terms $\langle S_{ab}^{\mathrm{fl}}(E)(S_{cd}^{\mathrm{fl}}(E))^*\rangle$ where all channel indices refer to the same quantum numbers J and Π. This statement implies that average CN cross sections are symmetric about 90° in the center-of-mass (c.m.) system. The terms $\langle S_{ab}^{\mathrm{fl}}(E)(S_{cd}^{\mathrm{fl}}(E))^*\rangle$ are subject to assumption (6) which reduces the average CN cross section to a sum over averages of squares of S-matrix elements. Each such term $\langle|S_{ab}^{\mathrm{fl}}(E)|^2\rangle$ describes the formation of the CN from channel a and its decay into channel b or vice versa. The Bohr assumption (independence of formation and decay of the CN) is used to write $\langle|S_{ab}^{\mathrm{fl}}(E)|^2\rangle$ in factorized form as

$$\langle S_{ab}^{\mathrm{fl}}(E)(S_{cd}^{\mathrm{fl}}(E))^*\rangle = (\delta_{ac}\delta_{bd} + \delta_{ad}\delta_{bc})T_a f_b. \tag{7}$$

Here T_a denotes the probability of formation of the CN from channel a and is defined by

$$T_a = 1 - |\langle S_{aa}(E)\rangle|^2. \tag{8}$$

The factor f_b gives the relative probability of CN decay into channel b and is normalized, $\Sigma_b f_b = 1$. Using the symmetry and unitarity of S and neglecting a term that is inversely proportional to the number of channels, we obtain from Eqs. (7) and (8) that $f_b = T_b/\Sigma_c T_c$. Thus,

$$\langle S_{ab}^{\mathrm{fl}}(E)(S_{cd}^{\mathrm{fl}}(E))^{*}\rangle = (\delta_{ac}\delta_{bd} + \delta_{ad}\delta_{bc})T_aT_b \Big/ \sum_c T_c, \tag{9}$$

while the average of the CN part of the cross section takes the form (we recall that α,β denote the fragmentation while $a,b,\ldots$ denote the channels)

$$\langle d\sigma_{\alpha\beta}^{\mathrm{CN}}/d\omega\rangle = \sum \text{ coefficients}\left((1+\delta_{ab})T_aT_b \Big/ \sum_c T_c\right) \times P_\ell(\cos\Theta). \tag{10}$$

Here ω is the solid angle, Θ is the scattering angle, and P_ℓ is the Legendre polynomial. The sum extends over all values of J,ℓ,a,b and contains geometric and kinematical coefficients not specified here [see Blatt and Biedenharn (1952)]. Except for the factor $1+\delta_{ab}$, Eq. (10) was originally proposed by Wolfenstein (1951) and by Hauser and Feshbach (1952) and is commonly referred to as the Hauser-Feshbach formula. The factor $1+\delta_{ab}$ was later shown (Vager, 1971) to be a necessary consequence of the symmetry of S and, for obvious reasons, is referred to as the "elastic enhancement factor." Here we apply the expression Hauser-Feshbach formula to both Eqs. (9) and (10).

Because of the unitarity of S, the average S matrix is subunitary. The "transmission coefficients" T_a defined in Eq. (8) measure the unitarity deficit of $\langle S\rangle$ [we recall Eq. (4)]. The T's obey $0\leqslant T_a\leqslant 1$. It is natural to interpret the unitarity deficit as the probability of CN formation (or, by detailed balance, of CN decay) from (into) channel a. We speak of weak (strong) absorption in channel a when T_a is close to zero (to unity). The T's are central elements of the theory. In the early years of CN theory (Blatt and Weisskopf, 1952), the CN was assumed to be a black box, so that $T_a=1$ ($T_a=0$) for all channels with angular momenta $\ell\leqslant\ell_{\max}$ ($\ell>\ell_{\max}$). Here $\ell_{\max}$ is the angular momentum corresponding to a grazing collision between both fragments. According to Eq. (8), the assumption $T_c=1$ implies $\langle S\rangle=0$, and the decomposition (3) was, in fact, only introduced when Feshbach *et al.* (1954) proposed the optical model of elastic scattering. The model was originally formulated for neutrons but soon extended to other projectiles. The model changed the view of CN reactions: The CN was not a black box but was partly transparent. The transmission coefficients T_a in Eq. (8) were not set equal to unity but could be calculated from the optical model which provided the first dynamical input for CN theory (aside from the average level density that is needed to calculate the energy dependence of CN emission products). The optical model for nucleons and the shell model are closely connected concepts: both involve a single-particle central potential (see Sec. V.D).

The average time τ for decay of the CN or, equivalently, the average width $\Gamma=\hbar/\tau$ of the CN resonances can be estimated using an argument due to Weisskopf (Blatt and Weisskopf, 1952). For bound levels with constant spacing d, the time-dependent wave function (a linear superposition of the eigenfunctions) is, aside from an overall phase factor, periodic with period $d/(2\pi\hbar)$. The wave function reappears regularly at time intervals $2\pi\hbar/d$ at the opening of any channel a where it escapes with probability T_a. For the time τ_a for escape into channel a this gives $\tau_a=2\pi\hbar/(dT_a)$, the partial width for decay into channel a is $\Gamma_a=\hbar/\tau_a=(d/2\pi)T_a$, and the total width Γ is

$$\Gamma = \frac{d}{2\pi}\sum_c T_c. \tag{11}$$

Although the derivation of Eq. (11) is based on equally spaced levels, it is also used for CN resonances, with d the average resonance spacing. A precursor to Eq. (11) by Bohr and Wheeler (1939), $\Gamma=\Lambda d/(2\pi)$, was based on the assumption of strong absorption $T_a=1$ in all Λ open channels.

Equation (5) predicts symmetry of the CN cross section about 90° c.m., while the Hauser-Feshbach formula with $T_c=1$ in all channels predicts that the energy distribution of CN decay products is proportional to the density of states in the final nucleus. Early tests of the Bohr assumption were focused on these predictions. Examples are shown in Figs. 2 and 3.

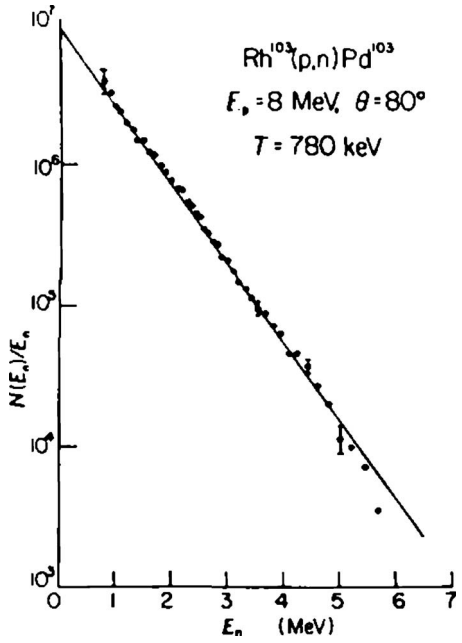

FIG. 2. Spectrum of neutrons ("evaporation spectrum") emitted from the CN ^{104}Pd in the (p,n) reaction on ^{103}Rh at an angle of 80° vs neutron energy E_n (semilogarithmic plot). With all transmission coefficients set equal to unity ("black box" model for the CN), the cross section $\propto\exp(-E_n/T)$ mirrors the level density in the residual nucleus and permits the determination of the nuclear temperature T. From Holbrow and Barschall, 1963.

B. Ericson fluctuations

In the early days of CN theory it was widely held that in the "continuum region" of strongly overlapping reso-

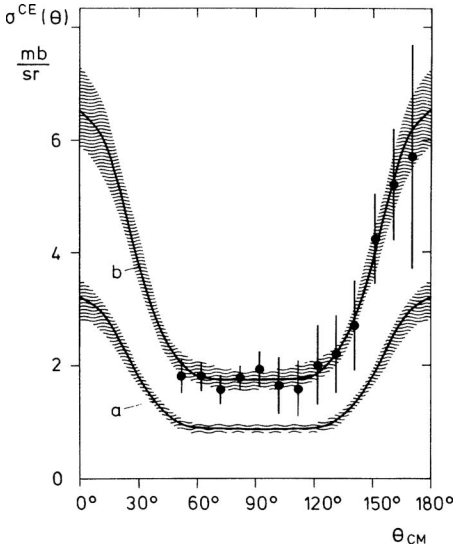

FIG. 3. Angular distribution of the compound-elastic cross section for the ^{30}Si(p,p) reaction at a bombarding energy E_p =9.8 MeV. The data (dots), taken in the regime $\Gamma \gg d$, show the symmetry of the CN cross section about 90° c.m. The solid lines (a) and (b) are predictions of the Hauser-Feshbach formula (9) without and with an elastic enhancement factor 2, respectively. From Kretschmer and Wangler, 1978.

nances, $\Gamma \gg d$, the cross section would be a smooth function of energy (Blatt and Weisskopf, 1952). The numerous overlapping resonances contributing randomly at each energy were thought to yield a scattering amplitude that varies slowly with energy. Ericson (1960) realized that this is not the case. He predicted strong and random fluctuations of CN cross sections that would be correlated over an energy interval of length Γ, the average width of the CN resonances as defined in Eq. (11). Ericson refined his earlier conjecture in a seminal article (Ericson, 1963). Together with theoretical work by Brink and Stephen (1963) and Brink *et al.* (1964), this paper became the basis for a large number of experimental investigations. The almost simultaneous advent of electrostatic tandem van de Graaff accelerators that produced ion beams with sufficiently small energy spread and with the beam energy required to produce compound nuclei in the Ericson regime, led to intense experimental and theoretical activity and confirmed Ericson's conjecture. A recent example is shown in Fig. 14. "Ericson fluctuations," as the phenomenon came to be known, have since been found and investigated in many areas of physics and constitute one of the most characteristic features of chaotic scattering in the regime of strongly overlapping resonances.

To estimate the magnitude of cross-section fluctuations, Ericson argued that for $\Gamma \gg d$ all resonances have approximately the same width Γ. To justify that statement he used the fact that for each resonance the total width can be written as the sum over fluctuating contributions from the open channels (Ericson, 1963). The fluctuations of the sum are, thus, inversely proportional to Λ, the number of open channels. From the Weisskopf estimate (11) we see that $\Gamma \gg d$ is possible only for $\Lambda \gg 1$. Thus, the fluctuations of resonance widths should become negligible for $\Gamma \gg d$ (see, however, Sec. VI.F).

We simplify the presentation by excluding the case of strictly elastic scattering and by assuming that Eq. (4) applies. Taking all resonance widths to be equal to Γ, we write the S matrix in the form

$$S_{ab}(E) = -i\sum_{\mu} \frac{\gamma_{a\mu}\gamma_{\mu b}}{E - E_\mu + (i/2)\Gamma} \quad (a \neq b). \tag{12}$$

The parameters $\gamma_{a\mu}$ are the partial width amplitudes for the decay of resonance μ into channel a. The fluctuations of the resonances are due to the stochastic nature of the resonance parameters E_μ and $\gamma_{a\mu}$. The resonance energies E_μ and the complex partial width amplitudes $\gamma_{\mu a} = \gamma_{a\mu}$ are assumed to be uncorrelated random variables; γ's are complex Gaussian random variables with mean value zero; pairs of γ's carrying different indices are assumed to be uncorrelated; we write $\langle|\gamma_{a\mu}|^2\rangle = 2\pi\nu_a^2$, where the angular brackets now stand for the ensemble average. We refer to Eq. (12) and to these statistical assumptions jointly as to the Ericson model.

According to Eq. (12), $S_{ab}(E)$ is, at fixed energy E and for $\Gamma \gg d$, a sum over many terms, each term containing the product of two Gaussian-distributed random variables and all terms being statistically independent of each other. We use the central limit theorem to conclude (Brink and Stephen, 1963) that $S_{ab}(E)$ is a Gaussian random process (i.e., the generalization of a random variable to a random function of some parameter, here the energy E). A Gaussian distribution is completely defined by its first and second moments. Hence, we need to determine only $\langle S_{ab}(E)\rangle$ and $\langle S_{ab}(E)S_{cd}^*(E+\varepsilon)\rangle$, where ε denotes the difference between the energy arguments of S_{cd}^* and S_{ab}. [We use that quite generally $\langle S_{ab}S_{cd}\rangle = \langle S_{ab}\rangle\langle S_{cd}\rangle$ (see Sec. V).] Then, all higher moments and correlation functions of S are known.

Rather than energy averages we actually calculate the ensemble averages of $\langle S_{ab}(E)\rangle$ and $\langle S_{ab}(E)S_{cd}^*(E+\varepsilon)\rangle$. This is done by averaging over the distributions of $\gamma_{a\mu}$ and E_μ. Energy and ensemble averages give identical results but ensemble averaging seems physically more transparent. It is obvious that $\langle S_{ab}(E)\rangle = 0$ in keeping with Eq. (4). In calculating $\langle S_{ab}(E)S_{cd}^*(E+\varepsilon)\rangle$, we first carry out the ensemble average over γ. In the remaining summation over E_μ we use that for an arbitrary function f we have $\Sigma_\mu f(E_\mu) = \int dE' f(E')\Sigma_\mu \delta(E' - E_\mu)$. We also use the definition $\rho(E) = \langle\Sigma_\mu \delta(E - E_\mu)\rangle$ of the average level density $\rho(E)$ of the resonances, and we assume that $\rho(E)$ is constant over an interval of length Γ. This yields

$$\langle S_{ab}(E)S_{cd}^*(E+\varepsilon)\rangle = (\delta_{ac}\delta_{bd} + \delta_{ad}\delta_{bc}) \times 8\pi^3\nu_a^2\nu_b^2\rho(E)\frac{1}{\Gamma + i\varepsilon}. \tag{13}$$

We compare Eq. (13) for $\varepsilon = 0$ with the Hauser-Feshbach formula (7). Complete agreement is obtained when we use the Weisskopf estimate (11), the identity $d = 1/\rho(E)$,

and write for the transmission coefficients $T_a = 4\pi^2 \nu_a^2 \rho(E)$. [In anticipation we mention that that result agrees with Eqs. (59) and (45) if $T_a \ll 1$ for all channels.] This shows that the Ericson model yields the Bohr assumption. It does so, however, only upon averaging. It is obvious that $|S_{ab}(E)|^2$ as given by Eq. (12) does not factorize as it stands. Calculating the energy average (rather than the ensemble average) with the help of a Lorentzian weight function of width I, we find that the averaging interval I must be large compared to Γ for Eq. (13) to hold. Thus, independence of formation and decay of the CN hold only for cross sections averaged over an interval of length $I \gg \Gamma$. CN cross sections measured with particle beams of sufficient energy resolution are expected to deviate from the Hauser-Feshbach formula. Since Eq. (5) involves an average, we expect the same statement to apply to the symmetry of CN cross sections about 90° c.m. In contrast to the presentation chosen in Sec. III.A, it had not always been clear prior to Ericson's work that the Bohr assumption holds only upon averaging.

The magnitude of cross-section fluctuations is estimated by calculating the normalized autocorrelation function of $|S_{ab}(E)|^2$. We use the Gaussian distribution of the S-matrix elements and Eq. (13) and obtain

$$\frac{\langle |S_{ab}(E)|^2 |S_{ab}(E+\varepsilon)|^2 \rangle - [\langle |S_{ab}(E)|^2 \rangle]^2}{[\langle |S_{ab}(E)|^2 \rangle]^2} = \frac{1}{1 + (\varepsilon/\Gamma)^2}. \tag{14}$$

Equation (14) shows that the fluctuations have the same size as the average cross section and a correlation width given by Γ, the average width of the CN resonances. These results suggest that Γ could be measured directly using Eq. (14). The Lorentzian on the right-hand side of Eq. (14) signals that the CN decays exponentially in time. The lifetime is $\hbar/\Gamma$.

The Ericson model can be extended to include the case of strictly elastic scattering (Brink and Stephen, 1963; Ericson, 1963). Moreover, the arguments can straightforwardly be extended to the fluctuations in both energy and angle of the actual CN cross section as given in Eq. (10) (Ericson, 1963).

In summary, in the regime of strongly overlapping resonances ($\Gamma \gg d$) the Ericson model leads to the following conclusions:

(i) The elements $S_{ab}(E)$ of the scattering matrix are Gaussian random processes.

(ii) The Bohr assumption (i.e., the Hauser-Feshbach formula) and the symmetry of the CN cross section about 90° c.m. hold only for the energy-averaged cross section but not for cross sections measured with high energy resolution. The averaging interval has to be larger than Γ.

(iii) CN cross sections (including the angular distributions) fluctuate. The fluctuations have the same magnitude as the average cross section. The correlation length of the fluctuations is Γ. This fact can be used to measure Γ.

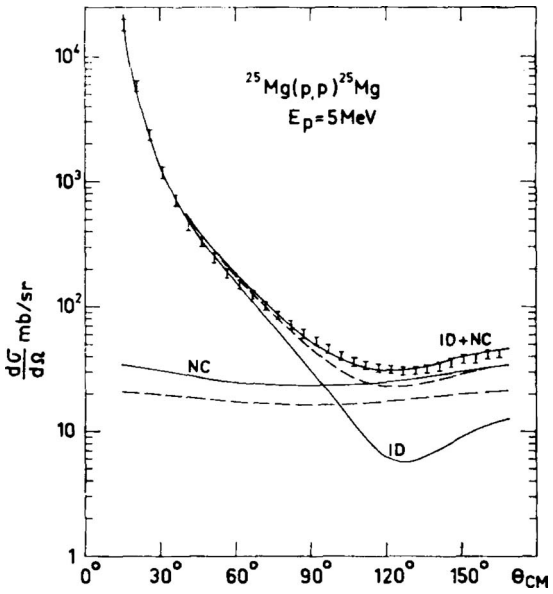

FIG. 4. Elastic cross section for protons at 5 MeV scattered on ^{25}Mg vs scattering angle. The data points with error bars are compared with predictions of the Hauser-Feshbach formula (NC) without (solid line) and with elastic enhancement factor (dashed line) and of the optical model (ID). From Gallmann *et al.*, 1966.

C. Direct reactions

Experiments in the 1950s performed with poor energy resolution showed that CN cross sections are not always symmetric about 90° c.m. These results were confirmed with better resolution. For the case of elastic scattering, an example is shown in Fig. 4. Although the data show the cross section versus laboratory angle, it is clear that the asymmetry also persists in the c.m. system. Similar results were also obtained for inelastic processes. Such deviations were attributed to a failure of Eq. (4), i.e., to inelastic-scattering processes without intermediate formation of the CN. Theoretical efforts to develop a theory of such "direct reactions" dominated nuclear reaction theory for some years and led to explicit expressions for the nondiagonal parts of $\langle S \rangle$. These efforts raised the question how the Hauser-Feshbach formula has to be modified in the presence of direct reactions, i.e., when $\langle S \rangle$ is not diagonal.

After contributions due to Moldauer (1961, 1963, 1964) and Satchler (1963), a definitive answer was proposed by Kawai *et al.* (1973). We describe the approach for $\Gamma \gg d$. The starting point is a decomposition of the scattering matrix of the form

$$S_{ab} = \langle S_{ab} \rangle - i \sum_{\mu} \frac{g_{\mu a} g_{\mu b}}{E - \mathcal{E}_{\mu}}. \tag{15}$$

The first term on the right-hand side is the average S matrix, and the last term (which is identical to S^{fl}) rep-

resents the resonance contributions, with $\mathcal{E}_\mu$ denoting the complex resonance energies. By definition, that term averages to zero. The decomposition (15) implies (Kawai *et al.*, 1973) correlations between $g_{\mu a}$ and $g_{\mu b}$ for $a \neq b$ if $\langle S_{ab} \rangle \neq 0$ for $a \neq b$. In that respect the approach differs fundamentally from the Ericson model. Subsequent developments are similar, however, to those sketched in Sec. III.B. In particular, the total widths of the resonances are effectively assumed to be constant (independent of μ). The average CN cross section is expanded in powers of d/Γ. The term of leading order is

$$\langle |S_{ab}^{\mathrm{fl}}|^2 \rangle = \frac{1}{\mathrm{Tr}\, P} \{ P_{aa} P_{bb} + P_{ab} P_{ab} \}. \tag{16}$$

Here

$$P_{ab} = \delta_{ab} - \sum_c \langle S_{ac} \rangle \langle (S_{bc})^* \rangle \tag{17}$$

is Satchler's transmission matrix (Satchler, 1963). It generalizes the transmission coefficients defined in Eq. (8) to the case where $\langle S \rangle$ is not diagonal. It measures the unitarity deficit of $\langle S \rangle$. According to Kawai *et al.* (1973), Eq. (16) replaces the Hauser-Feshbach formula (9) when direct reactions are present. We observe that if $\langle S \rangle$ is diagonal, Eq. (16) reduces to the Hauser-Feshbach formula, including the elastic enhancement factor.

D. Limitations of the compound-nucleus picture

Nuclear reaction cross sections begin to show deviations from the CN picture some 20 MeV or so above the first particle threshold. This failure of the CN model is attributed to "preequilibrium" or "precompound" processes. The deviations occur because basic assumptions on characteristic time scales of the reaction made in CN theory do not apply any longer. In Eq. (3) such an assumption is implicitly made. The average taken to calculate $\langle S \rangle$ must obviously extend over an energy interval containing many resonances. By the uncertainty relation, a large energy interval relates to a short-time interval for the duration of the reaction (see Sec. VI.C). Thus, $\langle S \rangle$ describes the fast part of the CN reaction. We estimate the minimum duration time of the reaction by the time of passage R/ν_F of a nucleon with Fermi velocity ν_F through a nucleus with radius R. In contrast, the fluctuating part of S with its rapid energy dependence describes the slow part of the CN reaction: decay of the CN with an average lifetime $\hbar/\Gamma$, with Γ given by the Weisskopf estimate (11). For the decomposition (3) to be meaningful, these two time scales must be well separated, $R/\nu_F \ll \hbar/\Gamma$.

An even more stringent constraint on time scales is hidden in the assumption that the CN resonances obey GOE statistics. As shown in part I, the assumption is experimentally validated in the regime of isolated resonances. But does it also hold for higher excitation energies where $\Gamma \gg d$? The assumption implies that the partial width amplitudes of the CN resonances [defined here as the eigenfunctions of the GOE Hamiltonian introduced in Eq. (36) below] have a Gaussian distribution in each channel. In other words, the couplings of all resonances to a given channel are, within statistics, equally strong, and there does not exist a preferred state or configuration, or a group of such states. (The coupling strengths may differ, of course, for different channels.) This is the formal expression of Bohr's assumption that the CN "equilibrates." To display the time scale hidden in that assumption, we consider a nucleon-induced reaction. The nucleon shares its energy with the nucleons in the target in a series of two-body collisions. Configurations of ever greater complexity are created. It takes several or perhaps even many such collisions until the energy of the incident particle is shared among many nucleons and the situation described by assuming GOE statistics for the resonances is attained. The time elapsed between the first collision and the attainment of equilibrium is the "equilibration time" τ_{eq}. The GOE description of CN scattering holds if decay of the CN sets in after the nucleus is equilibrated, i.e., if τ_{eq} is smaller than the average decay time $\hbar/\Gamma$. We have $R/\nu_F < \tau_{\mathrm{eq}}$ and the condition $\tau_{\mathrm{eq}} < \hbar/\Gamma$ for applicability of RMT is usually more stringent than the condition $R/\nu_F \ll \hbar/\Gamma$ deduced from the decomposition (3). We observe that $\hbar/\tau_{\mathrm{eq}}$ can be interpreted as the spreading width of the simple configuration created in the first collision between the incident particle and the target nucleus. The condition $\tau_{\mathrm{eq}} < \hbar/\Gamma$ then requires that spreading width to be large compared to the CN decay width Γ.

Precompound decay sets in when these conditions are violated. Simple estimates show that $\tau_{\mathrm{eq}} \ll \hbar/\Gamma$ for isolated resonances where $\Gamma \ll d$. But the complexity of CN resonances and, therefore, τ_{eq} increases with E. More importantly, Γ increases strongly with excitation energy, and $\hbar/\Gamma$ decreases correspondingly. Thus, while $\tau_{\mathrm{eq}} \ll \hbar/\Gamma$ for isolated resonances, $\hbar/\Gamma$ becomes comparable with and eventually smaller than τ_{eq} as E increases: Particle decay is possible before the equilibrated CN is reached in its full complexity. The associated reaction times cover the entire range from R/ν_F to $\hbar/\Gamma$, and both the GOE description of resonances and the decomposition (3) no longer apply. By the same token, precompound decay does not have the characteristic features of CN reactions: The average energy of the emitted particles is larger than for CN decay; the emitted particles "remember" the incident channel(s) and emission is preferentially in the forward direction. Preequilibrium reactions obviously call for a different approach, although the large number of configurations involved cannot be handled without statistical assumptions. Phenomenological models designed for these reactions (Blann, 1975) were later followed by theories aiming at a quantum-statistical description. The latter were compared and analyzed by Koning and Akkermans (1991). The theory of CN reactions reviewed in this paper is a closed theory based on the concept of quantum chaos as embodied in RMT and on strong empirical evidence reviewed in part I of this review. In its essential aspects CN scattering is universal and occurs likewise in the trans-

mission of waves through disordered media. The theory of precompound reactions is specific to nuclei. It requires additional assumptions that go beyond chaos and RMT that cannot be tested directly. It is not reviewed here.

Precompound processes occur in reactions induced by light particles (mass $A<6$ or 8 or so) impinging on a target of mass $A>20$ or so. A very different situation is that of reactions between "heavy ions," i.e., of two nuclei of mass $A>50$ or 100 each. The energy of relative motion is usually given per nucleon. An energy of 5 MeV per nucleon may then easily amount to a total kinetic energy of several hundreds of MeV. In the case of a grazing collision, the reaction transports energy and angular momentum of relative motion into intrinsic excitations of either fragment. This is accompanied by the transfer of nucleons between both reaction partners. Excitation energies of several tens of MeV are easily reached in either fragment. But the two fragments basically keep their identity; the CN, corresponding to complete fusion of both fragments, is typically not reached in a grazing collision. The theory of such processes uses concepts such as friction and dissipation developed in the theory of nonequilibrium processes and methods of quantum statistical mechanics. Naturally these are inspired by RMT and chaos but have never been strictly derived from such a basis. This is why, in the present review, we will not cover that area of the statistical theory of nuclear reactions either. In central collisions between two heavy ions, fusion is possible even though the density of CN resonances is limited: Quasibound states of the shell model with too large single-particle widths do not qualify as CN resonances (Weidenmüller, 1964). Such fusion processes are mainly investigated via the gamma rays emitted in the decay of the highly excited CN; the resulting data do yield statistically relevant information on excited states of the CN; this information is discussed in part I of this review. The literature on the subject is vast because the available energies have been much increased over the past 20 years and because highly segmented gamma-ray arrays have become available. We confine ourselves to citing two early reviews (Nörenberg and Weidenmüller, 1980; Weidenmüller, 1980).

IV. RANDOM-MATRIX APPROACH TO QUANTUM CHAOTIC SCATTERING

The statistical models reviewed in Sec. II, although inspired by RMT, are not derived from a random-matrix description of CN resonances. The Bohr assumption is intuitively appealing. But it is not clear in which range of Γ/d it applies and with what accuracy. The Ericson model leads to interesting predictions that agree with experiment. However, completing the model formulated in Eq. (12) by an equation for the elastic case, i.e., for S_{aa}, one finds that the resulting S matrix violates unitarity. The same statement applies to the inclusion of direct reactions in the Hauser-Feshbach formula (Kerman and Sevgen, 1976). As for the Weisskopf estimate (11), the physical significance of the parameter Γ is not clear. A width parameter appears in the context of the S-matrix autocorrelation function [see Eq. (14)]. We may also define Γ as twice the mean distance of the poles of S from the real axis. Are the two definitions identical? If not, which of the two (if any) is given by the Weisskopf estimate? What is the accuracy of the estimate? What are the correction terms of next order? A theoretical approach based on a random-matrix description of CN resonances that yields S-matrix distributions and S-matrix correlation functions within controlled approximations is clearly called for. This approach is reviewed in the present and in the following two sections. In this section we formulate the approach and, at the end of the section, give a brief historical survey. The approach uses the average S matrix as input. Properties of phenomenological models for $\langle S\rangle$ are reviewed in Sec. V. Results of the random-matrix approach are given in Sec. VI. The approach reviewed in this and the following sections is not confined to CN reactions but applies, in general, to a random-matrix description of quantum chaotic scattering.

A. Resonance reactions

A statistical theory based on RMT can be formulated only on the basis of a theory of resonance reactions. Only when the S matrix is written explicitly in terms of resonance contributions can we implement the statistical properties of those resonances. We describe an approach that is based on the coupling of N quasibound states to a number of channels and yields the S matrix directly in terms of the Hamiltonian governing those quasibound states. We show why this approach is very well suited for calculating GOE averages.

1. Single resonance

We begin with the simplest case, a single resonance without any background scattering. The S matrix has the Breit-Wigner form

$$S_{ab}(E)=\delta_{ab}-i\frac{\gamma_a\gamma_b}{E-E_0+(i/2)\Gamma}. \tag{18}$$

The partial width amplitudes $\gamma_a,\gamma_b,\ldots$ give the probability amplitudes for the decay of the resonance into channels $a,b,\ldots$. Factorization of the numerator in the last term in Eq. (18) is implied by quantum mechanics if the resonance is caused by a single quasibound state (see below). The matrix $S(E)$ is symmetric. We impose the unitarity condition (1) for all energies E and find that all partial width amplitudes must be real and that

$$\sum_a \gamma_a^2=\Gamma. \tag{19}$$

The sum of the eigenphase shifts $\Sigma_a\delta_a$ of S increases by π as E increases from a value far below to a value far above E_0. To see this, we note that the form (2) for S implies $\det S=\exp(2i\Sigma_a\delta_a)$. To calculate $\det S$ we use Eq.

(18) and find in matrix notation $\det S=\det\{1-i\vec{\gamma}\vec{\gamma}^T/[E-E_0+(i/2)\Gamma]\}$, where T denotes the transpose. The last determinant is easily worked out and yields $[E-E_0-(i/2)\Gamma]/[E-E_0+(i/2)\Gamma]$. This term has magnitude 1; the phase increases by 2π as E passes through the resonance. The resulting increase by π of the sum of the eigenphase shifts of S over the resonance does not imply that one of the eigenphase shifts grows by π while all others remain unchanged. On the contrary, the nonCrossing theorem of the eigenphases (Weidenmüller, 1967) referred to above implies that generically all eigenphases increase as E passes through the resonance, the average increase of every eigenphase being π/Λ, where Λ is the number of open channels.

Equation (18) can be derived by considering a single quasibound state $|\phi\rangle$ with energy ε which interacts with a number Λ of continuum states $|\chi_a(E)\rangle$ (the range of the channel index a is Λ). The continuum wave functions are orthonormal, $\langle\chi_a(E)|\chi_b(E')\rangle=\delta_{ab}\delta(E-E')$, for all a,b and orthogonal to the quasibound state, $\langle\chi_a(E)|\phi\rangle=0$, which in turn is normalized, $\langle\phi|\phi\rangle=1$. In keeping with the absence of any background scattering in Eq. (18) we neglect the dynamical coupling of the continuum states with each other and assume that the states $|\chi_a(E)\rangle$ describe free relative motion so that the scattering phase shift for each $|\chi_a(E)\rangle$ vanishes. We focus our attention on the coupling between the continuum states and the quasibound state mediated by the real matrix elements $W_a(E)$. The coupling causes $|\phi\rangle$ to become a resonance. The Hamiltonian is

$$H=\varepsilon|\phi\rangle\langle\phi|+\sum_a\int dEE|\chi_a(E)\rangle\langle\chi_a(E)| + \sum_a\int dEW_a(E)[|\phi\rangle\langle\chi_a(E)|+|\chi_a(E)\rangle\langle\phi|]. \quad (20)$$

To determine the scattering eigenstates of H we write (Dirac, 1958; Fano, 1961; Mahaux and Weidenmüller, 1969)

$$|\Psi_a^+(E)\rangle=\sum_c\int dE'a_c^{(a)}(E,E')|\chi_c(E')\rangle+b^{(a)}(E)|\phi\rangle. \quad (21)$$

Here $|\Psi\rangle$ has an incoming wave in channel a only. We insert Eq. (21) into the Schrödinger equation $H|\Psi\rangle=E|\Psi\rangle$ and multiply the result from the left with $\langle\phi|$ and $\langle\chi_a(E)|$. This gives a set of coupled linear equations for the coefficients $a(E,E')$ and $b(E)$. These are solved by imposing the boundary condition for $|\Psi_a^+(E)\rangle$. We define

$$F(E)=\sum_c\int dE'\frac{W_c^2(E')}{E^+-E'}=\Delta-\sum_c i\pi W_c^2(E). \quad (22)$$

Here E^+ carries an infinitesimal positive increment which corresponds to the boundary condition on $|\Psi^+\rangle$. The shift function Δ is defined in terms of a principal-value integral. We obtain

$$b^{(a)}(E)=\frac{W_a(E)}{E-\varepsilon-F(E)}, \qquad a_c^{(a)}(E,E')=\delta_{ac}\delta(E-E')+\frac{1}{E^+-E'}\frac{W_a(E)W_c(E')}{(E-\varepsilon-F(E))}. \quad (23)$$

In the second of these equations we have again used the boundary condition: After insertion into Eq. (21) the delta function yields an incoming wave in channel a while the denominator $1/(E^+-E')$ in the last term makes sure that all other contributions to $|\Psi_a^+(E)\rangle$ produce only outgoing waves at infinity. The amplitude of these waves can be easily worked out to be

$$S_{ab}^{\rm res}(E)=\delta_{ab}-2i\pi\frac{W_a(E)W_b(E)}{E-\varepsilon-\Delta+(i/2)\Gamma}. \quad (24)$$

Here $\Gamma=2\pi\Sigma_cW_c^2(E)$. We have used the superscript "res" on S to indicate the origin of Eq. (24) from a dynamical calculation employing a quasibound state. Equation (24) agrees with Eq. (18) if we set $\gamma_a=\sqrt{2\pi}W_a(E)$ and $E_0=\varepsilon+\Delta$. The factorization of the numerator in the second equation of Eqs. (23) causes the factorization of the resonance numerator in Eq. (24) and holds for all resonances caused by a single quasibound state.

To interpret Eqs. (22) and (24), we note that $F(E)$ is the sum of the resolvents for free motion in the channels: The first factor $W_c(E')$ is the amplitude for decay of the quasibound state into channel c at energy E', the denominator $1/(E^+-E')$ is the propagator for channel c, and the second factor $W_c(E')$ is the amplitude for returning to the resonance. We have to sum over all energies E'. The occurrence of $F(E)=\Delta-(i/2)\Gamma$ in the denominator of Eq. (24) signals repeated decay of and return to the quasibound state. With this mechanism the quasibound state turns into a resonance. The real part Δ of $F(E)$ corresponds to off-shell processes and gives the shift of the resonance energy ε. While Im F is due to the open channels only, Δ receives contributions from both open and closed channels.

We turn now to the general case where the background scattering is not negligible and leads to a background scattering matrix $S^{(0)}$. The S matrix for a single resonance takes the form

$$S_{ab}(E)=S_{ab}^{(0)}-i\frac{\tilde{\gamma}_a\tilde{\gamma}_b}{E-E_0+(i/2)\Gamma}. \quad (25)$$

The matrix $S^{(0)}$ is unitary. This follows from the unitarity of S at energies far from the resonance energy E_0. Unitarity of S at all energies E implies that the complex partial width amplitudes obey $\Sigma_c|\tilde{\gamma}_c|^2=\Gamma$. The matrix $S^{(0)}$ is also symmetric. This is implied by time-reversal invariance. Therefore, $S^{(0)}$ possesses an eigenvalue decomposition of the form (2), $S_{ab}^{(0)}=\Sigma_c\mathcal{O}_{ac}^{(0)}\exp(2i\delta_c^{(0)})\mathcal{O}_{bc}^{(0)}$. We use that relation and matrix notation to write Eq. (25) in the form

$$S_{ab}(E) = \{\mathcal{O}^{(0)} \exp(i\delta^{(0)}) S^{\rm res}(E) \exp(i\delta^{(0)}) (\mathcal{O}^{(0)})^T\}_{ab}, \tag{26}$$

where the matrix $S^{\rm res}$ in the eigenchannel representation of S^0 has exactly the form of Eq. (18),

$$S^{\rm res}_{cd}(E) = \delta_{cd} - i\frac{\gamma_c \gamma_d}{E - E_0 + (i/2)\Gamma}. \tag{27}$$

For the unitarity condition (1) to hold for all energies E, the partial width amplitudes $\gamma_c = \exp(-i\delta_c^{(0)}) \Sigma_a \mathcal{O}_{ca} \tilde{\gamma}_a$ must be real and must obey Eq. (19). It is normally assumed that $S^{(0)}$ and $\tilde{\gamma}$'s are independent of energy. This approximation assumes that angular-momentum and Coulomb penetration factors and all relevant matrix elements depend smoothly on energy and are typically justified over the width of a resonance although counterexamples exist (see Sec. VIII.A.2). The assumption does not apply for reactions at threshold energies which are not treated here. Analogous assumptions are also made when we later deal with many resonances; these are not mentioned explicitly again. It is easy to check that the sum of the eigenphases of S increases by π over the width of the resonance.

As in the case of Eq. (18), it is possible to derive Eq. (26) from a dynamical model. The Hamiltonian differs from the one in Eq. (20) in two respects. First, the continuum states $|\chi_a(E)\rangle$ are true scattering states with nonzero phase shifts. Second, the continuum states carrying different channel indices interact with each other. Taking into account these phase shifts and continuum-continuum interactions first and neglecting the quasibound state yield the background matrix $S^{(0)}(E)$. The actual calculation of that matrix involves a coupled-channel problem and may be rather involved. We show in Sec. V how that problem is overcome. In the eigenchannel representation (2) of $S^{(0)}$, the radial part of relative motion of the continuum wave functions $\exp(-i\delta_c^{(0)})\Omega_c(E)\rangle$ is real. [These functions are defined below Eq. (2). For neutral particles the radial part in any channel c is essentially given by a spherical Bessel function $j_{\ell_c}(k_c r_c + \delta_c)$.] Therefore, the matrix elements $W_a(E)$ coupling the quasibound state to the continuum wave functions are also real in the eigenchannel representation. A calculation analogous to the one leading to Eq. (24) then yields Eq. (26) with $\gamma_a = \sqrt{2\pi} W_a(E)$ and the resonance energy E_0 given by $\varepsilon + \Delta$ as before. We do not give that calculation here but refer the interested reader to Mahaux and Weidenmüller (1969). In summary, the S matrix is given by Eq. (26) and $S^{\rm res}(E)$ has the form of Eq. (24) except that the real matrix elements $W_c(E)$ now refer to the eigenchannel representation of $S^{(0)}$. Equation (26) is very convenient as it clearly separates the effects of the continuum-continuum interaction and the effect of resonance scattering.

2. N resonances

Except for the factorization of the numerator in the last term in Eq. (18), it is straightforward to guess the form of the S matrix for a single resonance. In the case of several or many overlapping resonances it is difficult to guess a form for S that fulfills the unitarity condition (1) for all values of the resonance parameters (partial width amplitudes, resonance energies, and total widths). Therefore, it is useful to derive that form from a dynamical model. We describe the model but omit the derivation because it is quite similar to the derivation leading to Eq. (24).

We consider a set of Λ orthonormal continuum states $|\chi_a(E)\rangle$ and a set of N orthonormal quasibound states $|\phi_\mu\rangle$. The continuum states interact with each other. As in Sec. IV.A.1 this interaction gives rise to a smooth unitary and symmetric background scattering matrix $S^{(0)}_{ab}$ for which we can write $S^{(0)}_{ab} = \Sigma_c \mathcal{O}^{(0)}_{ac} \exp(2i\delta_c^{(0)}) \mathcal{O}^{(0)}_{bc}$. The quasibound states span an N-dimensional Hilbert space. The unperturbed energies of and the interactions among the quasibound states are not specified in detail but are represented jointly by the real and symmetric N-dimensional matrix H, the projection of the total Hamiltonian onto the N-dimensional Hilbert space of quasibound states. In this space, we use an arbitrary basis of orthonormal states and write the matrix elements of H as $H_{\mu\nu}$ with $\mu, \nu = 1, \ldots, N$. As before we define the interaction between the quasibound states and the continuum states in the eigenchannel representation of the matrix $S^{(0)}$ with scattering eigenfunctions $\exp(-i\delta_a^{(0)})\Omega_a(E)$. Then the matrix elements $W^{(0)}_{\mu a}(E) = W^{(0)}_{a\mu}(E)$ of that interaction are real. The upper index zero indicates that we use the eigenchannel representation of $S^{(0)}$. The total S matrix again has the form of Eq. (26) but the resonance part now differs and is given by

$$S^{\rm res}_{ab}(E) = \delta_{ab} - 2i\pi \sum_{\mu\nu} W^{(0)}_{a\mu}(E) (D^{-1})_{\mu\nu} W^{(0)}_{\nu b}(E). \tag{28}$$

Here $D(E)$ is a matrix in the space of quasibound states and given by

$$D_{\mu\nu}(E) = E\delta_{\mu\nu} - H_{\mu\nu} - F_{\mu\nu}(E), \tag{29}$$

with

$$F_{\mu\nu}(E) = \sum_c \int dE' \frac{W^{(0)}_{\mu c}(E') W^{(0)}_{c\nu}(E')}{E^+ - E'} = \Delta^{(0)}_{\mu\nu} - i\pi \sum_c W^{(0)}_{\mu c}(E) W^{(0)}_{c\nu}(E). \tag{30}$$

It is easy to check that $S^{\rm res}(E)$ in Eq. (28) is unitary. According to Eq. (26) this statement implies unitarity of the total S matrix. Also $S^{\rm res}$ is obviously symmetric and so is, therefore, $S(E)$. We note that the clear separation of the influence of the continuum-continuum interaction and of the quasibound states given by Eq. (26) is not restricted to the case of a single resonance but holds in general. We also observe that Eqs. (28)–(30) apply for any strength of the coupling between resonances and channels. The equations are not restricted to the regime of weakly overlapping resonances and will serve as a basis for a statistical theory that applies for all values of Γ/d.

As for the case of a single resonance, $F(E)$ given in Eq. (30) describes virtual (real) decay of and return to the quasibound states via all channels by its real (imaginary) parts. This gives rise to the real shift matrix $\Delta^{(0)}$ and the real width matrix with elements $2\pi\Sigma_c W^{(0)}_{\mu c}(E)W^{(0)}_{c\nu}(E)$. Qualitatively speaking, the resonances are isolated (they overlap) if the average resonance spacing is large (small) compared to typical elements of the matrix $F(E)$. This statement is quantified in Secs. V and VI.F below.

To define the analog of the total width for a single resonance, we have to write the matrix $S^{\rm res}$ as a sum over poles in the complex energy plane, which is straightforward only for isolated resonances. The Hermitian matrix H can be diagonalized by an orthogonal transformation O. We denote the eigenvalues of H by E_μ and write for the transformed matrix elements $\tilde{W}^{(0)}_{\mu a}=\Sigma_\nu O_{\mu\nu}W^{(0)}_{\nu a}$. With a corresponding notation for F the transformed matrix D takes the form $(E^+-E_\mu)\delta_{\mu\nu}-\tilde{F}_{\mu\nu}$. The N eigenvalues E_μ are coupled to each other by the nondiagonal elements of $\tilde{F}$. For isolated resonances, that coupling can be neglected, and only the diagonal elements of $\tilde{F}$ are retained. We omit $\Delta^{(0)}$ in Eq. (28), define $\Gamma_\mu=2\pi\Sigma_c(\tilde{W}^{(0)}_{\mu c})^2$, and obtain for isolated resonances the form

$$S^{\rm res}_{ab}(E)=\delta_{ab}-2i\pi \times\sum_\mu \tilde{W}^{(0)}_{a\mu}(E)[E-E_\mu+(i/2)\Gamma_\mu]^{-1}\tilde{W}^{(0)}_{\mu b}. \quad (31)$$

This equation explicitly displays N resonances. For the resonance labeled μ, the partial width amplitude $2\pi\tilde{W}^{(0)}_{\mu b}$ gives the probability amplitude for decay into channel a, and the total width Γ_μ is the sum of the partial widths $\sqrt{2\pi}|\tilde{W}^{(0)}_{\mu b}|^2$. The scattering matrix (31) is unitary if we neglect the overlap of different resonances. The more general equation (28) obviously describes an S matrix with N resonances too, but applies also outside the regime of isolated resonances.

The S matrix in Eq. (28) possesses N poles in the complex energy plane. All poles of $S^{\rm res}$ are located below the real energy axis. To see that we observe that the positions of the poles are given by the eigenvalues of $H_{\mu\nu}+F_{\mu\nu}$. Let z be one such eigenvalue. It obeys

$$\sum_\nu (H_{\mu\nu}+F_{\mu\nu})\Psi_\nu=z\Psi_\mu. \quad (32)$$

We multiply Eq. (32) by the complex conjugate eigenfunction $(\Psi_\mu)^*$, sum over μ, and take the imaginary part of the resulting equation. This yields the Bell-Steinberger relation

$$-\pi\sum_c\left|\sum_\mu W_{c\mu}\Psi_\mu\right|^2=\sum_\mu|\Psi_\mu|^2\,{\rm Im}[z]. \quad (33)$$

This shows that indeed ${\rm Im}[z]<0$ unless $\Sigma_\mu W_{c\mu}\Psi_\mu=\gamma_c=0$ for all c. In the latter case we deal with a bound state embedded in the continuum with vanishing partial width amplitudes γ_c. Then z is real and $S^{\rm res}$ does not have a pole at $E=z$.

The scattering matrix $S^{\rm res}$ in Eq. (28) can be rewritten in terms of the K matrix, a matrix in channel space. The ensuing relations (34) and (35) are quite general and not restricted to isolated resonances. They may be used (Mahaux and Weidenmüller, 1969) to establish the relation between the R-matrix approach (Wigner and Eisenbud, 1947) and the present framework. Using the orthogonal transformation that leads to Eq. (31) we define

$$K_{ab}(E)=\pi\sum_\mu\frac{\tilde{W}^{(0)}_{a\mu}\tilde{W}^{(0)}_{\mu b}}{E-E_\mu} \quad (34)$$

and find after a straightforward calculation

$$S^{\rm res}_{ab}(E)=\left(\frac{1-iK}{1+iK}\right)_{ab}. \quad (35)$$

B. Stochastic scattering matrix

The result of Sec. IV.A.2 puts us into the position to introduce the stochastic description of the resonances in terms of the GOE. In a dynamical treatment of the resonances based on the shell model we express the matrix H in Eq. (29) in terms of the single-particle energies and the matrix elements of the residual interaction. We replace such a dynamical treatment by a stochastic one and consider H as a member of the GOE. In other words, in Eq. (29) we replace the actual Hamiltonian matrix H by the ensemble $H^{\rm GOE}$. This replacement generates an ensemble of scattering matrices S, each member of which is obtained by drawing H from the GOE. For completeness we recall the definition and some properties of the GOE and refer the interested reader to part I for further details. The independent elements $H^{\rm GOE}_{\mu\nu}$ of the real and symmetric N-dimensional matrix $H^{\rm GOE}$ are uncorrelated Gaussian-distributed random variables with zero mean values and a second moment given by

$$\langle H^{\rm GOE}_{\mu\nu}H^{\rm GOE}_{\rho\sigma}\rangle=\frac{\lambda^2}{N}(\delta_{\mu\rho}\delta_{\nu\sigma}+\delta_{\mu\sigma}\delta_{\nu\rho}). \quad (36)$$

Here λ is a parameter. The average spectrum of $H^{\rm GOE}$ has a semicircular shape. The radius of the semicircle is given by 2λ. Near the center of the spectrum the average level spacing d is given by $d=\pi\lambda/N$. The GOE is invariant under orthogonal transformations of the underlying Hilbert space. The energy argument E of S is taken close to (i.e., a finite number of spacings away from) the center. All observables are calculated in the limit $N\to\infty$. As pointed out in Sec. I, we expect the replacement of H by $H^{\rm GOE}$ to be valid at bombarding energies of up to 10 or 20 MeV where the internal equilibration time of the CN is smaller than the decay time $\hbar/\Gamma$.

The statistical approach defined by the replacement $H\to H^{\rm GOE}$ seems to contain a large number of parameters, i.e., the $N\Lambda$ matrix elements $W^{(0)}_{a\mu}$ and the param-

eter λ of the GOE. To appreciate the simplifications due to a statistical treatment, it is instructive to visualize the effort required in case we want to determine these parameters from a dynamical model such as the shell model. Using a shell-model basis of scattering states we first calculate the background matrix $S^{(0)}$. We would then have to calculate the matrix elements $W^{(0)}_{a\mu} = \exp(-i\delta_a)\langle\Omega_a|V|\phi_\mu\rangle$ in the eigenchannel representation of $S^{(0)}$ in terms of the residual interaction V by constructing the quasibound states ϕ_μ. For large N that effort would be huge. We now show that in the statistical approach, all this is much simplified by the invariance properties of the GOE.

The statistical theory uses as input the elements $\langle S_{ab}\rangle$ of the average S matrix $\langle S\rangle$ defined by the decomposition (3). These elements must be given in terms of some dynamical calculation or some suitable model. Options for calculating $\langle S\rangle$ are reviewed in Sec. V. The statistical theory aims at predicting moments and correlation functions (defined as ensemble averages) of $S^{\rm fl}(E)$ in terms of $\langle S\rangle$ in the limit $N\to\infty$. The orthogonal invariance of the GOE implies that all such moments and correlation functions can depend only on orthogonal invariants of the parameters $W^{(0)}_{a\mu}$. The only such invariants are the bilinear forms $\Sigma_\mu W^{(0)}_{a\mu}W^{(0)}_{\mu b}$. But the S matrix is dimensionless and can depend only on dimensionless combinations of the parameters of the statistical approach. These are the real quantities $\Sigma_\mu W^{(0)}_{a\mu}W^{(0)}_{\mu b}/\lambda$. Their number is $\Lambda(\Lambda+1)/2$, equal to the number of elements of $\langle S\rangle$. But the elements of $\langle S\rangle$ are complex and it even seems that the model is overdetermined. We show in Sec. V below that the moments and correlation functions of S actually depend, aside from overall phase factors, only on the magnitudes $|\langle S_{ab}\rangle|$ of the elements of the average scattering matrix. Thus, the statistical theory is well defined. We also show below that $\langle S\rangle$ determines not only the invariants $\Sigma_\mu W^{(0)}_{a\mu}W^{(0)}_{\mu b}/\lambda$ but also the orthogonal matrix $\mathcal{O}^{(0)}$ and the phase shifts $\delta^{(0)}_c$ appearing in Eq. (26). In other words, knowledge of $\langle S\rangle$ suffices for a complete calculation of CN scattering processes.

The quantities $\Sigma_\mu W^{(0)}_{a\mu}W^{(0)}_{\mu b}/\lambda$ are the effective parameters of the statistical theory. We use this fact to further simplify the resonance part of the scattering matrix in Eq. (28). The real and symmetric matrix $\Sigma_\mu W^{(0)}_{a\mu}W^{(0)}_{\mu b}$ can be diagonalized by an orthogonal transformation $\mathcal{O}^{\rm CN}_{ab}$ in channel space. We define the new real matrix elements

$$W_{a\mu} = \sum_b \mathcal{O}^{\rm CN}_{ba} W^{(0)}_{b\mu}, \tag{37}$$

which obey

$$\sum_\mu W_{a\mu}W_{\mu b} = \delta_{ab} N\nu_a^2. \tag{38}$$

To express S_{ab} in terms of the $W_{a\mu}$'s we define the unitary matrix

$$U_{ab} = (\mathcal{O}^{(0)}\exp(i\delta^{(0)})\mathcal{O}^{\rm CN})_{ab} \tag{39}$$

and write

$$S_{ab}(E) = (US^{\rm CN}(E)U^T)_{ab}. \tag{40}$$

Here

$$S^{\rm CN}_{ab}(E) = \delta_{ab} - 2i\pi\sum_{\mu\nu} W_{a\mu}(E)(D^{-1})_{\mu\nu}W_{\nu b}(E) \tag{41}$$

and

$$D_{\mu\nu}(E) = E\delta_{\mu\nu} - H^{\rm eff}_{\mu\nu}, \tag{42}$$

where

$$H^{\rm eff} = H^{\rm GOE}_{\mu\nu} + F_{\mu\nu} \tag{43}$$

is the non-Hermitian "effective Hamiltonian" that describes the dynamics of the resonances. The non-Hermitian part of $H^{\rm eff}$ is due to the imaginary part of the matrix $F_{\mu\nu}(E)$ given by

$$F_{\mu\nu}(E) = \sum_c \int dE' \frac{W_{\mu c}(E')W_{c\nu}(E')}{E^+ - E'}. \tag{44}$$

This matrix describes the effect of the coupling to the channels.

The matrix $S^{\rm CN}(E)$ of Eq. (41) is the S matrix for CN scattering in its purest form: the absence of all continuum-continuum interactions and of all elastic-scattering phase shifts, with real coupling matrix elements $W_{a\mu}$ obeying Eq. (38). Thus, $S^{\rm CN}$ is the central object of study of the statistical theory. The ensemble of matrices $S^{\rm CN}(E)$ constitutes a matrix-valued random process. (For fixed E, every element of $S^{\rm CN}$ is a random variable. Because of the dependence on energy, a generalization of the concept of random variable is called for, and one speaks of a random process.) The moments of $S^{\rm CN}$ depend on the dimensionless parameters

$$x_a = \frac{\pi N\nu_a^2}{\lambda} = \frac{\pi^2\nu_a^2}{d} \tag{45}$$

[see Eq. (38)], where we have taken the average GOE level spacing d at the center of the GOE spectrum. The form of Eq. (45) is reminiscent of Fermi's golden rule. The S-matrix correlation functions depend, in addition, on energy differences given in units of d (see Sec. VI).

The unitary matrix U in Eq. (39) contains all of the nonstatistical effects that connect $S^{\rm CN}$ with the physical channels: The transformation to the eigenchannel representation, the eigenphase shifts of $S^{(0)}$, and the transformation that diagonalizes the bilinear form of the $W^{(0)}$'s [see Eq. (37)]. Statistical assumptions are made only with respect to the matrix $H^{\rm GOE}$ that describes the interaction among quasibound states. We do not impose any statistical requirements on the matrix elements $W_{\mu c}(E)$, on $S^{(0)}$, or on U. This is in keeping with the evidence on chaos in nuclei reviewed in part I. It also corresponds to chaotic features of quantum dots and microwave billiards.

In many cases it is possible to simplify the matrix $F_{\mu\nu}(E)$. As in Eq. (30) we decompose $F_{\mu\nu}(E)$ into its real and imaginary parts. Often the coupling matrix elements $W_{\mu a}(E)$ are smooth functions of E (so that

$d[\partial \ln W_{\mu c}(E)/\partial E] \ll 1$). Then the principal-value integral is small, the real shift matrix can be neglected, and $F_{\mu\nu} \approx -(i/2)\Gamma_{\mu\nu}$ where the width matrix $\Gamma_{\mu\nu}$ is given by

$$\Gamma_{\mu\nu} = 2\pi \sum_c W_{\mu c}(E) W_{c\nu}(E). \tag{46}$$

The assumption $d[\partial \ln W_{\mu c}(E)/\partial E] \ll 1$ is not justified near the threshold of a channel, say a, where the $W_{\mu a}$'s with $\mu = 1, \ldots, N$ depend strongly on energy. A better approximation is obtained when we write the principal-value integral giving the real part of $F_{\mu\nu}$ in the approximate form (Mahaux and Weidenmüller, 1969) $\Sigma_c W_{\mu c} \Delta_c W_{c\nu}$, where the Δ_c's are some channel-dependent constants. Then $F_{\mu\nu} \approx \pi \Sigma_c W_{\mu c}(\Delta_c - i) W_{c\nu}$. This form differs from the first approximation by the replacement of the channel propagator $-i$ by $\Delta_c - i$. Agassi *et al.* (1975) showed that such a replacement only modifies the dependence of the transmission coefficients T_c on the coupling strengths x_c and leaves the theory otherwise unchanged. However, the coefficients T_c serve as phenomenological input parameters and the coupling strengths x_c do not appear explicitly anywhere in the final expressions for the moments or correlation functions of S^{CN}. Therefore, we use in the sequel the simple approximation $F_{\mu\nu} \approx -i\Sigma_c W_{\mu c} W_{c\nu}$. With this approximation, the effective Hamiltonian H^{eff} in Eq. (43) takes the form

$$H^{\mathrm{eff}}_{\mu\nu} = H^{\mathrm{GOE}}_{\mu\nu} - i\pi \sum_c W_{\mu c} W_{c\nu}. \tag{47}$$

Equations (40)–(42) and (47) together with Eq. (38) are the basic equations of the statistical model as used in the present paper. They are used throughout except for Sec. VIII.A.2: Isobaric analog resonances occur for proton energies below or at the Coulomb barrier where the energy dependence of the matrix elements $W_{c\mu}(E)$ cannot be neglected.

In some cases it is useful to write S^{CN} in the diagonal representation of H^{GOE}. We diagonalize every realization of H^{GOE} with an orthogonal matrix O. The eigenvalues E_μ, $\mu = 1, \ldots, N$, follow the Wigner-Dyson distribution (see Sec. I.II.D). For $N \to \infty$ the elements of O are uncorrelated Gaussian-distributed random variables and so are, therefore, the transformed matrix elements $\tilde{W}_{\mu a} = \Sigma_b O_{\mu\nu} W_{\nu a}$. These are not correlated with E_μs, have zero mean values, and have second moments given by

$$\langle \tilde{W}_{\mu a} \tilde{W}_{\nu b} \rangle = \nu_a^2 \delta_{ab} \delta_{\mu\nu} \tag{48}$$

[see Eq. (38)]. It is assumed that the ν_a^2's are independent of energy. In this representation the matrix S^{CN} of Eq. (41) is given by

$$S^{\mathrm{CN}}_{ab}(E) = \delta_{ab} - 2i\pi \sum_{\mu\nu} \tilde{W}_{a\mu}(E)(\tilde{D}^{-1})_{\mu\nu} \tilde{W}_{\nu b}(E), \tag{49}$$

where

$$\tilde{D}_{\mu\nu}(E) = (E - E_\mu)\delta_{\mu\nu} + i\pi \sum_c \tilde{W}_{\mu c} \tilde{W}_{c\nu}. \tag{50}$$

As done for S^{res} in Eq. (35), S^{CN} in Eq. (41) can also be written in terms of the K matrix. This form was, in fact, the starting point of some work on the statistical theory reviewed in Sec. IV.C. The forms (41) and (35), although mathematically equivalent, differ in one essential aspect. The S matrix in Eq. (41) depends explicitly on H^{GOE}. Ensemble averages of moments of S^{CN} as given by Eq. (41) are calculated by integrating over the Gaussian-distributed matrix elements of H^{GOE}. The orthogonal invariance of the GOE makes it possible to perform the calculation analytically for some of these averages (see Sec. VI). In contrast, the K matrix depends on the eigenvalues and eigenvectors of H^{GOE}. Thus, the orthogonal invariance of the GOE is not manifest in the form (35), and ensemble averages require a separate integration over the distribution of eigenvalues and of eigenvectors of the GOE. The calculation turns out to be prohibitively difficult. That is why the K matrix formalism has only been used for numerical simulations.

We have derived Eqs. (40)–(42) and (47) in the framework of the shell-model approach to nuclear reactions (Mahaux and Weidenmüller, 1969). This approach directly yields the dependence of the scattering matrix on the Hamiltonian for the quasibound states. Feshbach's unified theory of nuclear reactions (Feshbach, 1958, 1962, 1964) yields similar but more formal expressions written in terms of the projection operators onto the closed and open channels. To actually implement an RMT approach into these expressions and to work out averages from the resulting formulas, one has to write Feshbach's expressions explicitly in terms of nuclear matrix elements (Lemmer and Shakin, 1964). Such an approach yields (Lewenkopf and Weidenmüller, 1991) formulas quite similar in structure and content to Eqs. (40)–(42) and (47). The removal of direct reaction contributions by the matrix U in Eq. (40) and the reduction of the S matrix to the canonical form in Eq. (41) go back to Engelbrecht and Weidenmüller (1973) and Nishioka and Weidenmüller (1985).

Averages of observables are theoretically worked out as averages over the ensemble of scattering matrices, i.e., over H^{GOE}, and are denoted by the same angular brackets as used to indicate energy averages. The theoretical result $\langle \mathcal{A} \rangle$ for an observable $\mathcal{A}$ is compared with the experimental running average over energy of the same observable measured for a specific nucleus, i.e., for a specific nuclear Hamiltonian. It is stipulated that the nuclear Hamiltonian is a member of the GOE. Ergodicity would then guarantee the equality of both averages (see Sec. I.II.C.3). Ergodicity holds true for $\mathcal{A}$ if the energy-correlation function of $\mathcal{A}$ goes to zero for large values of the argument. In the case of the scattering matrix S^{CN}, this property is analytically fully established for all observables formed from S^{CN} only in the domain of strongly overlapping resonances. There is no reason to doubt, however, that ergodicity also applies in the regime of isolated and weakly overlapping resonances.

As discussed in Sec. I.II.C.2 the local spectral fluctuation measures of the GOE do not depend on the Gauss-

ian distribution assumed for the matrix elements $H_{\mu\nu}^{\mathrm{GOE}}$ in Eq. (36) but apply for a wide class of random-matrix ensembles. This property is referred to as universality. The fluctuation properties of the S matrix are studied over energy intervals that are measured in units of the mean level spacing of the resonances. The relevant observables (S-matrix correlation functions) are, thus, likewise local fluctuation measures. The proof of universality of such measures given by Hackenbroich and Weidenmüller (1995) also applies to these observables.

The theoretical framework of Eqs. (40)–(42) and (47) is quite flexible and allows for extensions of the theory. These may account for violation of isospin symmetry, of parity, or for tests of time-reversal invariance in CN reactions. Such applications of the statistical theory are reviewed in Secs. VIII.A–VIII.C. Violation of isospin symmetry or parity is treated by replacing H^{GOE} in Eq. (47) by a block matrix (Rosenzweig and Porter, 1960) as done in Eq. (I.30) and in Eq. (98) below. Each diagonal block refers to states with the same isospin (or parity) quantum numbers while the off-diagonal blocks contain the matrix elements of the symmetry-breaking interaction (see Sec. I.III.D.1). Time-reversal invariance is broken when H^{GOE} is replaced by $H^{\mathrm{GOE}}+\alpha iA$, where α is a real parameter and A is a real and antisymmetric random matrix [see Eqs. (I.32) and (I.33) and Sec. VIII.C below].

The statistical theory for S formulated so far applies to every set of fixed quantum numbers (total spin and parity) of the CN. In keeping with Eq. (5) we assume that S matrices referring to different quantum numbers are statistically uncorrelated. This assumption is not as innocent as it may look. Indeed, let us imagine that H^{eff} in Eq. (42) is determined not from the GOE but from the shell model. That calculation would yield the matrices $H_{\mu\nu}$ (and, thereby, the S matrices) simultaneously for all conserved quantum numbers. A change of the residual interaction of the shell model would cause all these matrices to change simultaneously. Different realizations of the GOE may be thought of as corresponding to different choices of the residual interaction. Therefore, the matrices H^{GOE} appearing in S matrices carrying different quantum numbers are expected to be correlated (Mulhall *et al.*, 2000). Such correlations among Hamiltonian matrices referring to states with different quantum numbers do indeed exist (Papenbrock and Weidenmüller, 2007) and were discussed in Sec. I.V.B.5. To what extent is the assumption formulated in Eq. (5) invalidated by the existence of such correlations? As remarked in Sec. III.A, Eq. (5) implies that CN cross sections are symmetric about 90° in the c.m. system. The available experimental evidence supports this prediction and we expect, therefore, that deviations from Eq. (5) are not significant. We return to this point in Sec. VI.G.

C. History

The theory developed in Secs. IV.A and IV.B may appear quite natural. However, it took several decades to arrive at that formulation. Since the phenomenological models reviewed in Secs. III.A and III.B led to predictions that were in good agreement with experiment, a deeper understanding of these models was called for from the outset. By way of justification of their work, Hauser and Feshbach (1952), Ericson (1960), and Brink and Stephen (1963), referred to the statistical properties of isolated resonances (which were then supposed and are now known to agree with GOE predictions). But the actual derivation of the Hauser-Feshbach formula and of Ericson fluctuations from a GOE model for CN resonances posed a severe challenge, especially if the aim was a comprehensive statistical theory based on the GOE that would apply for all values of the parameter Γ/d. This resulted in a large number of publications in 1950–1985. Here we can give only an outline of the main developments.

The development of the statistical theory of CN reactions depended on the availability of a suitable theoretical framework to describe resonance reactions. Such a framework is needed to formulate statistical assumptions on the resonance parameters. But to a large extent the availability of such a framework depended on the development of nuclear-structure theory. Early attempts to formulate statistical models mirror the development of the dynamical theory of nuclei.

The R-matrix theory by Wigner and Eisenbud (1947) was formulated at a time when virtually nothing was known about nuclear structure and is, by necessity, a very formal theory: Except for the short range of the nucleon-nucleon interaction, it does not refer to any specific feature of the nuclear Hamiltonian. Resonances are constructed as follows. The nucleus is thought to be enclosed by fictitious boundaries (one for each two-body fragmentation). On these boundaries fictitious boundary conditions are imposed. As a result, the spectrum of the nuclear Hamiltonian in the "internal region" (the domain enclosed by the boundaries) is discrete. The eigenvalues and eigenfunctions depend on numerous parameters (distance of the boundaries from the center of mass and values of the boundary conditions). Green's theorem is used to connect these discrete levels with the channels, and the levels become CN resonances. Even today the resulting form of the scattering matrix is extremely useful for the analysis of experimental data containing several partly overlapping resonances ("multilevel R-matrix fit"). However, few-level approximations to the S matrix are not automatically unitary. Moreover, the form of the S matrix is rather unwieldy and depends explicitly on the parameters just mentioned. For these reasons, the R matrix has never been used as the starting point of a statistical approach.

Lane and Lynn (1957) calculated the average cross section for neutron capture reactions in the regime of isolated resonances. The calculation was possible without referring to a comprehensive theory of resonance reactions. Indeed, in the regime $\Gamma \ll d$ each resonance is independently described by a Breit-Wigner formula as in Eq. (18) or Eq. (25). If one assumes that the distribution of resonance parameters of isolated resonances follows

the GOE, the partial width amplitudes in each channel are Gaussian-distributed random variables. For each resonance the total width Γ_μ is related to the partial widths $\Gamma_{a\mu}$ by the sum rule (19). The resonance energies do not enter the calculation of the energy-averaged cross section. The task consists in calculating the ensemble average of $\Gamma_{a\mu}\Gamma_{b\mu}/\Gamma$, where a and b are two specific channels (here the neutron and the gamma decay channel). This can be done using the GOE and as input values for the averages of the partial widths, the strength functions $\langle\Gamma_{a\mu}\rangle/d$ (see Sec. VI.A). A correction factor deduced from R-matrix theory accounted for the effect of weak resonance overlap. Moldauer (1961) extended the result of Lane and Lynn perturbatively to weakly overlapping resonances.

The first attempt to construct a comprehensive statistical theory is due to Moldauer (1961, 1963, 1964, 1969, 1975b, 1976, 1980), and references therein. In order to go beyond the regime of isolated resonances, Moldauer used an expansion of the scattering matrix in terms of its poles in the complex energy plane. This form of the S matrix had been proposed by Humblet and Rosenfeld (1961). In contrast to the R-matrix theory, the Humblet-Rosenfeld theory is a dynamical theory: The parameters of the pole expansion are, in principle, completely determined by the Hamiltonian, and there are no arbitrary parameters. Unfortunately, an explicit analytical connection between the Hamiltonian, the positions of the poles, and the values of the residues is not known. Thus, the Humblet-Rosenfeld theory is effectively a formal theory like the R-matrix theory. Moreover, the following difficulty arises. For isolated resonances there is a one-to-one correspondence between a resonance and a pole of the scattering matrix [see Eq. (18)]. The parameters of the pole possess a direct physical interpretation as partial width amplitudes and as energy and total width of the resonance. In the general case of many overlapping resonances the Humblet-Rosenfeld expansion uses the same parameters (residues and locations of the poles of the S matrix plus a smooth background matrix). But the simple interpretation valid for isolated resonances does not apply. Moreover, the theory is not manifestly unitary. For isolated resonances the unitarity constraint leads to the simple sum rule (19), while it imposes complicated relations between the pole parameters for overlapping resonances. These have never been untangled. Therefore, the choice of statistical assumptions for the pole parameters was far from obvious. At some point, Moldauer used the K-matrix formulation (35) of the S matrix, assumed that the energies E_μ and matrix elements $W_{a\mu}$ in Eq. (34) obeyed GOE statistics, and determined the distribution of pole parameters via a numerical simulation. His relentless efforts met with limited success but kept interest in the problem. Some of his results are reviewed in Sec. VI.F.

Feshbach's unified theory of nuclear reactions (Feshbach, 1958, 1962, 1964) was the first theory of CN reactions which expressed the scattering matrix in terms of the Hamiltonian of the system without the help of arbitrary parameters. It uses projection operators onto the spaces of open and closed channels. The projection of the nuclear Hamiltonian onto the space of closed channels defines a self-adjoint operator with a discrete spectrum. The bound states of the self-adjoint operator generate the resonances in the full problem. The theory was used by Lemmer and Shakin (1964) for a first calculation of the elastic neutron scattering on ^{15}N using the nuclear shell model. Quasibound shell-model states appeared as neutron resonances. Although not related to the statistical theory, this work demonstrated the possibility to account for CN resonances in terms of a dynamical approach using the nuclear shell model. Later work by the MIT group (Kawai *et al.*, 1973) used Feshbach's theory to formulate an extension of the Hauser-Feshbach formula that accounts for the presence of direct reactions (see Sec. III.C). The approach used plausible assumptions but is not based on a random-matrix approach.

The general theory of nuclear resonance reactions developed in the 1960s by Mahaux and Weidenmüller (1969) was based on the nuclear shell model and work by Dirac (1958) and Fano (1961). It was more explicit than Feshbach's theory of nuclear reactions. This was a natural consequence of the fact that nuclear-structure theory had made significant progress since the early 1950s. Resonances were shown to be mainly due to quasibound states of the shell model. The approach expresses the scattering matrix in terms of the Hamiltonian governing the dynamics of the quasibound states as in Eq. (28). This was the starting point of later developments. The theory is connected with the R-matrix theory of Wigner and Eisenbud (1947) through relations of the form of Eq. (35).

Independently of that development, Engelbrecht and Weidenmüller (1973) showed that there exists a unitary transformation which diagonalizes $\langle S\rangle$. The transformation acts on channel space and, therefore, leaves the statistical properties of the resonances unchanged (Hofmann, Richert, Tepel, and Weidenmüller, 1975). As a consequence, the transformation reduces the problem of calculating CN cross sections in the presence of direct reactions to the problem without direct reactions (i.e., for a diagonal $\langle S\rangle$). This was an important simplification [see Eq. (40)].

The conspicuous lack of a comprehensive theory of CN reactions with predictive power motivated Tepel *et al.* (1974), Hofmann, Richert, and Tepel (1975), and Hofmann, Richert, Tepel, and Weidenmüller (1975) to perform numerical simulations with the aim of establishing fit formulas for average CN cross sections valid for all values of Γ/d. The authors used the transformation mentioned in the previous paragraph and focused their attention on S^{CN}. They proved that aside from overall phase factors, the distribution of S-matrix elements depends only on the transmission coefficients. This fact simplified the construction of the fit formulas. For the numerical simulations, they used the K-matrix form (35) of the stochastic scattering matrix (41). The K-matrix parameters were determined by the eigenvalues and

eigenfunctions of GOE matrices. Repeated random drawings from a Gaussian distribution of the elements of GOE matrices led to statistically meaningful averages and determined the parameters in the fit formulas (see Sec. VI.D.1). Similar formulas were subsequently also developed by Moldauer (1975b).

The first use of the explicit dependence of Eq. (29) on the Hamiltonian H in the calculation of CN processes was made by Agassi *et al.* (1975). CN scattering theory was extended so as to include precompound reactions. They used a stochastic model for the matrix H in Eq. (29) which allowed for the existence of classes of shell-model states of increasing complexity. Averages of cross sections were calculated in terms of an asymptotic expansion valid for $\Gamma \gg d$. The Ericson regime was obtained as a special case of strong coupling between classes so that the internal equilibration time of the CN becomes small compared to the decay time $\hbar/\Gamma$. As a result, the Hauser-Feshbach formula and predictions of the Ericson model were first derived from a microscopic statistical theory. This was possible because resonance spacings were assumed to be constant (i.e., not to follow GOE predictions). Later work showed that for $\Gamma \gg d$ that simplification led to correct results.

In 1984, a connection was established (Verbaarschot *et al.*, 1984a) between statistical nuclear theory and quantum field theory. More precisely, field-theoretical concepts used in condensed-matter theory and in statistical mechanics were applied to the RMT description of both nuclear spectra and nuclear reactions. In a very concrete sense, RMT as applied to nuclei became part of the statistical mechanics of many-body systems. Specifically, generating functionals familiar from condensed-matter theory were used to describe fluctuations both of nuclear spectra and of S-matrix elements in a common framework. In the limit $N \gg 1$, the evaluation of the generating functionals permitted a clear separation of average properties of observables and of their fluctuations. The stochastic scattering matrix was defined in the form given by Eq. (41) and was written as a suitable derivative of a generating functional Z. As a first application, the S-matrix correlation function was calculated with the help of the replica trick (Weidenmüller, 1984). This yields an asymptotic expansion in powers of d/Γ (see Sec. VI.B). Later, Z was expressed in terms of Efetov's supersymmetry approach (Efetov, 1983). This led (Verbaarschot *et al.*, 1984b, 1985) to the exact expression for the S-matrix correlation function given in Sec. VI.C. Equations (40)–(42) and (47) and the supersymmetry approach have since been established as the main tools to study chaotic scattering based on RMT.

V. AVERAGE S MATRIX

The average S matrix serves as input for the statistical theory of nuclear reactions. In the present section we display central properties of $\langle S \rangle$ and review ways to determine $\langle S \rangle$ phenomenologically.

A. Calculation of $\langle S^{\mathrm{CN}}(E) \rangle$

We focus our attention on the only stochastic element in the scattering matrix, i.e., on the CN part $\langle S^{\mathrm{CN}} \rangle$ [see Eq. (41)]. The calculation of averages of S^{CN} (and of powers of S^{CN}) is simpler than of terms involving both S^{CN} and $(S^{\mathrm{CN}})^*$ because as shown in Eq. (33) all poles of $S^{\mathrm{CN}}(E)$ lie below the real E axis.

We calculate $\langle S^{\mathrm{CN}}(E) \rangle$ by replacing the ensemble average by a running average over energy with a Lorentzian weight function of width I centered at energy E_0 (Brown, 1959). We choose the center of the GOE spectrum $E_0 = 0$ as the center of the weight function and have

$$\langle S^{\mathrm{CN}}(E) \rangle = \frac{1}{\pi} \int_{-\infty}^{+\infty} dE S^{\mathrm{CN}}(E) \frac{I}{E^2 + I^2}. \tag{51}$$

The average in Eq. (51) extends over very many resonances so that $I \gg d$ with d the average level spacing in the center of the GOE spectrum. The integration contour can be closed in the upper half of the energy plane. We obtain

$$\langle S^{\mathrm{CN}}(E) \rangle = S^{\mathrm{CN}}(iI). \tag{52}$$

We use Eqs. (49) and (50) and expand $S^{\mathrm{CN}}(iI)$ in a Born series with respect to the imaginary part of H^{eff},

$$\langle S^{\mathrm{CN}}(E) \rangle_{ab} = \delta_{ab} + 2 \sum_{n=1}^{\infty} [(-i\pi \mathcal{W})^n]_{ab}. \tag{53}$$

Here $\mathcal{W}$ is a matrix in channel space given by

$$\mathcal{W}_{ab} = \sum_{\mu} \tilde{W}_{a\mu} [iI - E_\mu]^{-1} \tilde{W}_{\mu b}. \tag{54}$$

Since $I \gg d$, it is legitimate to neglect the fluctuations of the E_μ in the denominator in Eq. (54), i.e., to assume for the E_μ a picket-fence model with fixed nearest-neighbor spacing d. The sum over μ amounts to averaging the product $\tilde{W}_{a\mu} \tilde{W}_{\mu b}$. We have $(1/N) \Sigma_\mu \tilde{W}_{a\mu} \tilde{W}_{\mu b} = (1/N) \Sigma W_{a\mu} W_{\mu b}$. We use Eq. (38), change the summation into an energy integration, and find

$$\mathcal{W}_{ab} = (-i\pi \nu_a^2/d) \delta_{ab}. \tag{55}$$

Inserting the result into Eq. (53) and using the definition (45), we find

$$\langle S_{ab}^{\mathrm{CN}} \rangle = \frac{1 - x_a}{1 + x_a} \delta_{ab}. \tag{56}$$

Equation (56) relates the average scattering matrix to the parameters x_a of the statistical theory. The result (56) is also obtained in the limit $N \to \infty$ via the replica trick (see Sec. VI.B.2) and the supersymmetry approach (see Sec. VI.C). The average S matrix given by Eq. (56) is real because we have chosen E in the center of the GOE spectrum, $E = 0$. For a different choice of E, $\langle S_{aa}^{\mathrm{CN}} \rangle$ would not be real. The additional phase caused by such a choice is not part of the matrix U constructed in Sec. IV.B.

Equation (56) shows that $\langle S^{\rm CN}\rangle$ is always diagonal. However, this does not imply that $\langle S\rangle$ is diagonal too. In fact, Eq. (40) demonstrates that $\langle S\rangle$ is diagonal only if the matrix U is diagonal. That matrix embodies the effect of couplings between channels. That is why a nondiagonal form of $\langle S\rangle$ is taken to be synonymous with the presence of "direct reactions" (i.e., reactions that proceed without intermediate CN formation).

The average of a product of S-matrix elements can be worked out in the same way. Let $\{a_i,b_i\}$ with $i=1,\ldots,k$ denote k arbitrary pairs of channels and consider the average of the product of the matrix elements $S^{\rm CN}_{a_ib_i}(E_i)$ taken at energies $E_1,E_2,\ldots,E_k$. Again using a Lorentzian averaging function, closing the contour in the upper half of the complex energy plane, and using Eq. (52) we find

$$\left\langle \prod_i S^{\rm CN}_{a_ib_i}(E_i)\right\rangle = \prod_i \langle S^{\rm CN}_{a_ib_i}(E_i)\rangle. \tag{57}$$

More generally, we have for any function $f(S^{\rm CN})$ that is analytic in the upper half of the complex energy plane the relation

$$\langle f(S^{\rm CN})\rangle = f(\langle S^{\rm CN}\rangle). \tag{58}$$

This is an important result. It shows that S-matrix elements taken at the same or at different energies are uncorrelated. The result (57) does not hold for products involving both $S^{\rm CN}$ and $(S^{\rm CN})^*$ since these have poles on both sides of the real energy axis, and closing the integration contour does not yield a simple expression. The calculation of such terms poses the main technical difficulty in the statistical theory.

B. Physical interpretation of $\langle S\rangle$

The decomposition (3) of the scattering matrix into an average part and a fluctuating part applies likewise to the CN part $S^{\rm CN}$ of S. The discussion in Sec. III.D of the physical significance of that decomposition in terms of time scales for the CN reactions then applies to $S^{\rm CN}$ too, as do the limitations of the statistical theory established there.

Equation (56) shows that the average CN S matrix is subunitary, $|\langle S^{\rm CN}_{aa}\rangle|\leqslant 1$. The equality sign holds only when x_a vanishes, i.e., when there is no coupling between channel a and the N resonances. We emphasize that the lack of unitarity of $\langle S^{\rm CN}\rangle$ is due to taking the average over N resonances (and, since $\langle S^{\rm CN}\rangle$ is diagonal, not to inelastic scattering processes that would deplete the elastic channel). To see how averaging reduces the magnitude of $S^{\rm CN}$, we consider the simplest case of a single channel coupled to N resonances. There are no inelastic processes by definition. The scattering amplitude has the form $S^{\rm CN}(E)=\exp[2i\delta(E)]$ and can be viewed as a point on the unit circle of the complex plane. As E increases, $\delta(E)$ increases by π over the width of every resonance, and $S^{\rm CN}(E)$ moves counterclockwise on the unit circle once around the origin. The average of $S^{\rm CN}(E)$ over N resonances must then lie in the interior of the unit circle, i.e., be subunitary. These points have been illuminated in Friedman and Weisskopf (1955).

It is remarkable that $\langle S^{\rm CN}_{aa}\rangle$ as given in Eq. (56) depends only on the coupling coefficient x_a and not on the other coupling coefficients x_b with $b\neq a$. This shows that $\langle S^{\rm CN}_{aa}\rangle$ taken all by itself describes the loss of probability amplitude in channel a due to CN formation. Information on the manner in which the CN eventually decays back into the various channels is not contained in $\langle S^{\rm CN}_{aa}\rangle$. The information as to where the lost probability eventually reappears (in quantum mechanics, probability is conserved) is supplied by the fluctuating part of $S^{\rm CN}$. Thus, CN scattering theory can be viewed as a special case of quantum transport theory (Agassi *et al.*, 1975).

In Eq. (8), the transmission coefficients were defined under the assumption that $\langle S\rangle$ is diagonal. This assumption is met by $\langle S^{\rm CN}\rangle$. We calculate T_a from Eq. (8) using Eq. (56) for $\langle S^{\rm CN}\rangle$ and find

$$T_a = 4x_a/(1+x_a)^2. \tag{59}$$

(For a nondiagonal $\langle S\rangle$ the connection with the transmission coefficients is given in Sec. V.C.) The form (59) for the transmission coefficients applies when we choose the energy E in the center of the GOE spectrum, $E=0$. For a different choice of E, the form of T_a differs. This difference is irrelevant in practice because the transmission coefficients serve as phenomenological input parameters of the theory anyway.

In the theory of resonance reactions formulated in Secs. IV.A.2 and IV.B the coupling between levels and channels seems to increase monotonically with increasing strength of the coupling matrix elements $W_{a\mu}$ or, equivalently, the parameters x_a defined in Eq. (45). However, Eq. (59) shows that this is not the case. With increasing x_a, the transmission coefficient T_a increases monotonically until it reaches its maximum value $T_a=1$ at $x_a=1$. Thereafter, T_a decreases monotonically with increasing x_a and tends toward zero as $x_a\to\infty$. Similarly, Eq. (56) shows that $\langle S^{\rm CN}_{aa}\rangle$ decreases from unity to zero as x_a approaches unity from zero. As x_a increases further, $\langle S^{\rm CN}_{aa}\rangle$ approaches -1. We also note that under the substitution $x_a\to 1/x_a$, T_a is invariant while $\langle S^{\rm CN}_{aa}\rangle$ changes sign, $\langle S^{\rm CN}_{aa}\rangle(1/x_a)=-\langle S^{\rm CN}_{aa}\rangle(x_a)$. All this shows that there is a maximum value of the coupling strength, $x_a=1$, beyond which a further increase of x_a effectively reduces the coupling between channel a and the resonances.

To make that fact physically plausible we consider the matrix D in Eq. (42). We follow the work of Sokolov and Zelevinsky (1988, 1989, 1992, 1997). For large values of the x_a (all a), the width matrix $\Gamma_{\mu\nu}$ [Eq. (46)] dominates $H^{\rm GOE}$ in $H^{\rm eff}$ [see Eq. (47)]. Therefore, one chooses a basis in which $\Gamma_{\mu\nu}$ is diagonal. Equation. (38) shows that $\Gamma_{\mu\nu}$ possesses Λ nonzero eigenvalues $2\pi N\nu_a^2$ with $a=1,\ldots,\Lambda$. The associated orthonormal eigenvectors are given by $(1/\sqrt{N\nu_a^2})W_{a\mu}$. Completing in some arbitrary fashion these Λ eigenvectors to a set of N orthonormal

vectors, denoting the resulting orthogonal matrix by G and transforming the matrix $D \to \tilde{D} = GDG^T$, we obtain

$$\tilde{D}_{\mu\nu} = (E + i\pi N\nu_\mu^2)\delta_{\mu\nu} - \tilde{H}_{\mu\nu}, \tag{60}$$

where $\tilde{H} = GH^{\mathrm{GOE}}G^T$ and where the first Λ diagonal entries $\pi N\nu_\mu^2$ are given in terms of the Λ nonvanishing eigenvalues $2\pi N\nu_a^2$ with $a = 1, \ldots, \Lambda$ of the width matrix $\Gamma_{\mu\nu}$ while $\nu_\mu^2 = 0$ for $\mu > \Lambda$. Concerning these first Λ resonances, we consider $\tilde{H}$ as a small perturbation. This is justified as long as the decay widths $2\pi N\nu_\mu^2$ of the resonant states $\mu = 1, \ldots, \Lambda$ are large compared with their spreading widths $2\pi\langle[\tilde{H}_{\mu\nu}]^2\rangle/d$ due to mixing with the other resonances. (We recall that the concept of the spreading width was introduced in the context of doorway states in Sec. I.II.G. The entire discussion there applies likewise to the present case.) With $d = \pi\lambda/N$ and with the help of Eq. (36) that implies $\nu_a^2 \gg d$ or $x_a \gg 1$ for all a. In zeroth order in $\tilde{H}$ we then deal with Λ poles located at $-i\pi N\nu_\mu^2$, $\mu = 1, \ldots, \Lambda$ and with $N - \Lambda$ poles located on the real axis. Taking into account $\tilde{H}$ we obtain a "cloud" of $N - \Lambda$ poles located below but close to the real axis and Λ poles very far from that axis. Each of the latter contributes only a smooth phase to the S matrix (smooth over a typical distance d). The additional phase causes the minus sign in the relation $\langle S_{aa}^{\mathrm{CN}}\rangle(1/x_a) = -\langle S_{aa}^{\mathrm{CN}}\rangle(x_a)$. Aside from the additional phase, the Λ far-away poles do not affect the CN scattering process. On the other hand, CN scattering due to the cloud of $N - \Lambda$ narrow resonances is, for Λ fixed and $N \to \infty$, indistinguishable from the cloud of N narrow CN resonances. That is why, aside from overall phase factors, all moments and correlation functions of S^{CN} do not depend on the phase shifts due to the Λ far-away poles and can be expressed in terms of the transmission coefficients T_a. The picture of the distribution of poles that emerges from this qualitative discussion is quantitatively confirmed in Sec. VI.F: As all the coefficients x_a increase monotonically from zero, the N poles of S move away from the real energy axis into the complex plane. As x_a increases beyond $x_a = 1$ (all a), the cloud of N poles begins to separate into a small cloud containing Λ poles that move ever further away from the real axis and a big cloud of $N - \Lambda$ poles that moves back toward the real axis (see Fig. 5).

According to Eq. (8), the transmission coefficients measure the unitarity deficit of the average S matrix. As mentioned in Sec. III.A, they also measure the probability of CN formation. It is now clear why the T_a's are better suited for that purpose than the coupling coefficients x_a.

C. Satchler's transmission matrix

In Sec. V.B we have used S^{CN} (which is diagonal on average) to express $\langle S_{aa}^{\mathrm{CN}}\rangle$ and T_a in terms of the coupling coefficients x_a [see Eqs. (56) and (59)]. We now address

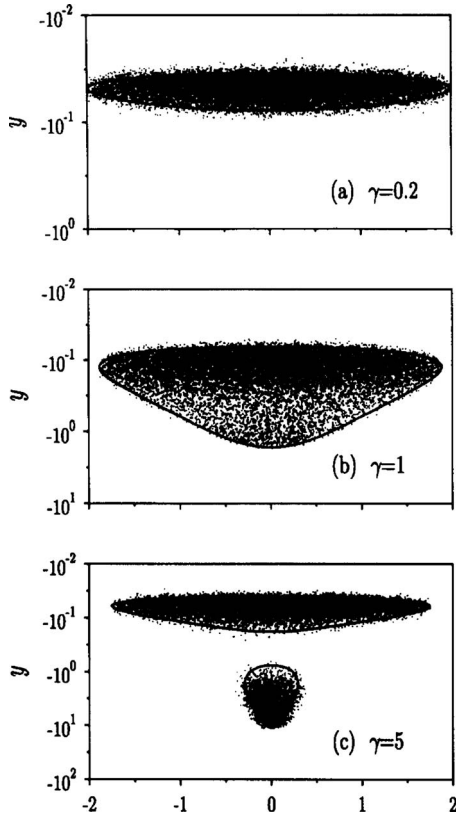

FIG. 5. Distribution of the poles of the S matrix in the complex energy plane. The distribution is shown for several values of the strength γ of the average coupling to the channels. The abscissa spans the entire range of the spectrum. From Lehmann, Saher, *et al.* 1995.

the question how to determine the transmission coefficients if $\langle S\rangle$ is not diagonal, which is the generic case. In principle, the question can simply be answered with the help of Eq. (40): To find the T_a's, take the matrix $S^{\mathrm{CN}} = U^\dagger SU^*$. By definition, the average of S^{CN} is diagonal, and Eq. (8) yields the transmission coefficients. But historically the question came up before the form (40) with U defined in Eq. (39) was known. It arose in conjunction with the experimental discovery of direct reactions mentioned in Sec. III.C and with the theoretical treatment of such reactions which are described by nondiagonal average scattering matrices (see Sec. V.D).

A general measure of the unitarity deficit of $\langle S\rangle$ is given by Satchler's transmission matrix P (Satchler, 1963), a matrix in channel space defined in Eq. (17). Since P is Hermitian, it can be diagonalized by a unitary matrix $\tilde{U}$. We denote the eigenvalues by p_a with $a = 1, \ldots, \Lambda$ and have

$$(\tilde{U}^\dagger P\tilde{U})_{ab} = \delta_{ab}p_a, \quad \text{where } 0 \leqslant p_a \leqslant 1. \tag{61}$$

Applying the transformation $\tilde{U}$ to the right-hand side of Eq. (17) and using $\tilde{U}^*\tilde{U}^T = 1_\Lambda$, we are led to consider the matrices $A = \tilde{U}^\dagger\langle S\rangle\tilde{U}^*$ and $A^* = \tilde{U}^T\langle S\rangle\tilde{U}$. Equation (61) implies that $(AA^*)_{ab} = \delta_{ab}(1 - p_a) = (A^*A)_{ab}$ which in turn shows that the symmetric matrices A and A^* are normal

and can be diagonalized simultaneously (Engelbrecht and Weidenmüller, 1973). The matrix product AA^* being diagonal already, we conclude that A and A^* are diagonal too (except for accidental degeneracies of the p_a which we do not consider). Thus,

$$(\tilde{U}^\dagger \langle S \rangle \tilde{U}^*)_{ab} = \delta_{ab}\sqrt{1-p_a}\,\exp(2i\phi_a), \tag{62}$$

where the ϕ_a's are real. Defining $U_{ab}=\tilde{U}_{ab}\exp(i\phi_b)$ we conclude that the average of the matrix $U^\dagger S U^*$ is real and diagonal, $\langle U^\dagger S U^* \rangle_{ab}=\delta_{ab}\sqrt{1-p_a}$. This shows that the transmission coefficients are given by the eigenvalues p_a of Satchler's transmission matrix, $T_a=p_a$, $a=1,\ldots,\Lambda$. Moreover, the function $F_{\mu\nu}$ in Eq. (44) is invariant under an arbitrary unitary transformation in the space of channels. Therefore, the matrix $S^{\mathrm{CN}}=U^\dagger S U^*$ is identical with the scattering matrix of pure CN scattering in the absence of direct reactions. In other words, the matrix U reduces the CN scattering problem in the presence of direct reactions to the pure CN scattering problem without direct reactions.

The transformation U introduced by Engelbrecht and Weidenmüller (1973) and defined in terms of Satchler's transmission matrix is a purely formal device. Nishioka and Weidenmüller (1985) have shown how U is defined physically. We do not retrace the steps of the argument here because we have used it to construct the matrix U in Eq. (39). The present construction of the matrix U via Satchler's transmission matrix yields exactly the same matrix U as in Eq. (39) if the energy E is chosen in the center of the GOE spectrum, so that $E=0$. Otherwise, the matrix U obtained from Eqs. (61) and (62) contains an additional phase [the phase of the average S matrix; see the remark below Eq. (56)].

D. Optical model and strength function. Direct reactions

The average S matrix serves as input for the statistical theory and must be determined phenomenologically. It is intuitively clear that the fast part $\langle S \rangle$ of the reaction amplitude S can involve only few degrees of freedom. Therefore, models that do not take into account the full complexity of the many-body problem suffice for an accurate determination of $\langle S \rangle$. These are the optical model of elastic scattering and the coupled-channels approach. The latter describes fast inelastic processes that are referred to as direct reactions. We do not review these models in detail but confine ourselves to those aspects that are essential for the understanding of the statistical theory.

In the optical model (Hodgson, 1963), elastic scattering of nucleons is described in terms of a radial Schrödinger equation with a central potential $V(r)+iW(r)$. The bulk of the real part $V(r)$ is due to the shell-model potential. (The shell model is the subject of Sec. I.IV.A.) The imaginary part $W(r)$ describes CN formation by nucleon absorption. Via a dispersion relation, the imaginary part $W(r)$ also modifies the real (shell-model) part $V(r)$. Because of the presence of $W(r)$, the scattering amplitude calculated from the optical model is subunitary and identified with the average scattering amplitude in the nucleon channel of the statistical theory. Obvious generalizations apply to the scattering of composite particles. Figure 4 shows results of an optical-model calculation.

As mentioned in Sec. IV.C, the CN was originally considered a black box. The novel aspect of the optical model introduced by Feshbach *et al.* (1954) was the partial transparency of the target nucleus. That aspect modified Bohr's picture of the CN as a system of strongly interacting particles: Nucleons in the nucleus had a finite mean free path. The nuclear shell model had indicated such behavior already for the ground state and low-lying excited states. Now that feature was extended to resonances (states above neutron threshold). The influence of shell structure on the CN cross section is manifest in the neutron strength function. In analogy to the spreading width introduced in Sec. I.II.G, the neutron s-wave strength function $s(E)$ is defined as $s(E)=2\pi\langle\Gamma_{\mu a}\rangle/d$. Here $\Gamma_{\mu a}$ is the partial width for s-wave neutron emission of resonance μ. With $\Gamma_{\mu a}=2\pi W_{\mu a}^2$ and Eq. (45) this yields $s(E)=4x_a$ and for $x_a \ll 1$, $s(E)=T_a$ [see Eq. (59)]. The strength function $s(E)$ measures the intensity with which a group of resonances is coupled to the s-wave neutron channel. The strength function can both be measured (by performing a running average over a number of resonances) and be calculated directly from the optical model. We recall that the radius of the real part of the optical-model potential (i.e., essentially the shell-model potential) increases with A. The strength function displays maxima versus A whenever a single-particle s-wave state is about to be pulled into the potential well.

The phenomenological description of direct reactions is based on an extension of the optical model for elastic scattering. For a set of channels, the radial equations describing elastic scattering with the help of the optical model are coupled. The term which couples two channels is obtained as the matrix element of the interaction between projectile and target sandwiched between the two channel wave functions [see the reviews by Austern (1970), Koning and Delaroche (2003), and Glendenning (2004)]. Direct reactions are most important for strongly coupled channels. Often these are channels where the target nucleus is in different states of collective excitation. Nucleon transfer between projectile and target may also lead to strong interchannel coupling. In many cases, the solution of the coupled-channels problem can be simplified by using the Born approximation. The result is the distorted-wave Born approximation: The plane waves in the entrance and exit channels are distorted by the optical potentials; the transition between both channels is calculated perturbatively to first order.

Direct reactions induce correlations between partial width amplitudes relating to different channels (Hüfner *et al.*, 1967; Kawai *et al.*, 1973). In the present context, that is seen as follows. Equation (48) shows that for $a \neq b$, the partial width amplitudes $\sqrt{2\pi}\tilde{W}_{\mu a}$ and $\sqrt{2\pi}\tilde{W}_{\mu b}$

are uncorrelated random variables. But in the presence of direct reactions, the matrix U in Eq. (40) is not diagonal, and the partial width amplitudes $\gamma_{\mu a}$ of the full S matrix in channel a are given by $\Sigma_b U_{ab}\sqrt{2\pi}\tilde{W}_{\mu b}$. For two channels $a \neq b$ connected by a direct reaction these are, in general, correlated. Indeed, using Eq. (48) we find that $\langle \gamma_{\mu a}\gamma^*_{\mu b}\rangle = 2\pi\Sigma_c U_{ac}U^*_{bc}\nu_c^2 \neq 0$.

VI. RESULTS OF THE STATISTICAL THEORY

According to Eqs. (40)–(42), $S(E)$ is a matrix-valued random process. The goal of the statistical theory consists in finding the joint probability distribution of $S(E)$ and $S^*(E)$. Because of Eq. (40) it would actually suffice to determine the joint probability distribution of $S^{\mathrm{CN}}(E)$ and $(S^{\mathrm{CN}}(E))^*$. The probability distribution should be given in terms of the transmission coefficients T_c, of energy differences in units of the mean GOE level spacing d, and of overall phase factors. We are far from that goal because averaging over the $N(N+1)/2$ random variables of H^{GOE} that appear in the denominator of S^{CN} [see Eqs. (41), (42), and (47)] turns out to be extremely difficult in general. We possess only partial information mainly on low moments and correlation functions of $S^{\mathrm{CN}}(E)$ and $(S^{\mathrm{CN}}(E))^*$. This information suffices for a comparison with the available experimental data and is now reviewed, together with the various methods that have been used to calculate the answers. We do not go into the full complexity of some of the calculations as these are technically quite demanding, and refer the reader to the original literature.

In the calculation of moments and correlation functions, a simplification arises because the coupling matrix elements obey Eq. (38). It follows that all moments and correlation functions of $S^{\mathrm{CN}}(E)$ and $(S^{\mathrm{CN}}(E))^*$ vanish unless the channel indices are pairwise equal. For instance, using the unitary transformation of Eq. (40) to calculate $\langle|S_{ab}|^2\rangle$, we find that only terms of the form $\langle|S^{\mathrm{CN}}_{cd}|^2\rangle$ and $\langle S^{\mathrm{CN}}_{cc}(S^{\mathrm{CN}}_{c'c'})^*\rangle$ give nonvanishing contributions.

A. Isolated resonances ($\Gamma \ll d$)

Isolated resonances occur in two limiting cases: The coupling coefficients x_a defined in Eq. (45) may be either very small or very large compared to unity, $x_a \ll 1$ or $x_a \gg 1$ for all a. The two cases differ only in the phases of the average S-matrix elements and lead to identical expressions for the CN cross section. Therefore, we consider only the case $x_a \ll 1$ for all a. We use the form (49) and (50) of S^{CN} and the statistical properties listed above those equations. We replace the ensemble average by an energy average and use contour integration. That is possible for $\Gamma \ll d$ because the resonances are isolated. We define $\Gamma_{\mu a} = 2\pi\tilde{W}^2_{\mu a}$ and $\Gamma_\mu = \Sigma_c \Gamma_{\mu c}$. The partial widths $\Gamma_{\mu a}$ are squares of Gaussian-distributed random variables and follow the Porter-Thomas distribution given in Eq. (I.18). According to Eq. (I.17) the distribution depends on a single parameter, the average width $\langle\Gamma_{\mu a}\rangle$. We find (Bethe, 1937; Lane and Lynn, 1957; Moldauer, 1961, 1963, 1964, 1969, 1975a, 1975b)

$$\langle|S^{(\mathrm{CNfl})}_{ab}|^2\rangle = \frac{2\pi}{d}\left\langle \frac{\Gamma_{\mu a}\Gamma_{\mu b}}{\Gamma_\mu}\right\rangle. \tag{63}$$

The average on the right-hand side is over the Porter-Thomas distribution of the $\Gamma_{\mu a}$'s. Since $\Gamma_\mu = \Sigma_a \Gamma_{\mu a}$, the variables in the numerator and denominator are not statistically independent. For $x_a \ll 1$ we have that $T_a \approx 4x_a = (2\pi/d)\langle\Gamma_{\mu a}\rangle$. Thus, it is possible to express the right-hand side of Eq. (63) (including the Porter-Thomas distribution of the $\Gamma_{\mu a}$) completely in terms of the transmission coefficients T_a, as required by the statistical theory. We rewrite Eq. (63) in the form

$$\langle|S^{(\mathrm{CNfl})}_{ab}|^2\rangle = \frac{T_a T_b}{\sum_c T_c}\mathbf{W}_{ab}. \tag{64}$$

Here $\mathbf{W}_{ab}$ is referred to as the "width fluctuation correction" (to the Hauser-Feshbach formula) and is defined as

$$\mathbf{W}_{ab} = \left\langle \frac{\Gamma_{\mu a}\Gamma_{\mu b}}{\Gamma_\mu}\right\rangle \frac{\langle\Gamma_\mu\rangle}{\langle\Gamma_{\mu a}\rangle\langle\Gamma_{\mu b}\rangle}. \tag{65}$$

Equation (65) shows that for the single-channel case we have $\mathbf{W}=1$. For the general case (several open channels), $\mathbf{W}_{ab}$ has been calculated numerically by Lane and Lynn (1957) and especially by Reffo *et al.* (1976). The values range from 1 to 3. This shows that for isolated resonances the Hauser-Feshbach formula is only approximately valid. For the special case of a large number of channels with very small transmission coefficients each (so that $\Lambda \gg 1$ but $\Sigma_c T_c \ll 1$) numerator and denominator in the first term on the right-hand side of Eq. (65) become uncorrelated, we have $\mathbf{W}_{ab} \approx \langle\Gamma_{\mu a}\Gamma_{\mu b}\rangle/\langle\Gamma_{\mu a}\rangle\langle\Gamma_{\mu b}\rangle = 1+2\delta_{ab}$, and the Hauser-Feshbach formula applies with an elastic enhancement factor of 3. This is why it is sometimes stated that the elastic enhancement factor increases from the value 2 for $\Gamma \gg d$ (see Sec. VI.B) to the value 3 for $\Gamma \ll d$ although the last value actually applies only in a special situation.

Equation (65) holds for completely isolated resonances. A correction taking into account weak resonance overlap and using R-matrix theory was given by Lane and Lynn (1957). Moldauer (1961) went beyond Eq. (65) by using a perturbative expansion of the S matrix in powers of the nondiagonal elements of the width matrix. The expressions become soon very cumbersome. Therefore, Moldauer (1961, 1963, 1964, 1969, 1975b, and references therein) tried to go beyond the limit $\Gamma \ll d$ using the pole expansion of the S matrix as formulated by Humblet and Rosenfeld (1961). But the pole parameters (locations of poles and values of the residues) are linked by unitarity in a complicated way and, thus, not statistically independent. This difficulty has never been resolved. We return to some aspects of Moldauer's work in Sec. VI.F.

Equation (64) predicts average cross sections for elastic and inelastic scattering as functions of the transmission coefficients. It would be of interest to calculate perturbatively also the cross-section autocorrelation function $\langle |S_{ab}^{(\mathrm{CNfl})}(E_1)|^2 |S_{ab}^{(\mathrm{CNfl})}(E_2)|^2 \rangle$. This seems not to have been done yet. Likewise, the quantity $\langle S_{aa}^{\mathrm{CNfl}} (S_{bb}^{\mathrm{CNfl}})^* \rangle$ seems not to have been worked out explicitly for $\Gamma \ll d$. As remarked in the introduction to Sec. VI, this quantity is needed for the average CN cross section in the presence of direct reactions. The reason for the neglect is probably that $\Gamma \ll d$ is strictly realized only for a single open channel.

B. Ericson regime ($\Gamma \gg d$)

The Ericson model reviewed in Sec. III.B leads to interesting predictions which agree with experiment but has the shortcomings listed at the beginning of Sec. IV. While it is probably not possible to derive the Ericson model as such from the RMT approach developed in Sec. IV we now show that it is indeed possible to derive both the Hauser-Feshbach formula and all results of the Ericson model from that approach. This is done with the help of an asymptotic expansion in powers of d/Γ. Two methods have been used, a diagrammatic approach (Agassi *et al.*, 1975) and the replica trick (Weidenmüller, 1984). These are reviewed in turn. Combining the results of both, one obtains a complete theory of CN reactions in the regime $\Gamma \gg d$.

1. Diagrammatic expansion

We use the form (49) and (50) of S^{CN} and the statistical properties that come with that representation. We note that with $\tilde{F}_{\mu\nu}(E) = -i\pi \Sigma_c \tilde{W}_{\mu c} \tilde{W}_{c\nu}$, we have

$$\langle \tilde{F}_{\mu\nu} \rangle = -i\pi \delta_{\mu\nu} \sum_c \nu_c^2 = -i \delta_{\mu\nu} f. \tag{66}$$

The last equation defines f. With $\delta F_{\mu\nu} = F_{\mu\nu} - \delta_{\mu\nu} f$, the matrix $\tilde{D}$ is written as $\tilde{D}_{\mu\nu} = (E - E_\mu - if)\delta_{\mu\nu} - \delta F_{\mu\nu} = \tilde{D}_\mu^{(0)} \delta_{\mu\nu} - \delta F_{\mu\nu}$. In the approach of Agassi *et al.* (1975), each of the two S-matrix elements in the product $S_{ab}^{\mathrm{CN}}(E_1)(S_{cd}^{\mathrm{CN}}(E_2))^*$ is expanded in a Born series with respect to $\delta F_{\mu\nu}$. To calculate $\langle S_{ab}^{\mathrm{CN}}(E_1)(S_{cd}^{\mathrm{CN}}(E_2))^* \rangle$, one first performs the ensemble average over the $\tilde{W}$'s. The average is taken separately for each term of the double Born series. The matrix $\delta F_{\mu\nu}$ is bilinear in the Gaussian-distributed $\tilde{W}$'s. Each term of the double Born series therefore contains a product of $\tilde{W}$'s. The ensemble average over such a product is taken by Wick contraction: The $\tilde{W}$'s are grouped in pairs; each pair is replaced by its ensemble average [see Eq. (48)]. All possible ways of pairing the $\tilde{W}$'s must be taken into account, including pairs where one member stems from the Born series of S^{CN} and the other from that of $(S^{\mathrm{CN}})^*$. The number of ways of pairing the $\tilde{W}$'s increases dramatically with the order of the double Born series. Among these, only those which contribute to leading order in d/Γ are kept. These are identified with the help of two rules. (i) Contraction patterns are neglected that yield terms of the form $\Sigma_\mu (\tilde{D}_\mu^{(0)})^{n_1} ((\tilde{D}_\mu^{(0)})^*)^{n_2}$ with $n_1 \geqslant 2$ and/or $n_2 \geqslant 2$. When the summation over μ is changed into an energy integration and the integrals are done via contour integration, the result vanishes. (ii) The second rule is illustrated by the following example. We compare two simple contraction patterns both of which occur as parts in the Born series and yield a term proportional to $(\tilde{D}_\mu^{(0)})^3$. The first one occurs in the term $\tilde{D}_\mu^{(0)} [(\tilde{W} i \tilde{W} \tilde{D}^{(0)})^2]_{\mu\nu}$ and involves the contraction of the first with the third and of the second with the fourth factor $\tilde{W}$. From Eq. (48) the result is $-\delta_{\mu\rho} (\tilde{D}_\mu^{(0)})^3 \Sigma_a (\nu_a^2)^2$. The second pattern occurs in the term $\tilde{D}_\mu^{(0)} [(\tilde{W} i \tilde{W} \tilde{D}^{(0)})^4]_{\mu\nu}$ and involves the contraction of the first with the fourth, of the second with the third, of the fifth with the eighth, and of the sixth with the seventh factor $\tilde{W}$. The result is $\delta_{\mu\nu} (\tilde{D}_\mu^{(0)})^3 [(-i\pi/d) \Sigma_a (\nu_a^2)^2]^2$. The first (second) pattern yields a single (double) sum over channels. Thus, the first pattern is small, of order d/Γ compared to the second, and is neglected. Denoting the contraction of a pair of $\tilde{W}$'s with an overbar, one finds that only those contractions survive in leading order in d/Γ where no two contraction lines intersect (nested contributions).

In evaluating these patterns we have replaced the summation over eigenvalues E_μ by an integration over energy. This yields the factors $1/d$ in the second pattern. Doing so corresponds to the neglect of correlations between eigenvalues (the actual eigenvalue distribution is replaced by one with constant spacings). The Wigner-Dyson eigenvalue correlations have a typical range given by d, and for $d \ll \Gamma$ one expects that the neglect is justified. With the help of the same approximation the remaining terms in the double Born series can be resummed. With $\varepsilon = E_2 - E_1$ this yields

$$\langle S_{ab}^{(\mathrm{CNfl})}(E_1)(S_{cd}^{(\mathrm{CNfl})}(E_2))^* \rangle = (\delta_{ac}\delta_{bd} + \delta_{ad}\delta_{bc}) \times \frac{T_a T_b}{\sum_e T_e + 2i\pi\varepsilon/d}. \tag{67}$$

For $\varepsilon = 0$ that coincides with the Hauser-Feshbach formula (9) and for $\varepsilon \neq 0$ agrees with Ericson's prediction (13) if we identify in the latter the factors $4\pi^2 \nu_a^2/d$ with the transmission coefficients T_a [see the text following Eq. (13)]. Moreover, in the framework of the diagrammatic approach, the Weisskopf estimate (11) is seen to yield the exact expression for the width of the S-matrix correlation function in the Ericson regime. Equation (67) implies that the elastic ($a=b$) CN cross section is enhanced over the inelastic one by a factor of 2 ("elastic enhancement factor"). This result is beautifully confirmed experimentally (see Fig. 3). In Agassi *et al.* (1975) the terms of next order in d/Γ were also calculated. We return to this point in Sec. VI.B.2.

The diagrammatic expansion can also be used to calculate higher-order S-matrix correlation functions. It is found (Agassi *et al.*, 1975) that to leading order in d/Γ such correlations can be expressed completely in terms of correlations of pairs of S-matrix elements. This implies that in the Ericson regime the S-matrix elements possess a Gaussian distribution.

In summary, the diagrammatic approach shows that for $\Gamma \gg d$ the S-matrix elements are Gaussian-distributed random processes, with first and second moments given in Eqs. (56) and (57), respectively, and with a correlation width given by the Weisskopf estimate (11). All of this agrees with the predictions of the Ericson model. We conclude that within the diagrammatic approach (i.e., under the neglect of eigenvalue correlations), the distribution of the S-matrix elements is completely known and is determined in terms of the average S-matrix element (56) via the transmission coefficient (8).

2. Replica trick

Calculation of the average of $|S_{ab}^{\mathrm{CN}}|^2$ is difficult because H^{GOE} appears in the denominator of S^{CN}. A way to overcome this problem consists in the use of a generating functional Z (Weidenmüller, 1984). The observable (here $|S_{ab}^{\mathrm{CN}}|^2$) is given in terms of a suitable derivative of Z, and H^{GOE} appears in Z as the argument of an exponential. This fact would greatly simplify the integration over the random variables (the matrix elements of H^{GOE}) were it not for the need to normalize Z. The normalization problem is overcome by the replica trick originally developed in condensed-matter physics (Edwards and Anderson, 1975).

We introduce N real integration variables ψ_μ, $\mu=1,\ldots,N$, and define the generating functional

$$Z(E,J)=\left(\prod_{\mu=1}^{N}\int_{-\infty}^{+\infty}d\psi_\mu\right)\exp\left\{(i/2)\sum_{\mu}\psi_\mu E\psi_\mu\right\}\times\exp\left\{(i/2)\sum_{\mu\nu}\psi_\mu\left(-H_{\mu\nu}+i\pi\sum_{c}\hat{W}_{\mu c}\hat{W}_{c\nu}\right)\psi_\nu\right\}. \tag{68}$$

Here the matrix elements $\hat{W}$ include the source terms J and are defined as

$$\hat{W}_{\mu c}=W_{\mu c}+J\delta_{ca}W_{\mu b}+J\delta_{cb}W_{\mu a}. \tag{69}$$

The CN scattering matrix is given by

$$S_{ab}^{\mathrm{CN}}=\delta_{ab}+\frac{\partial}{\partial J}\ln Z(E,J)|_{J=0}. \tag{70}$$

Unfortunately, little has been gained because calculating $\langle S_{ab}^{\mathrm{CN}}\rangle$ or $\langle S_{ab}^{\mathrm{CN}}(S_{cd}^{\mathrm{CN}})^*\rangle$ from Eq. (70) involves averaging the logarithmic derivative of Z or the product of two logarithmic derivatives of Z and is next to impossible to do. The difficulty is that, at $J=0$, Z is not and cannot easily be normalized to unity. The problem is overcome by using the identity

$$\ln Z=\lim_{n\to 0}\frac{1}{n}(Z^n-1). \tag{71}$$

For integer values of n, the average of Z^n (or of a product of such terms) can be calculated, and Eq. (71) is then used to calculate $\langle \ln Z\rangle$ or $\langle(\ln Z)^2\rangle$. Instead of $\ln Z$ we use n replicas of Z to calculate averages, hence the name of the method. The calculation must be done analytically as otherwise the limit $n\to 0$ cannot be taken. This is possible only for positive integer values of n. However, Eq. (71) is strictly valid only when n is not restricted to integer values. Otherwise, one may miss nonzero contributions that happen to vanish for all positive integer n. This is why the method is not guaranteed to be exact and is referred to as a "trick." Later investigations have shown, however, that when used for an asymptotic expansion as is done below, the replica trick gives correct answers (Verbaarschot and Zirnbauer, 1985).

A detailed description of the calculation (Weidenmüller, 1984) exceeds the frame of this review. We only sketch the essential steps. In the case of $\langle Z^n\rangle$, we deal with $n\times N$ real integration variables ψ_μ^k, with $k=1,\ldots,n$ and $\mu=1,\ldots,N$. With the help of Eq. (36), averaging over H^{GOE} yields a quartic term in ψ_μ^k's. This term can be written as the trace of the square of the symmetric real $n\times n$ matrix $A_{kk'}=\Sigma_\mu\psi_\mu^k\psi_\mu^{k'}$. The form of A reflects the orthogonal invariance of the GOE. The bilinear term in A is removed by means of a Hubbard-Stratonovich transformation,

$$\exp\left\{-\frac{\lambda^2}{4N}\mathrm{Tr}(A^2)\right\}\propto\prod_{k\le k'}\int_{-\infty}^{+\infty}d\sigma_{kk'}\exp\left\{-\frac{N}{4}\mathrm{Tr}(\sigma^2)\right\}\times\exp\{-i\lambda\,\mathrm{Tr}(\sigma A)\}. \tag{72}$$

In Eq. (72) we have introduced a set of new integration variables which appear in the form of the symmetric real n-dimensional matrix $\sigma_{kk'}$. After removal of the quartic term, the remaining integral over the ψ_μ^k's is Gaussian and can be done. The integral over $\sigma_{kk'}$ is performed with the help of the saddle-point approximation. For $N\gg 1$ the approximation is excellent. For $\langle S^{\mathrm{CN}}\rangle$, it yields an asymptotic expansion in inverse powers of N with the right-hand side of Eq. (56) as the leading term. Proceeding in the same way for $\langle S_{ab}^{(\mathrm{CNfl})}(E_1)(S_{cd}^{(\mathrm{CNfl})}(E_2))^*\rangle$ one finds instead of a single saddle point a continuum of saddle points. In a seminal paper, Schäfer and Wegner (1980) have shown in a different context how to deal with that manifold. This is done with the help of a suitable parametrization of the matrix $\sigma_{kk'}$ which displays both the massive integration variables (that describe integration points outside the saddle-point manifold) and the Goldstone mode (which defines the coordinates within the saddle-point manifold). After these steps, one finds that the energy difference $E_2-E_1=\varepsilon$ appears in the integrand only in the combination $\Sigma_c T_c+(2i\pi\varepsilon/d)$. This shows that the correlation width Γ of the correlation function is given by the Weisskopf estimate (11). The integrals over the saddle-point manifold cannot be done

exactly. For the calculation of $\langle S_{ab}^{(\mathrm{CNfl})}(E_1)(S_{cd}^{(\mathrm{CNfl})}(E_2))^*\rangle$, the replica trick can only be used to calculate an asymptotic expansion in inverse powers of $\Sigma_c T_c$. The leading term agrees with Eq. (67). Terms of higher order also agree with the result given by Agassi *et al.* (1975). Moreover, these terms can be used to confirm unitarity for each order of the expansion and to show that the leading term gives reliable answers for $\Sigma_c T_c \geqslant 10$ or so (see also Sec. VI.C).

In the case of direct reactions, we use Eq. (40) and obtain from Eq. (67), the definition (17) and with $T_a = p_a$ as a result [Eq. (16)]. This shows that to leading order in d/Γ the result of Kawai *et al.* (1973) agrees with that of the statistical theory.

3. Summary

The replica trick yields an asymptotic expansion in inverse powers of $\Sigma_c T_c$ for the S-matrix correlation function. The leading term is given by Eq. (67). This form implies that the correlation width agrees exactly with the Weisskopf estimate (11). The diagrammatic approach neglects eigenvalue correlations of the GOE Hamiltonian in favor of a constant-spacing model but leads likewise to Eq. (67). This shows that for $\Gamma \gg d$ such correlations are indeed negligible and that the results of the diagrammatic approach are trustworthy. Investigating higher-order correlation functions within the diagrammatic approach (which seems prohibitively difficulty in the framework of the replica trick), one finds that the S-matrix elements are Gaussian-distributed random variables with first and second moments given by Eqs. (56) and (67), respectively. We see that combining the replica trick and the diagrammatic approach we obtain a complete theoretical understanding of the distribution of the elements of S^{CN} in the Ericson regime. The results agree with predictions of the Ericson model and, in the presence of direct reactions, with those of Kawai *et al.* (1973).

C. *S*-matrix correlation function

The replica trick yields only an asymptotic expansion but not the full S-matrix correlation function. The correlation function can be obtained exactly using "supersymmetry" (Efetov, 1983; Verbaarschot and Zirnbauer, 1985). We briefly motivate the use of this method.

The use of the generating functional defined in Eq. (68) would greatly simplify if it were possible to normalize Z so that $Z(E,0)=1$. Then, in Eq. (70) we would have $[\partial \ln Z(E,J)/\partial J]|_{J=0} = [\partial Z(E,J)/\partial J]|_{J=0}$. Averaging S would amount to averaging Z (and not $\ln Z$), and it would not be necessary to use the replica trick. Since in Z the random variables appear in the exponent, the calculation of $\langle Z\rangle$ would be straightforward.

The goal is achieved by defining the normalized generating functional as the product of two factors. The first factor is Z^2 with Z as defined in Eq. (68). The second factor has the same form as Z except that the integration variables anticommute. Integration with anticommuting variables is a well-known mathematical technique (Berezin, 1986). In the present context, we use the following property. The normalization factor of a Gaussian integral involving N commuting real integration variables ψ_μ, $\mu=1,\ldots,N$, and a symmetric matrix A is given by

$$\prod_\mu \int_{-\infty}^{+\infty} d\psi_\mu \exp\left\{(i/2)\sum_{\mu\nu} \psi_\mu A_{\mu\nu}\psi_\nu\right\} = \{\det[A/(2i\pi)]\}^{-1/2}. \tag{73}$$

The same integral with the commuting variables ψ_μ replaced by anticommuting variables χ_μ and χ_μ^* is given by

$$\prod_\mu \int d\chi_\mu^* d\chi_\mu \exp\left\{i\sum_{\mu\nu} \chi_\mu^* A_{\mu\nu}\chi_\nu\right\} = \det[A/(2i\pi)]. \tag{74}$$

Combining two factors of the form of the left-hand side of Eq. (73) with one factor of the form of the left-hand side of Eq. (74), we obtain a normalized generating functional involving both commuting and anticommuting integration variables. The term "supersymmetry" commonly used in that context is somewhat inappropriate. It stems from relativistic quantum field theory (Wess and Zumino, 1974a, 1974b) where fermionic (i.e., anticommuting) and bosonic (i.e., commuting) fields are connected by a supersymmetry. That specific symmetry does not occur in the present context.

In a formal sense, the calculation of $\langle S^{\mathrm{CN}}\rangle$ and of the correlation function runs in parallel to the one for the replica trick. In content, the steps differ because of the simultaneous use of commuting and anticommuting variables. The steps are averaging the generating functional over the GOE, replacing the quartic terms in the integration variables generated that way with the help of a Hubbard-Stratonovich transformation, executing the remaining Gaussian integrals over the original integration variables, and using the saddle-point approximation for the remaining integrals over the supermatrix σ. That matrix is introduced via the Hubbard-Stratonovich transformation and has both commuting and anticommuting elements. For $N \gg 1$ the saddle-point approximation is excellent and yields for $\langle S^{\mathrm{CN}}\rangle$ an asymptotic expansion in inverse powers of N, the leading term being given by the right-hand side of Eq. (56) when E is taken in the center of the GOE spectrum. When the same formalism is used for the S-matrix correlation function instead of S itself, the saddle-point changes into a saddle-point manifold. With the help of a suitable parametrization (Schäfer and Wegner, 1980) of σ, the integration over that manifold can be done exactly. The result is again valid to leading order in $1/N$. With $\varepsilon = E_2 - E_1$, one obtains (Verbaarschot *et al.*, 1985)

$$\langle S_{ab}^{(\mathrm{CNfl})}(E_1)(S_{cd}^{(\mathrm{CNfl})}(E_2))^*\rangle = \prod_{i=1}^{2}\int_0^{+\infty} d\lambda_i \int_0^1 d\lambda \frac{1}{8}\mu(\lambda_1,\lambda_2,\lambda) \times \exp\left\{-\frac{i\pi\varepsilon}{d}(\lambda_1+\lambda_2+2\lambda)\right\} \times \prod_e \frac{1-T_e\lambda}{(1+T_e\lambda_1)^{1/2}(1+T_e\lambda_2)^{1/2}} J_{abcd}(\lambda_1,\lambda_2,\lambda). \tag{75}$$

The factor $\mu(\lambda_1,\lambda_2,\lambda)$ is an integration measure and given by

$$\mu(\lambda_1,\lambda_2,\lambda) = \frac{(1-\lambda)\lambda|\lambda_1-\lambda_2|}{\prod_{i=1}^{2}\{[(1+\lambda_i)\lambda_i]^{1/2}(\lambda+\lambda_i)^2\}}, \tag{76}$$

while

$$J_{abcd}(\lambda_1,\lambda_2,\lambda) = (\delta_{ac}\delta_{bd}+\delta_{ad}\delta_{bc})T_aT_b\left(\sum_{i=1}^{2}\frac{\lambda_i(1+\lambda_i)}{(1+T_a\lambda_i)(1+T_b\lambda_i)} + \frac{2\lambda(1-\lambda)}{(1-T_a\lambda)(1-T_b\lambda)}\right) + \delta_{ab}\delta_{cd}T_aT_c\langle S_{aa}^{\mathrm{CN}}\rangle\langle (S_{cc}^{\mathrm{CN}})^*\rangle \times\left(\sum_{i=1}^{2}\frac{\lambda_i}{1+T_a\lambda_i}+\frac{2\lambda}{1-T_a\lambda}\right)\left(\sum_{i=1}^{2}\frac{\lambda_i}{1+T_c\lambda_i} + \frac{2\lambda}{1-T_c\lambda}\right) \tag{77}$$

describes the dependence of the correlation function on those channels which appear explicitly on the left-hand side of Eq. (75).

Equations (75)–(77) give the S-matrix correlation function in closed form, i.e., in terms of an integral representation. It does not seem possible to perform the remaining integrations analytically for an arbitrary number of channels and for arbitrary values of the transmission coefficients. In the way it is written, Eq. (75) is not suited very well for a numerical evaluation because there seem to be singularities as the integration variables tend to zero. Moreover, the exponential function oscillates strongly for large values of the λ's. These difficulties are overcome by choosing another set of integration variables. Details are given in Verbaarschot (1986). For the case of unitary symmetry, formulas corresponding to Eqs. (75)–(77) were given in Fyodorov *et al.* (2005).

We now turn to the physical content of Eqs. (75)–(77). The unitarity condition (1) must hold for S^{CN} also after averaging. Using a Ward identity one finds that unitarity is indeed obeyed (Verbaarschot *et al.*, 1985). Except for the overall phase factors of the average S matrices appearing on the right-hand side of Eq. (77), the S-matrix correlation function depends only on the transmission coefficients, as expected. Equations (75)–(77) apply over the entire GOE spectrum if d is taken to be the average GOE level spacing at $E=(1/2)(E_1+E_2)$. That stationarity property enhances confidence in the result. When E is chosen in the center of the GOE spectrum, $E=0$, then $\langle S^{\mathrm{CN}}\rangle$ is real [see Eq. (56)], and the complex conjugate sign in the last term in Eq. (77) is redundant. Writing the product over channels in Eq. (75) as the exponential of a logarithm, expanding the latter in powers of λ_1, λ_2, and λ and collecting terms, one finds that ε appears only in the combination $(2i\pi\varepsilon/d)+\Sigma_c T_c$. This fact was also established in the framework of the replica trick. It shows that Γ as defined by the Weisskopf estimate (11) defines the scale for the dependence of the correlation function on ε. Put differently, the energy difference ε appears universally in the dimensionless form ε/Γ (and not ε/d), and for $\{a,b\}=\{c,d\}$ the correlation function (75) has the form $f(1+i\varepsilon/\Gamma;T_a,T_b;T_1,T_2,\ldots,T_\Lambda)$. The right-hand side of Eq. (77) is the sum of two terms. These correspond to $\langle S_{ab}^{(\mathrm{CNfl})}(E_1)(S_{ab}^{(\mathrm{CNfl})}(E_2))^*\rangle$ and $\langle S_{aa}^{(\mathrm{CNfl})}(E_1)(S_{bb}^{(\mathrm{CNfl})}(E_2))^*\rangle$ and are exactly the terms expected (see the introduction to Sec. VI).

The limiting cases ($\Gamma \ll d$ and $\Gamma \gg d$) of Eqs. (75)–(77) were studied and compared with previous results (Verbaarschot, 1986). The case $\Gamma \ll d$ is obtained by expanding the result in Eqs. (75)–(77) in powers of the transmission coefficients. The result agrees with Eq. (63). Conversely, expanding the result in Eqs. (75)–(77) in inverse powers of $\Sigma_c T_c$ one generates the same series as obtained from the replica trick (see Sec. VI.B.2). This shows that the Hauser-Feshbach formula (9), the extension (16) of that formula to the case of direct reactions, and the Ericson result (67) all are leading terms in an asymptotic expansion of the relevant expressions in powers of d/Γ. Moreover, in the limit $\Gamma \gg d$ the Weisskopf estimate (11) gives the exact expression for the correlation width. All of these facts were also obtained previously with the help of the replica trick (see Sec. VI.B.2). A more detailed investigation using supersymmetry (Davis and Boosé, 1988, 1989) has shown that the elastic S-matrix elements S_{aa} possess the Gaussian distribution assumed by Ericson only for strong absorption ($T_a \approx 1$). If this condition is not met, deviations from the Gaussian are caused by unitarity (see Sec. VI.E).

Equations (75)–(77) contain the central result of the statistical theory. The S-matrix correlation function is given analytically for all values of Γ/d. These equations supersede both the perturbative approach (Sec. VI.A) and the replica trick (Sec. VI.B.2) because the results of both these approaches turn out to be special cases of the general result. It would be highly desirable to extend the supersymmetry approach to the calculation of moments and correlation functions involving higher powers of S^{CN} and $(S^{\mathrm{CN}})^*$ than the first. For the correlation function (77), the supermatrix σ has dimension 8. For the cross-section correlation function, the supermatrix matrix has dimension 16. Integration over all matrix elements must be done analytically. While that is feasible for the func-

tion (77), it seems beyond reach for the cross-section correlation. This is why the results of the diagrammatic approach (Sec. VI.B.1) are needed to complete the theory in the Ericson regime: They show that the S-matrix elements have a Gaussian distribution. There is no analytical information about cross-section fluctuations versus energy outside the Ericson regime.

We note that in both limits $\Gamma \ll d$ and $\Gamma \gg d$ the fluctuation properties of the S matrix are completely determined by the Gaussian distribution of the eigenvectors of H^{GOE} and are independent of the fluctuation properties of the eigenvalues of that matrix. Indeed, for $\Gamma \ll d$ the value of $\langle |S_{ab}^{\mathrm{CNfl}}|^2 \rangle$ in Eqs. (64) and (65) is determined entirely by the Porter-Thomas distribution of the partial widths (which in turn is a consequence of the Gaussian distribution of the eigenvectors of H^{GOE}). And for $\Gamma \gg d$ (Ericson limit) the asymptotic expansion (Agassi *et al.*, 1975) based on a picket-fence model for the eigenvalues gives the same result as the calculation that takes fully into account the eigenvalue correlations of H^{GOE}. A significant dependence of the S-matrix fluctuations on the distribution of the eigenvalues of H^{GOE} can, thus, occur only in the intermediate domain $\Gamma \approx d$.

A dynamical model for an interacting fermionic many-body system coupled to a number of open channels was investigated by Celardo *et al.* (2007, 2008). Spinless fermions are distributed over a number of single-particle states with Poissonian level statistics and interact via a two-body interaction of the EGOE(2) type (see Sec. I.V.A). The Hilbert space is spanned by Slater determinants labeled $\mu = 1, \ldots, N$. These are coupled to the open channels labeled $a, b, \ldots$ by amplitudes A_μ^a which are assumed to have a Gaussian distribution with mean value zero and a second moment given by $\langle A_\mu^a A_\nu^b \rangle = \delta_{ab}\delta_{\mu\nu}\gamma^a/N$. The parameters γ^a determine the strength of the coupling to the channels. One focus of these papers is on the way the S-matrix fluctuations change when the intrinsic dynamics is changed from regular (Poisson statistics) to chaotic (Wigner-Dyson statistics) by increasing the strength of the two-body interaction. Many of the features discussed in this review are illustrated by the numerical simulations by Celardo *et al.* (2007, 2008). The assumption that the amplitudes A_μ^a have a Gaussian distribution with a second moment that is proportional to the unit matrix in the space of Slater determinants puts a constraint on the calculations as it implies that the distribution of the A_μ^a is invariant under orthogonal transformations in the space of Slater determinants. Put differently, together with the intrinsic Hamiltonian $H_{\mu\nu}$ all Hamiltonian matrices obtained from $H_{\mu\nu}$ by orthogonal transformations yield the same distribution for the S-matrix elements. This induced orthogonal invariance of H implies that the eigenvectors of H are Gaussian-distributed random variables, completely independent of the detailed form of H, and that only the distribution of the eigenvalues of H depends on whether the intrinsic dynamics is regular or chaotic. The statistical assumption on the amplitudes A_μ^a is physically justified when many channels are open and when the channel wave functions describe states that are chaotic themselves. But the assumption allows for a partial test only of the transition from regular to chaotic motion.

Equations (75)–(77) have been derived in the limit $N \to \infty$ and Λ fixed. Lehmann, Savin, *et al.* (1995) pointed out that in the extreme Ericson regime $\Sigma_c T_c \gg 1$ another limit [first considered by Sokolov and Zelevinsky (1988, 1989, 1992)] may be more appropriate: Λ and N tend jointly to ∞ while the ratio $m = \Lambda/N$ is kept fixed. The authors calculated the S-matrix correlation function in that limit. Using supersymmetry, they found corrections of order m to the saddle-point equation. These modify the S-matrix correlation function but keep the correlation width (given by the Weisskopf estimate) unchanged. The modifications are due to the fact that in the limit considered the range of the correlation function becomes comparable to the range of the GOE spectrum, and the universality that characterizes the regime $\Gamma \ll \lambda$ (where 2λ is the radius of the GOE semicircle) is lost. Further details are given in Sec. VI.F.

1. Decay in time of the compound nucleus

Rather than studying the dependence of the correlation function (75) on the energy difference ε, we investigate the Fourier transform of that function. We confine ourselves to pure CN scattering [so that the matrix U in Eq. (40) is the unit matrix]. We first show that for a very short wave packet incident in channel a the time dependence of the CN decay feeding channel b is given by the Fourier transform of the correlation function (75) (Lyuboshitz, 1978a, 1978b; Dittes *et al.*, 1992; Harney *et al.*, 1992). We then use the explicit form of that function to determine the time dependence of CN decay.

Let $\int dE \exp(-iEt) g(E) |\Psi_a(E)\rangle$ with $\int dE |g(E)|^2 = 1$ be a normalized wave packet incident in channel a. The functions $|\Psi_a(E)\rangle$ are solutions of the Schrödinger equation for a CN system with Λ channels and $N \gg 1$ quasibound states subject to the boundary condition that there is an incident wave with unit flux in channel a only. We set $\hbar = 1$. The wave packet is short in time if $g(E)$ is very broad, i.e., covers many resonances. The outgoing flux in any channel b is asymptotically (large distance) given by

$$F = \int dE_1 \int dE_2 \exp[i(E_2 - E_1)t] \times g(E_1) g^*(E_2) S_{ab}^{\mathrm{CN}}(E_1) (S_{ab}^{\mathrm{CN}}(E_2))^*. \tag{78}$$

We introduce new integration variables $\varepsilon = E_2 - E_1$ and $E = (1/2)(E_1 + E_2)$ and obtain

$$F = \int dE \int d\varepsilon \exp[i\varepsilon t] g(E - (1/2)\varepsilon) g^*(E + (1/2)\varepsilon) \times S_{ab}^{\mathrm{CN}}(E - (1/2)\varepsilon) \{S_{ab}^{\mathrm{CN}}(E + (1/2)\varepsilon)\}^*. \tag{79}$$

Under the assumption that $g(E)$ changes very slowly over a scale of order d or Γ (whichever is larger), we may write the expression as

$$F = \int d\varepsilon \exp[i\varepsilon t] \int dE |g(E)|^2 S_{ab}^{\mathrm{CN}}[E-(1/2)\varepsilon] \times \{S_{ab}^{\mathrm{CN}}[E+(1/2)\varepsilon]\}^* = \int d\varepsilon \exp[i\varepsilon t] \langle S_{ab}^{\mathrm{CN}}[E-(1/2)\varepsilon] \times \{S_{ab}^{\mathrm{CN}}[E+(1/2)\varepsilon]\}^* \rangle. \quad (80)$$

We use the decomposition (3) and obtain a sum of two contributions. The first contribution, $\delta(t)|\langle S_{ab}^{\mathrm{CN}}\rangle|^2$, shows that the average S matrix describes the fast part of the reaction as claimed in Sec. V. The second contribution has the form

$$p_{ab}(t) = \int d\varepsilon \exp[i\varepsilon t] \langle S_{ab}^{(\mathrm{CNfl})}(E-(1/2)\varepsilon) \times \{S_{ab}^{(\mathrm{CNfl})}(E+(1/2)\varepsilon)\}^* \rangle. \quad (81)$$

This shows that the Fourier transform (FT) of the correlation function (75) gives the time dependence of the CN decay. More precisely, the FT is the derivative of the function which describes the decay in time of the CN in channel b within the statistical theory (Lyuboshitz, 1978a, 1978b; Dittes *et al.*, 1992; Harney *et al.*, 1992). The form (42) of the matrix D implies that $p_{ab}(t)=0$ for $t<0$ as expected (Dittes *et al.*, 1992; Harney *et al.*, 1992).

The function $p_{ab}(t)$ cannot be worked out analytically in its full generality. Some limiting cases are of interest (Dittes *et al.*, 1992; Harney *et al.*, 1992). For a single open channel, the decay is not exponential. Rather, it is asymptotically ($t\to\infty$) given by the power-law dependence $t^{-3/2}$. For Λ channels weakly coupled to the resonances (all $T_a \ll 1$), the decay has asymptotically the form $t^{-1-\Lambda/2}$. In both cases, the characteristic mean decay time is given by the average of the coupling strengths of the resonances to the channels. Exponential decay given by $\exp[-\Gamma t]$ with Γ given by the Weisskopf estimate (11) is realized only in the Ericson regime $\Gamma \gg d$. Deviations from the exponential decay law are due to the Porter-Thomas distribution of the partial widths (see Sec. I.II.D.1). The decay in time of an isolated resonance is exponential, of course, except for very short and very long times. But superposing many such resonances with different widths causes deviations from the exponential distribution. Such deviations have been observed experimentally (see Sec. VI.A). Hart *et al.* (2009) drew a somewhat different conclusion. The decay in time of excitations in a chaotic microwave cavity was investigated. The cavity mimics a chaotic quantum system. Therefore, the general RMT results should apply. The authors found that in the limit $t\to\infty$, the ensemble average considered by Dittes *et al.* (1992) and Harney *et al.* (1992) differs from the behavior of (every) single realization. For the latter, the longest-living resonances finally dominate, these are well separated in energy, and the decay, therefore, becomes eventually exponential. The transition from algebraic to exponential decay follows a universal law if time is properly normalized (Hart *et al.*, 2009). The apparent discrepancy with the result of Dittes *et al.* (1992) and Harney *et al.* (1992) is due (Ott, 2009) to a finite-size effect: Hart *et al.* (2009) considered the case of a finite number N of resonances, while the result of Dittes *et al.* (1992) and Harney *et al.* (1992) holds in the limit $N\to\infty$. The turning point in time wherein (Hart *et al.*, 2009) power-law decay changes into exponential decay increases with N and is moved to infinity for $N\to\infty$.

Another approach to time delay uses the Wigner-Smith time-delay matrix (Wigner, 1955b; Smith, 1960a, 1960b)

$$Q_{ab} = i\left\{ \frac{d}{d\varepsilon} \sum_c \langle S_{ac}^{(\mathrm{CNfl})}(E-(1/2)\varepsilon) \times \{S_{bc}^{(\mathrm{CNfl})}(E+(1/2)\varepsilon)\}^* \rangle \right\}_{\varepsilon=0}. \quad (82)$$

That matrix is the matrix of average time delays. Indeed, it is easy to see that $Q_{aa}=(2\pi)^{-1}\Sigma_b \int dt t p_{ab}(t)$. The eigenvalues of the Hermitian matrix Q are called the proper delay times. For Λ channels with $T_c=1$ for all c, the joint probability distribution and the density of the proper delay times have been worked out (Brouwer, 1995; Brouwer *et al.*, 1997, 1999). Savin *et al.* (2001) generalized the approach to Λ equivalent channels with $T_c \neq 1$. Analytical formulas valid for an arbitrary number of channels and arbitrary values of the transmission coefficients are given by Lehmann, Savin, *et al.* (1995). For time-reversal noninvariant systems these issues were treated by Fyodorov, Savin, and Sommers (1997) and Fyodorov and Sommers (1997). The single-channel case was studied by Ossipov and Fyodorov (2005).

D. Distribution of *S*-matrix elements

Except for the Ericson regime, correlation functions that relate to physical observables and involve higher powers of S than in Eq. (75) are not known. Is the situation better when we ask for the distribution of S-matrix elements all taken at the same energy? As we shall see, the answer lies strangely between yes and no.

1. Fit formulas

Fit formulas for the second moments of S based on an RMT simulation were developed prior to the derivation of the general result in Eqs. (75)–(77) and, in principle, have been superseded by that development. We give these formulas here because they are still frequently used in applications. Tepel *et al.* (1974), Hofmann, Richert, and Tepel (1975), and Hofmann, Richert, Tepel, and Weidenmüller (1975) used an ansatz for $\langle |S_{ab}^{(\mathrm{CNfl})}|^2\rangle$ that was inspired by the Hauser-Feshbach formula. It reads

$$\langle |S_{ab}^{(\mathrm{CN/fl})}|^2\rangle = \frac{V_a V_b}{\sum_c V_c}[1+(\mathbf{W}_a-1)\delta_{ab}]. \quad (83)$$

Unitarity relates the expressions on the right-hand side of Eq. (83) with the transmission coefficients T_a. The resulting equations possess unique solutions for the V_a's

provided the $\mathbf{W}_a$'s are known. This leaves the latter as the only parameters to be determined by fits to a numerical simulation. For numerous sets of transmission coefficients, the simulation was done using the K-matrix form (35) of S^{CN}, taking in Eq. (34) the E_μ's as eigenvalues and determining the $\tilde{W}^{(0)}_{a\mu}$'s in terms of the eigenfunctions of a GOE matrix, with a strength defined by T_a. The result is a fit formula for $\mathbf{W}_a$,

$$\mathbf{W}_a - 1 = \frac{2}{1 + (T_a)^{0.3+1.5(T_a/\Sigma_c T_c)}} + 2\left[\frac{T_a - T}{\sum_c T_c}\right]^2. \quad (84)$$

Here T is the arithmetic mean of the T_a's. The other nonvanishing bilinear form $\langle S^{(\mathrm{CNfl})}_{aa}(S^{(\mathrm{CNfl})}_{bb})^*\rangle$ was similarly assumed to factorize for $a \neq b$. Fit formulas for that function based on simulations are likewise given by Hofmann, Richert, Tepel, and Weidenmüller (1975). Numerical evaluation (Verbaarschot, 1986) of Eqs. (75)–(77) showed good agreement with Eqs. (83) and (84) within the expected statistical errors. Similar formulas were subsequently developed by Moldauer (1976).

2. Many open channels

Dyson (1962a) defined the orthogonal ensemble of unitary symmetric matrices S of dimension N (the "circular orthogonal ensemble") and studied the distribution of its eigenvalues for $N \to \infty$. The members of that ensemble may be interpreted as scattering matrices. By definition, these have average value zero and, thus, transmission coefficients $T_a = 1$ in all channels. Moreover, the limit $N \to \infty$ implies the (unrealistic) limit of infinitely many channels. It is perhaps for these reasons that the orthogonal circular ensemble has not found notable applications in nuclear physics.

The distribution of S-matrix elements is analytically accessible for systems with absorption. Absorption occurs, for instance, in microwave resonators where it is due to Ohmic losses. Absorption is described by introducing ficticious channels and associated transmission coefficients. If the resulting total widths of the levels are dominated by absorption, they become statistically independent of the partial width amplitudes of the physical channels. Calculation of the distribution of S-matrix elements is then much simplified (Fyodorov *et al.*, 2005; Savin *et al.*, 2006).

The approach may be used to obtain partial information on the distribution of S-matrix elements in CN reactions. One must focus attention on a distinct pair (a,b) of channels and assume that many channels are open (these may all have small transmission coefficients so that we do not necessarily work in the Ericson regime). All channels different from (a,b) then play the same role as the ficticious channels in the case of absorption, and the results obtained by Fyodorov *et al.* (2005) and Savin *et al.* (2006) may be used to determine the distribution of S_{ab}. The method obviously does not yield the joint distribution function of all elements of the scattering matrix. We are not aware of applications of this approach to CN reactions and do not reproduce the relevant formulas here (see, however, Sec. VI.E).

3. Exact results for low moments

The supersymmetry approach can be used to calculate the third and fourth moments of the scattering matrix (Davis and Boosé, 1988, 1989). The need to introduce supermatrices of dimension larger than 8 (unavoidable if one wishes to calculate higher-order correlation functions) is circumvented by writing these moments as higher-order derivatives of the very same generating functional that is used to calculate the result (75). The resulting analytical formulas are valid for all values of Γ/d. For more details, see Sec. VI.E. In view of the complexity of the calculations, an extension of that approach to higher moments than the fourth seems very difficult.

4. Maximum-entropy approach

The approach developed by Mello *et al.* (1985) is based on an appealing idea. If S^{CN} is determined by an RMT approach (as done in Sec. IV.B), then S^{CN} itself should be as random as is consistent with basic properties of that matrix. These properties are unitarity, symmetry, and the property [Eq. (57)] to which the authors refer as "analyticity-ergodicity." In addition, it is required that $\langle S^{\mathrm{CN}}_{aa}\rangle$ should have the value given by the S matrix S^{opt}_{aa} of the optical model. With these requirements used as constraints, expressions for the distribution $F(S)$ of S^{CN} are obtained from either an analytical approach or a variational principle. The results agree. In the latter case, the probability density for S^{CN} is determined by maximizing the entropy $-\int F(S)\ln F(S)d\mu(S)$ under the said constraints. Here $\mu(S)$ is the Haar measure for unitary and symmetric matrices (see Sec. I.II.B). With Λ the number of channels, 1_Λ the unit matrix in Λ dimensions, and V a Λ-dependent normalization factor, the result is

$$F(S^{\mathrm{CN}}) = \frac{1}{V}\frac{\{\det[1_\Lambda - (S^{\mathrm{opt}})^* S^{\mathrm{opt}}]\}^{(\Lambda+1)/2}}{|\det[1_\Lambda - (S^{\mathrm{opt}})^* S^{\mathrm{CN}}]|^{\Lambda+1}}. \quad (85)$$

The function F is the most likely distribution function for S^{CN} under the constraints mentioned. Do results calculated from $F(S)$ agree with those based on the RMT approach in Sec. IV.B? The answer is a (conditional) yes. First, the distribution (85) can be derived (Brouwer, 1995) from the stochastic S matrix in Eq. (41) under the assumption that the Hamiltonian is a member of the "Lorentzian ensemble" (rather than of the GOE). The Lorentzian ensemble and the GOE have the same eigenvector distribution and the same level-correlation functions in the large N limit (Brouwer, 1995). It is, therefore, extremely likely that the distribution (85) also holds for the stochastic S matrix in Eq. (41) with the Hamiltonian taken from the GOE. This view is supported further by the following facts. For strong absorption ($\langle S_{ab}\rangle = 0$ for all $\{a,b\}$), Eq. (85) reduces to $F(S^{\mathrm{CN}}) = \mathrm{const}$. In other words, the distribution of S-matrix elements is determined entirely by the Haar measure. In

that limit the ensemble (85) agrees, therefore, with Dyson's circular ensemble (Dyson, 1962a). In the Ericson regime, Eq. (85) yields the Hauser-Feshbach formula with an elastic enhancement factor of 2 (Friedman and Mello, 1985). Moreover, for $\Lambda=2$ and $\varepsilon=0$, Eq. (85) agrees (Verbaarschot, 1986) with Eqs. (75)–(77). Further support comes from results for the unitary case (Fyodorov and Sommers, 1997).

All these facts make it seem highly probable that Eq. (85) correctly describes the distribution of S-matrix elements for chaotic scattering. Unfortunately, in the general case of several open channels the expression on the right-hand side of Eq. (85) is so unwieldy that it has not been possible so far to evaluate it. This puts us into the strange situation that we do seem to know the distribution of S-matrix elements without being able to use it. It must also be remembered that the maximum-entropy approach does not yield information on S-matrix correlation functions.

E. Cross-section fluctuations

For the analysis or prediction of cross-section fluctuations, the theoretical results reviewed so far in this section do not suffice. While the third and fourth moments of $S^{\rm fl}(E)$ at fixed energy E are known analytically (Davis and Boosé, 1988, 1989), information on the corresponding correlation functions of $S^{\rm fl}(E)$ does not exist. The problem was addressed by Dietz, Harney, *et al.* (2010). The authors used the available analytical results and information obtained numerically and/or experimentally from microwave billiards (see Sec. VII.A) to investigate cross-section fluctuations and to identify the range of parameters where predictions can safely be made.

We use Eqs. (41)–(43) for $S^{\rm CN}$. The cross-section autocorrelation function $\mathcal{C}_{ab}(\varepsilon)$ is defined as

$$\mathcal{C}_{ab}(\varepsilon)=\langle|S^{\rm CN}_{ab}(E+\varepsilon/2)|^2|S^{\rm CN}_{ab}(E-\varepsilon/2)|^2\rangle - [\langle|S^{\rm CN}_{ab}(E)|^2\rangle]^2. \tag{86}$$

Using Eq. (3) we write $S^{\rm CN}(E)=\langle S^{\rm CN}\rangle+S^{\rm (CNfl)}$. We use the fact [see Eq. (56)] that $\langle S^{\rm CN}\rangle$ is real and obtain

$$\begin{aligned}\mathcal{C}_{ab}(\varepsilon)=2\delta_{ab}\{&|\langle S^{\rm CN}_{aa}\rangle|^2\,{\rm Re}[C^{(2)}_{aa}(\varepsilon)]\\&+\langle S^{\rm CN}_{aa}\rangle{\rm Re}[\langle S^{\rm (CNfl)*}_{aa}(E+\varepsilon/2)|S^{\rm (CNfl)}_{aa}(E-\varepsilon/2)|^2\rangle]\\&+\langle S^{\rm CN}_{aa}\rangle{\rm Re}[\langle S^{\rm (CNfl)*}_{aa}(E-\varepsilon/2)|S^{\rm (CNfl)}_{aa}(E+\varepsilon/2)|^2\rangle]\}\\&+\{\langle|S^{\rm (CNfl)}_{ab}(E+\varepsilon/2)|^2|S^{\rm (CNfl)}_{ab}(E-\varepsilon/2)|^2\rangle\\&-[\langle|S^{\rm (CNfl)}_{ab}|^2\rangle]^2\}.\end{aligned} \tag{87}$$

Here $C^{(2)}_{ab}(\varepsilon)$ is the S-matrix autocorrelation function in Eq. (75) taken at $c=a$, $d=b$. Equation (87) shows that there is a substantial difference between the elastic case ($a=b$) and the inelastic one ($a\neq b$) caused by the fact that $\langle S^{CN}\rangle$ is diagonal. We address the inelastic case first. In the Ericson regime, $S^{\rm (CNfl)}$ is Gaussian, and the autocorrelation function of $|S^{\rm (CNfl)}|^2$ is, therefore, given by the square of the S-matrix correlation function in Eq. (75). However, that relation cannot be expected to hold much outside the Ericson regime because we must expect the cross-section fluctuations (in units of the average cross section) to increase significantly as Γ/d decreases. This expectation is quantitatively confirmed by Dietz, Harney, *et al.* (2010): The autocorrelation function of $|S^{\rm (CNfl)}|^2$ is, at least approximately, given by the square of the S-matrix correlation function in Eq. (75) whenever $S^{\rm (CNfl)}$ possesses a bivariate Gaussian distribution, and that is essentially the case when $\Gamma>d$ or so. For the elastic case ($a=b$) the situation is difficult even in the Ericson regime unless $|\langle S^{CN}_{aa}\rangle|\ll 1$. Indeed, whenever that constraint is violated, the distribution of $S^{\rm (CNfl)}_{aa}$ cannot be Gaussian: Combined with the decomposition $S^{\rm CN}_{aa}=\langle S^{CN}_{aa}\rangle+S^{\rm (CNfl)}_{aa}$, the constraint $|S^{\rm CN}_{aa}|<1$ implied by unitarity forces the distribution of $S^{\rm (CNfl)}_{aa}$ to be skewed. The distortion of the Gaussian distribution grows with decreasing Γ/d and is strongest when the coupling to the channels becomes very small. [Then, $S^{\rm CN}_{aa}$ is dominated by the first term on the right-hand side of Eq. (41).] The terms in the second and third lines of Eq. (87) vanish only if the distribution of $S^{\rm (CNfl)}_{aa}$ is Gaussian so that the phase of $S^{\rm (CNfl)}_{aa}$ is uniformly distributed in the interval $\{0,2\pi\}$. This condition is found to be violated (Dietz, Harney, *et al.*, 2010) already when $\Gamma/d<4$, and a full evaluation of all terms on the right-hand side of Eq. (87) is then necessary.

This is possible with the help of the results of Davis and Boosé (1988, 1989) who calculated analytically the functions

$$\begin{aligned}F^{(4)}_{ab}(\varepsilon)&=\langle[S^{\rm fl*}_{ab}(E+\varepsilon/2)]^2[S^{\rm fl}_{ab}(E-\varepsilon/2)]^2\rangle,\\F^{(3)}_{ab}(\varepsilon)&=\langle S^{\rm fl*}_{ab}(E+\varepsilon/2)[S^{\rm fl}_{ab}(E-\varepsilon/2)]^2\rangle.\end{aligned} \tag{88}$$

We note that for $\varepsilon\neq 0$ these functions differ from the expressions appearing on the right-hand side of Eq. (87). However, numerical simulations and experimental data show (Dietz, Harney, *et al.*, 2010) that for all values of Γ/d the last curly bracket in Eq. (87) [denoted by $C^{(4)}_{ab}(\varepsilon)$] is well approximated by $C^{(4)}_{ab}(0)F^{(4)}_{ab}(\varepsilon)/F^{(4)}_{ab}(0)$ and that similarly we have ${\rm Re}[\langle S^{\rm (CNfl)*}_{aa}(E+\varepsilon/2)|S^{\rm (CNfl)}_{aa}(E-\varepsilon/2)|^2\rangle]\approx F^{(3)}_{aa}(\varepsilon)$. The last relation holds with good accuracy except for the regime $\Gamma\approx d$ of weakly overlapping resonances. With these results, Eq. (87) takes the form

$$\begin{aligned}\mathcal{C}_{ab}(\varepsilon)\approx 2\delta_{ab}(&|\langle S^{\rm CN}_{aa}\rangle|^2\,{\rm Re}[C^{(2)}_{aa}(\varepsilon)]\\&+\{\langle S^{\rm CN}_{aa}\rangle{\rm Re}[F^{(3)}_{ab}(\varepsilon)+F^{(3)}_{ab}(-\varepsilon)]\})\\&+\frac{C^{(4)}_{ab}(0)}{F^{(4)}_{ab}(0)}F^{(4)}_{ab}(\varepsilon).\end{aligned} \tag{89}$$

All terms in Eq. (89) are known analytically. Expressions useful for a numerical computation are given in the Appendix of Dietz, Harney, *et al.* (2010). Thus, from a practical point of view, theoretical expressions for cross-section fluctuations are available for all values of Γ/d except for the elastic case where relation (89) does not hold for $\Gamma\approx d$.

F. Poles of the S matrix

Resonances correspond to poles of the S matrix. The distribution of the poles of the stochastic S matrix defined in Eq. (41) has, therefore, attracted theoretical attention from the beginning. Obvious questions are the following: How is the correlation width (11) related to the distance of the poles from the real axis? Is it possible to verify quantitatively the picture drawn of the pole distribution in Sec. V.B?

It was mentioned in Sec. IV.C that Moldauer (1961, 1963, 1964, 1969, 1975b, 1976, 1980) based his approach to CN scattering on the pole expansion of the S matrix. He seems to have been the first author to determine the distribution of poles numerically (Moldauer, 1964). He made a number of important discoveries that stimulated later research. (i) There exists a gap separating the poles from the real axis. (ii) For strong coupling to the channels, some poles occur far away from the real energy axis (Moldauer, 1975b). (iii) A "sum rule" for resonance reactions [see Moldauer (1969), and references therein] relates the transmission coefficients and the mean distance of the poles from the real axis.

Later work by various authors has led to a deeper understanding of these results. We begin with the "Moldauer-Simonius sum rule for resonance reactions" and follow the derivation due to Simonius (1974). We assume that the unitary S matrix defined in Eq. (41) has N simple poles $\mathcal{E}_\mu$ only. [Coincidence of two poles is considered fortuitous and actually excluded by quadratic repulsion of poles (see below).] Then

$$\det S^{\mathrm{CN}} = \exp\{2i\phi\}\prod_{\mu=1}^{N}\frac{E-\mathcal{E}_\mu^*}{E-\mathcal{E}_\mu}. \tag{90}$$

The denominator on the right-hand side represents the N poles. The form of the numerator follows from the unitarity of S^{CN}: $\det[(S^{\mathrm{CN}})^*]$ is inverse to $\det[S^{\mathrm{CN}}]$. The only energy dependence is due to the poles of S^{CN}, and the phase ϕ is, therefore, constant. With $\mathrm{Im}\,\mathcal{E}_\mu = -(1/2)\Gamma_\mu$ we have

$$\ln\det S^{\mathrm{CN}} - 2i\phi = \sum_\mu \ln\left(1 - i\frac{\Gamma_\mu}{E-\mathcal{E}_\mu}\right). \tag{91}$$

To average Eq. (91) over energy, we use a Lorentzian averaging function with width I (see Sec. V.A) and expand the logarithm in powers of $\Gamma_\mu/(E-\mathcal{E}_\mu)$. Contour integration shows that only the linear term gives a nonvanishing contribution. With $I \gg \Gamma_\mu$ for all μ we find

$$\left\langle \ln\left(1 - i\frac{\Gamma_\mu}{E-\mathcal{E}_\mu}\right)\right\rangle = -i\frac{\Gamma_\mu}{E-\mathrm{Re}(\mathcal{E}_\mu)+iI}. \tag{92}$$

This yields

$$\langle \ln\det S^{\mathrm{CN}}\rangle + \langle \ln(\det S^{\mathrm{CN}})^*\rangle = -2\pi\sum_\mu \frac{\Gamma_\mu(I/\pi)}{[E-\mathrm{Re}(\mathcal{E}_\mu)]^2+I^2} = -2\pi\frac{\langle\Gamma_\mu\rangle}{d}. \tag{93}$$

We use Eq. (58) (i.e., the equality of $\langle \ln\det S^{\mathrm{CN}}\rangle$ and $\ln\det\langle S^{\mathrm{CN}}\rangle$) and the definition (8) and obtain the Moldauer-Simonius sum rule

$$\langle\Gamma_\mu\rangle = -\frac{d}{2\pi}\sum_c \ln(1-T_c). \tag{94}$$

Equation (94) implies $\langle\Gamma_\mu\rangle \geqslant \Gamma$, where Γ is the correlation width given by the Weisskopf estimate (11). Moreover, $\langle\Gamma_\mu\rangle$ diverges whenever a single (or several) transmission coefficients approach unity. The divergence is caused by the fact that one (or several) pole(s) of S^{CN} is (are) shifted far below the real E axis (see Sec. V.B and the text below). In deriving Eq. (94) we have assumed that the averaging interval I is large compared to Γ_μ for all μ. It is not clear from the derivation whether the Moldauer-Simonius sum rule applies as one of the T's approaches unity. However, work on the unitary case using the Gaussian unitary ensemble (GUE) (see Sec. I.II.B) (Fyodorov and Sommers, 1996) and on the single-channel case for the GOE (Sommers *et al.*, 1999) has shown that the distribution of the poles acquires a tail that causes the divergence as $T_c \to 1$.

The locations of the poles of S are given by the eigenvalues of the effective Hamiltonian (46). Sokolov and Zelevinsky (1988, 1989, 1992) used Eq. (46) in an effort to extend statistical spectroscopy (as based on the properties of H^{GOE}) to resonances. Numerical work of Kleinwächter and Rotter (1985) had amplified Moldauer's observation that for large coupling to the channels, one or several poles are located far from the real energy axis. Sokolov and Zelevinsky gave a semiquantitative analytical explanation of that observation summarized in Sec. V.B and showed that, at the same time, the majority of poles move back toward the real axis ("trapped states"). For the single-channel case they derived the distribution of poles in the complex energy plane. They connected the existence of one or several poles far from the real energy axis with the phenomenon of super-radiance (Dicke, 1954) in quantum optics. They showed that the non-Hermitian part of H^{eff} causes quadratic repulsion of the poles in the complex plane and that finding the density of poles of S in the complex energy plane is equivalent to the reconstruction of the two-dimensional charge density from a given electrostatic field.

To determine analytically the joint probability density of the poles in the complex energy plane for the S matrix defined in Eq. (41), two approaches have been taken. If the limit $N \to \infty$ is taken with Λ fixed, terms of order $m = \Lambda/N$ do not contribute to the saddle-point equation, neither in the replica approach (see Sec. VI.B.2) nor in the supersymmetry approach (see Sec. VI.C). A model different from but related to Eq. (41) introduced by Sokolov and Zelevinsky (1988, 1989, 1992) makes it possible to overcome the limitation and to discuss the pole distribution in the framework of the saddle-point approximation. The number Λ of channels is assumed to be large and to go with N to infinity while the ratio $m = \Lambda/N$ is held fixed. The parameters $W_{a\mu}$ describing the coupling of level μ with channel a are taken to be

Gaussian-distributed random variables with mean value zero and common second moment

$$\langle W_{a\mu} W_{b\nu} \rangle = (d\gamma/\pi^2)\delta_{ab}\delta_{\mu\nu}. \tag{95}$$

The Λ channels are all equivalent, and the resulting ensemble of S matrices is invariant with respect to orthogonal transformations of the channel space. The dimensionless strength γ of the coupling is the only parameter. In contrast to the use of H^{GOE} in Eq. (46), the invariance of the distribution of the W's under orthogonal transformations of the channels cannot be deduced from quantum chaos and is, therefore, somewhat arbitrary. Lehmann, Saher, *et al.* (1995) showed, however, that the pole distribution obtained from the model (95) is quite similar to the one where the W's are fixed. The limit $\Lambda \to \infty$ corresponds to the Ericson regime. However, by choosing $\gamma \ll 1$, one can approach the limit of weakly overlapping resonances.

The model (95) was used for an extensive discussion of the distribution of poles of the S matrix in Haake *et al.* (1992) (where the replica trick was used) and in Lehmann, Saher, *et al.* (1995) (where supersymmetry was applied). In both cases, the saddle-point equations differ from those obtained for fixed channel number by terms of order $m=\Lambda/N$. These equations are used to determine the average pole distribution in the complex energy plane with the help of an electrostatic analogy similar to the one mentioned above. Analytic expressions are obtained for the boundary curve separating the area of nonvanishing pole density from the empty one. Typical results are shown in Fig. 5, see text below.

As mentioned above, Moldauer discovered a gap separating the poles of S from the real energy axis. Later, Gaspard and Rice (1989a, 1989b) deduced the existence of a gap in the framework of the semiclassical approximation for chaotic systems with few degrees of freedom. This suggests that the gap is a universal feature of chaotic scattering. For the model of Eq. (95), the gap was shown to exist and the gap parameters were worked out analytically in Haake *et al.* (1992) and Lehmann, Saher, *et al.* (1995). In the center of the GOE semicircle, the width $\Gamma_{\mathrm{gap}}/2$ of the gap separating the cloud of poles and the real axis is given by (Lehmann, Saher, *et al.*, 1995)

$$\Gamma_{\mathrm{gap}} = \frac{d}{2\pi}\Lambda\frac{4\gamma}{1+\gamma^2}. \tag{96}$$

Using Eq. (59) and $x_a=\gamma$ we can write the right-hand side as $[d/(2\pi)]\Sigma_c T_c$. This is the Weisskopf estimate. In Lehmann, Saher, *et al.* (1995) the S-matrix correlation width for the model of Eq. (95) was also worked out and found to coincide with the one found in the framework of Eq. (41) (fixed number of channels), i.e., with the Weisskopf estimate. For the model of Eq. (95), the equality of gap width and Weisskopf estimate holds unless m approaches unity. Then, the correlation width becomes comparable to and is modified by the range of the GOE spectrum. Put differently and positively, the result implies that S-matrix fluctuations are universal as long as there is a clear separation of the two energy scales, the gap width, and the range of the GOE spectrum.

The joint probability density of the poles of S in the complex plane can be obtained from the above-mentioned algebraic equations. With $\mathrm{Re}(E)/\lambda=x$, $\mathrm{Im}(E)/\lambda=y$, Fig. 5 shows the distribution below the real E axis. The single cloud seen for $\gamma=0.2$ and for $\gamma=1$ splits into two as γ is increased further. The separation begins to develop at $\gamma=1$. From the Moldauer-Simonius sum rule, we would expect that many poles move to $-i\infty$ as γ approaches unity. This is not seen in the figure. We ascribe the discrepancy to the assumption (used in the derivation of the sum rule) that the entire energy dependence of S^{CN} is due to the poles [see Eq. (90)]. This assumption fails when the widths of the resonances become comparable with the range of the GOE spectrum.

The second approach (Fyodorov, Khoruzhenko, and Sommers, 1997; Fyodorov and Khoruzhenko, 1999; Fyodorov and Sommers, 2003) takes the limit $N \to \infty$ for fixed channel number Λ and arbitrary values of the transmission coefficients T_c ("almost Hermitian matrices"). For the unitary case (GUE Hamiltonian) it yields the complete joint probability density of the eigenvalues of the effective Hamiltonian in Eq. (43). Corresponding results for the GOE are not known except for the single-channel case $\Lambda=1$ (Ullah, 1969; Sokolov and Zelevinsky, 1989).

The first experimental study (Kuhl *et al.*, 2008) of the distribution of poles of the scattering matrix in the complex energy plane employed a microwave resonator and the method of harmonic analysis (see also Sec. VII.B). The results agree with theoretical predictions (Sommers *et al.*, 1999).

In summary, the distribution of the poles of S^{CN} in the complex energy plane gives valuable insight into the scattering mechanism even though the information is not sufficient to construct the scattering amplitude(s). The Moldauer-Simonius sum rule shows that, in general, the average distance of the poles from the real axis is bigger than would be concluded from the Weisskopf estimate (11). With increasing coupling to the channels, up to Λ poles are moved ever further away from the real axis, a fact related to super-radiance in quantum optics. An example for the actual distribution of poles in the regime of many strongly coupled channels ($N \to \infty$, $\Lambda \to \infty$, and $m=\Lambda/N$ fixed) is shown in Fig 5. A gap separates the cloud of poles from the real E axis. The width of the gap is given by the Weisskopf estimate. The regime of almost Hermitian matrices has also been worked out.

Unfortunately, the information available on the distribution of poles of the S matrix in the complex energy plane is not sufficient to draw conclusions on the energy dependence of $S(E)$. It might be tempting, for instance, to identify $\langle \Gamma_\mu \rangle$ as given by Eq. (94) with the width Γ of the S-matrix autocorrelation function. But that would be incorrect (Moldauer, 1975a; Brody *et al.*, 1981). In the framework of the two-body random ensemble (see Secs. VI.G and I.V.B) this fact was demonstrated by Celardo

et al. (2007). A systematic study of the relationship between Γ, $\langle\Gamma_\mu\rangle$, and the Weisskopf estimate in Eq. (11) was given by Dietz, Richter, and Weidenmüller (2010). For the case of a single channel and $T\approx 1$, Eq. (94) yields $\langle\Gamma_\mu\rangle \gg d$ while a calculation of the S-matrix autocorrelation function from Eqs. (75)–(77) with $\Lambda=1$ and $T=1$ yields $\Gamma\approx 0.3d$, in rough agreement with the Weisskopf estimate in Eq. (11). This shows that in the single-channel case we always deal with isolated resonances. Similarly, for two or three channels, all with $T\approx 1$, Eq. (94) yields $\langle\Gamma_\mu\rangle \gg d$ while Eqs. (75)–(77) show that one barely reaches the case of weakly overlapping resonances in that case. It is found that the Weisskopf estimate provides a good estimate for the S-matrix correlation width Γ in all cases.

To draw valid conclusions on the energy dependence of $S(E)$ from the distribution of the poles of $S(E)$ one needs, in addition to the location of the poles of $S(E)$, also information on the residues. Such information is presently available only to a limited extent mainly for the unitary case (Frahm *et al.*, 2000; Schomerus *et al.*, 2000). Let $\gamma_{\mu c}\gamma^*_{\mu c'}$ denote the residue of the complex pole labeled μ with width Γ_μ of $S_{cc'}$. For nonisolated resonances relation (19) is replaced by $\Sigma_c|\gamma_{\mu c}|^2=\sqrt{K_\mu}\Gamma_\mu$. The dependence of the statistical properties of the "Petermann factor" K_μ on the number of channels has been determined (Frahm *et al.*, 2000; Schomerus *et al.*, 2000).

G. Correlations of *S*-matrix elements carrying different quantum numbers

We return to the question raised in the last paragraph of Sec. IV.B: Is assumption (5) justified that S-matrix elements carrying different quantum numbers are uncorrelated?

While RMT *per se* is obviously not in a position to give an answer to that question, a realistic large-scale shell-model calculation would. We have in mind a calculation using the two-body random ensemble (TBRE) of the nuclear shell model. The TBRE was introduced in Sec. I.V.B where details and references to the original papers may be found. In the TBRE, several neutrons and protons occupy the single-particle states of a major shell of the shell model and interact via a two-body interaction. The matrix elements of the interaction are taken to be Gaussian-distributed random variables. Spin is a good quantum number, and the need to couple nucleon angular momenta and spins to good total spin creates considerable complexity. Matrix elements of S carrying different spin quantum numbers have to be calculated numerically for different realizations of the TBRE, and their correlations worked out. For reasons given below, the dimensions of the underlying shell-model spaces would have to be very large. We are not aware of any such calculation.

However, in the conclusions of Papenbrock and Weidenmüller (2007) the authors argued that for sufficiently large shell-model spaces, the correlations between S-matrix elements carrying different quantum numbers might be very weak. The arguments are based on the study of a model (Papenbrock and Weidenmüller, 2008) that is conceptually close to but technically simpler than the TBRE and, therefore, analytically accessible. In the model parity is the only quantum number, and m spinless fermions occupy ℓ_1 (ℓ_2) degenerate single-particle states with positive (negative) parity. The fermions interact via a parity-conserving two-body interaction with random Gaussian-distributed uncorrelated two-body matrix elements. The nth moments $\mathcal{M}_n(\pm)$ of the Hamiltonian H of the model (defined as normalized traces of H^n with positive integer n) can be worked out analytically for the many-body states of both positive ($+$) and negative ($-$) parities. The case of large matrix dimension is attained in the "dilute limit" defined by $\ell_1,\ell_2,m\to\infty$, $m/\ell_1\to 0$, and $m/\ell_2\to 0$. It is shown that $\mathcal{M}_n(+)=\mathcal{M}_n(-)$ for all n up to a maximum value that is bounded from above by m but tends to ∞ in the dilute limit and the two moments differ ever more strongly when n grows beyond that bound. This result shows that the spectra of states with positive and negative parity are strongly correlated. In particular, the shapes of the two average spectra are extremely similar. At the same time, the result suggests that the local spectral fluctuations of the two spectra are uncorrelated. Indeed, in their work on the use of moments for nuclear spectroscopy, French and collaborators concluded that such fluctuations are determined by the very highest moments of the Hamiltonian (Brody *et al.*, 1981).

The results just stated apply in the dilute limit only. They do not contradict earlier findings (Papenbrock and Weidenmüller, 2007) for the TBRE on correlations between spectra carrying different quantum numbers. These calculations involved Hilbert spaces of small dimension only.

Assuming that a result similar to the one just stated holds in the limit of large matrix dimension for the TBRE and observing that the fluctuation properties of the S matrix are caused by the local spectral fluctuation properties of the underlying Hamiltonian [see Eqs. (28) and (29)], we conclude that, within the framework of the nuclear shell model, S-matrix elements carrying different quantum numbers are likely to be uncorrelated, in agreement with Eq. (5).

VII. TESTS AND APPLICATIONS OF THE STATISTICAL THEORY

The statistical theory reviewed in Secs. V and VI has been tested thoroughly. Moreover, it has found numerous applications both within the realm of nuclear physics and beyond. In this section we review some recent such tests and applications.

A. Isolated and weakly overlapping CN resonances

In the regime of isolated resonances, thorough tests of the statistical theory of nuclear reactions ($\Gamma \ll d$) were

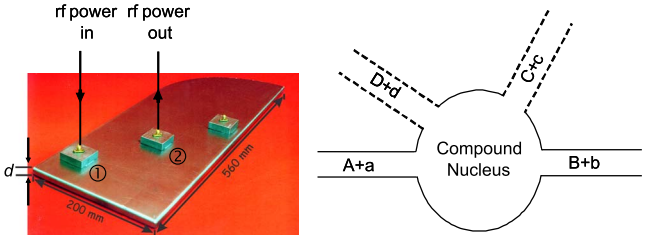

FIG. 6. (Color online) Flat microwave resonator (left-hand side) as a model for the compound nucleus (right-hand side). The height $d=0.84$ cm of the flat resonator makes it a chaotic quantum billiard up to a frequency of 18.75 GHz.

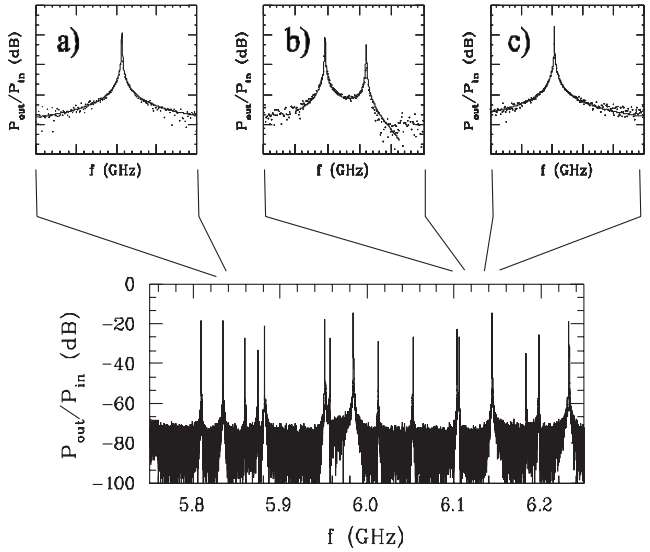

FIG. 7. Part of the transmission spectrum of a superconducting microwave billiard. We note the extremely high resolution of the resonances. Two singlets (a) and (c) and a doublet (b) of resonances are magnified in the upper part. For all three cases R-matrix resonance formulas (Beck *et al.*, 2003) based on expressions from Lane and Thomas (1958) were fitted to the data. From Dembowski *et al.*, 2005.

undertaken already many years ago. Especially for neutron resonances there exists a comprehensive review (Lynn, 1968). In the regime of weakly overlapping resonances, tests have so far not been performed in nuclei. Here we do not summarize the early works but rather focus attention on recent data and tests of the theory. These have become possible in microwave billiards (Dietz *et al.*, 2008). Such devices simulate the CN and its resonances or, for that matter, any other chaotic quantum-scattering system. Indeed, in sufficiently flat microwave resonators and for sufficiently low values of the radio frequency (rf)—the so-called quantum billiards—only one vertical mode of the electric field is excited, and the Helmholtz equation is mathematically equivalent to the Schrödinger equation for a two-dimensional quantum billiard (Stöckmann and Stein, 1990; Sridhar, 1991; Gräf *et al.*, 1992; So *et al.*, 1995; Richter, 1999; Stöckmann, 2000). If the classical dynamics (free motion within the microwave resonator and elastic scattering by its boundary) is chaotic, the statistical properties of the eigenvalues and eigenfunctions of the closed resonator in the quantum case follow RMT predictions (Bohigas *et al.*, 1984; Heusler *et al.*, 2007), and the scattering of rf amplitudes by the resonator corresponds to quantum chaotic scattering.

The left-hand side of Fig. 6 shows a typical quantum billiard realized in the form of a flat microwave resonator. For the measurement of the spectrum, rf power is coupled via an antenna labeled 1 into the resonator, thereby exciting an electric field mode within the resonator, and the reflected output signal at the same antenna (or the transmitted one at the antenna labeled 2) is determined in magnitude and phase in relation to the input signal. Hence, the resonator is an open scattering system where the antennas act as single scattering channels. The scattering process is analogous to that of a CN reaction as indicated schematically on the right-hand side of Fig. 6. The incident channel $A+a$ consists of a target nucleus A bombarded by a projectile a, leading to a compound nucleus which eventually decays after some time into the channel with the residual nucleus B and the outgoing particle b. (We disregard angular momentum and spin.) Attaching more antennas to the resonator (or dissipating microwave power in its walls) corresponds to more open channels $C+c$, $D+d$,… of the compound nucleus. The resonator in Fig. 6 has the shape of a so-called Bunimovich stadium billiard which is known to be fully chaotic in the classical limit (Bunimovich, 1985).

The resonator in Fig. 6 was made of niobium and operated in a superconducting mode. This strongly increases the quality factor of the resonator and yields very high resolution. The resonator was used for both the study of spectral properties, i.e., the statistics of the resonances in the cavity (Gräf *et al.*, 1992), and a measurement of their decay widths (Alt *et al.*, 1995). The latter are proportional to the square of the billiard eigenfunctions at the locations of the antennas. Figure 7 shows a transmission spectrum. Spectra of that quality can be typically obtained in superconducting billiards in the regime of isolated and weakly overlapping resonances. The measured ratio of $P_{\text{out},b}$, the rf power signal transmitted into antenna b, and $P_{\text{in},a}$, the incoming rf power signal at antenna a, is shown on a semilogarithmic plot. The ratio is equal to $|S_{ab}(f)|^2$, where $S_{ab}(f)$ with $a,b=1,2$ are the elements of the complex-valued frequency-dependent 2×2 scattering matrix S. More generally, measurements of the modulus and phase of the outgoing and incoming signals performed with a network vector analyzer determine magnitude and phase of all elements $S_{ab}(f)$ of S. Such detailed information is not usually available for other chaotic scattering systems where, in general, one can only measure intensities. For a number of isolated resonances labeled μ with $\mu=1,\ldots,N$ without any background scattering, the S matrix is a sum of Breit-Wigner terms,

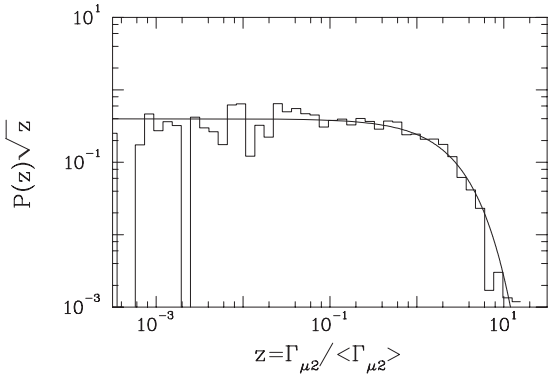

FIG. 8. The experimental distribution of the partial widths $\Gamma_{\mu 2}$ in units of their mean value $\langle\Gamma_{\mu 2}\rangle$. The solid line corresponds to a Porter-Thomas distribution. From Alt *et al.*, 1995.

$$S_{ab} = \delta_{ab} - i\sum_{\mu} \frac{\Gamma_{\mu a}^{1/2}\Gamma_{\mu b}^{1/2}}{f - f_{\mu} + (i/2)\Gamma_{\mu}}. \tag{97}$$

Here f_{μ} and Γ_{μ} are the real and imaginary parts of the eigenvalues of an effective Hamiltonian $\hat{H}_{\rm eff}=\hat{H}-i\pi\hat{W}\hat{W}^{\dagger}$ for the microwave billiard in which the $\hat{W}$'s denote the coupling of the resonator states to the antenna states and the walls of the billiard (see Sec. IV.A.2). With $\sqrt{2\pi}\tilde{W}_{a\mu}^{(0)}\to\Gamma_{a\mu}^{1/2}$, Eq. (97) is completely equivalent to Eq. (31) which describes the coupling of isolated nuclear quasibound states to the channels.

As discussed below Eq. (31) the partial width amplitude $\Gamma_{\mu a}^{1/2}$ is the probability amplitude for decay of resonance μ into channel a, and $\Gamma_{\mu}=\Sigma_a\Gamma_{\mu a}$ is the total width. In an experiment with the superconducting quantum billiard (shown on the left-hand side of Fig. 6) coupled to three antennas $c=1,2,3$ (corresponding to a CN reaction with three open channels), the complete set of resonance parameters (resonance energies, partial widths, and total widths) for 950 resonances was measured (Alt *et al.*, 1995). The total widths Γ_{μ} and the partial widths $\Gamma_{\mu 2}$ are found to fluctuate randomly about a slow secular variation with μ, i.e., with frequency. The GOE predicts a Gaussian distribution for the decay amplitudes $\Gamma_{\mu c}^{1/2}$ or, equivalently, a χ^2 distribution with one degree of freedom, the Porter-Thomas distribution [(Porter and Thomas, 1956); see Eq. (I.18)]. The distribution of $\Gamma_{\mu 2}$ in Fig. 8 exhibits this behavior impressively.

As a further test of the statistical theory, the autocorrelation function of the S matrix of the cavity, defined as $C_c(\varepsilon)=\langle S_{cc}(f)S_{cc}^{*}(\varepsilon+f)\rangle-|\langle S_{cc}(f)\rangle|^2$, was determined for channels $c=1$, 2, and 3. The average is taken over frequency. For $c=2$ the result is plotted as circles in the upper part of Fig. 9. The shaded band is a measure of the experimental uncertainty of $C_2(\varepsilon)$. The shape of the shaded band differs markedly but not unexpectedly (Lewenkopf and Weidenmüller, 1991) from that of a Lorentzian with width $\langle\Gamma_{\mu}\rangle$ shown as a solid line in the upper part of Fig. 9. The contribution of each of the over 900 individual resonances in Fig. 9 is, of course, Lorentzian in shape with width Γ_{μ}. However, different resonances

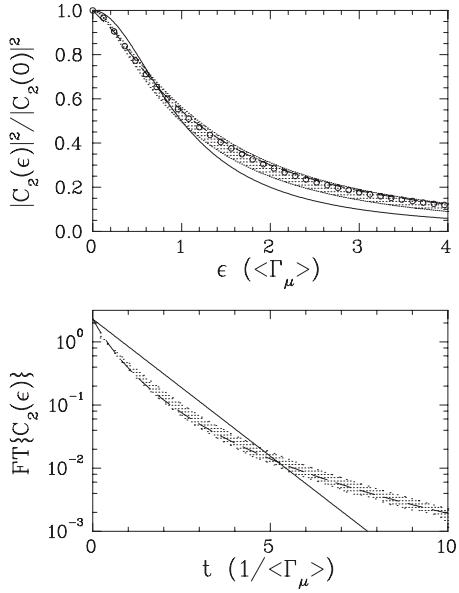

FIG. 9. Autocorrelation function for isolated resonances. Upper part: The experimental autocorrelation function $|C_2(\varepsilon)|^2$ (circles within the shaded band of errors), the prediction of the statistical theory (dashed line), and a Lorentzian (solid line). Lower part: Fourier coefficients of the autocorrelation function (dots) with errors indicated by the shaded band together with the prediction of the statistical theory (dashed line) and an exponential (Fourier transform of a Lorentzian). The nonexponential decay in time of the Fourier transform of the S-matrix autocorrelation functions is clearly visible. From Alt *et al.*, 1995.

have different widths, and the average over all resonances is not a Lorentzian. This happens only when the total widths Γ_{μ} fluctuate strongly with μ. Thus, both the number of open channels and the absorption in the walls of the microwave billiard (also contained in Γ_{μ}) must be small. Both conditions can be satisfied in experiments with superconducting microwave resonators but generally not in experiments at room temperature. [In the microwave experiment of Doron *et al.* (1990), for instance, absorption was strong and consequently the data did not display a non-Lorentzian line shape (Lewenkopf *et al.*, 1992).] Clearly, the observed non-Lorentzian shape is a quantum phenomenon: In the semiclassical approximation, i.e., for many open channels, we have purely exponential decay. The result displayed in the upper part of Fig. 9 is in quantitative agreement with the statistical theory, i.e., with Eqs. (75)–(77).

The Fourier transform (FT) of the autocorrelation function $C_2(\varepsilon)$ shown in the lower part of Fig. 9 decays nonexponentially as a function of time. This feature too reflects the non-Lorentzian shape of the autocorrelation function shown in the upper part of Fig. 9 and is in agreement with the statistical model. We refer to the discussion in the paragraph following Eq. (81). One may say that in the experiment nonexponential decay of a quantum system with chaotic dynamics has been "observed" for the first time.

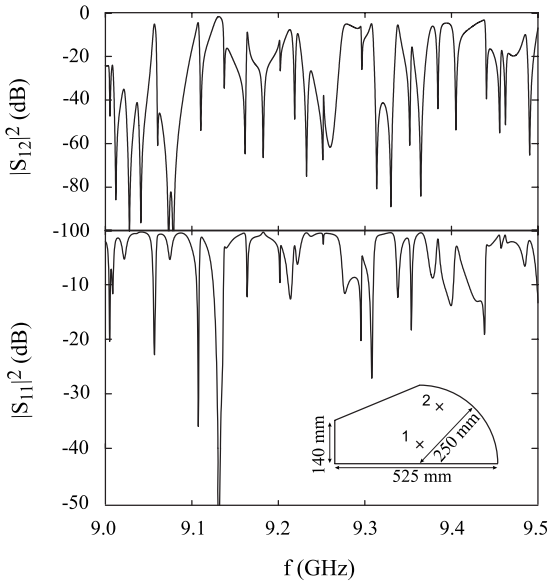

FIG. 10. Intensity measurements in microwave cavities. Transmitted (upper part) and reflected (lower part) intensity vs frequency between 9.0 and 9.5 GHz. The resonances overlap and create a fluctuation pattern. The shape of the two-dimensional quantum billiard used in the experiment is shown in the inset. Points 1 and 2 indicate the positions of the antennas. From Dietz *et al.*, 2008.

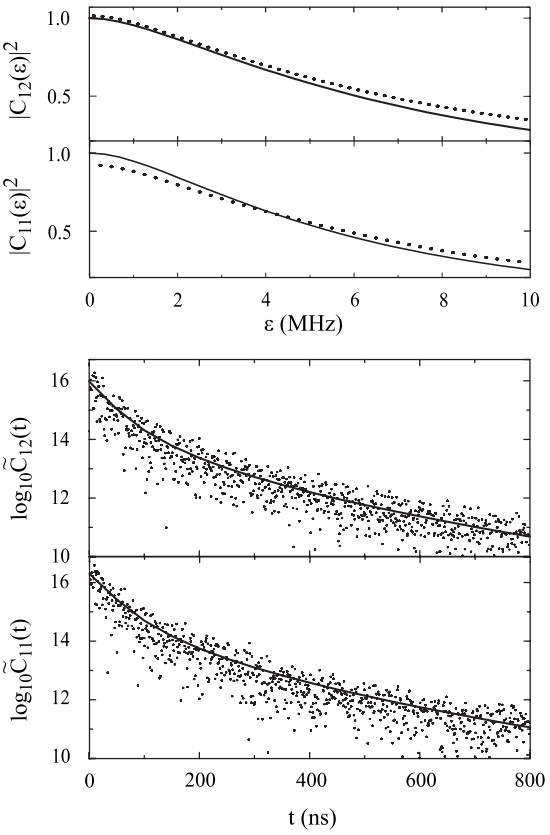

FIG. 11. Autocorrelation function for weakly overlapping resonances. Upper part: The autocorrelation function $|C_{ab}(\varepsilon)|^2$ for values of a and b as indicated. The values of $|C_{ab}(\varepsilon)|^2$ were calculated from the measured S-matrix elements (points) and from the fit of Eq. (75) of the statistical theory to the data (solid line). Lower part: Fourier coefficients $\tilde{C}_{ab}(t)$ of the autocorrelation function (points) and the Fourier transform of the fit of $C_{ab}(\varepsilon)$ [Eq. (75)] to the data (solid line). The nonexponential decay in time in the region of weakly overlapping resonances ($\Gamma/d \approx 0.2$) is striking. From Dietz *et al.*, 2008.

A thorough experimental investigation of chaotic scattering in microwave billiards has recently also been performed in the regime of weakly overlapping resonances ($\Gamma \lesssim d$), and the results have been analyzed with the help of the formulas of Sec. VI.C. A normally conducting flat microwave resonator made of copper was used as a quantum billiard (Dietz *et al.*, 2008). The resonator shown in the inset of Fig. 10 has the shape of a tilted stadium (Primack and Smilansky, 1994). The stadium has fully chaotic classical dynamics. The resonator carried two antennas, and the complex elements of the symmetric scattering matrix $S_{ab}(f)$ were measured versus frequency. Figure 10 shows examples of the measured transmission ($|S_{12}|^2$) and reflection ($|S_{11}|^2$) intensities as functions of resonance frequency. We note the strong fluctuations of both quantities with frequency.

As in the case of isolated resonances the S-matrix autocorrelation function $C_{ab}=\langle S_{ab}(f)S^*_{ab}(f+\varepsilon)\rangle - |\langle S_{ab}\rangle|^2$ for $a,b=1$ or 2 was computed from the data. The upper part of Fig. 11 shows that the values of the scattering matrix $S_{ab}(f)$ are correlated with a correlation width Γ of order several MHz. The values of $S_{ab}(f)$ measured at M equidistant frequencies with step width Δ have been Fourier transformed. The complex Fourier coefficients are denoted by $\tilde{S}_{ab}(t)$ with $t \geqslant 0$. We use the discrete time interval $t=d/M\Delta$ elapsed after excitation of the billiard resonator instead of the Fourier index k. The Fourier transform $\tilde{C}_{ab}(t)$ of $C_{ab}(\varepsilon)$ has Fourier coefficients $|\tilde{S}_{ab}(t)|^2$ and any two coefficients are uncorrelated random variables (Ericson, 1965). The lower part of Fig. 11 shows data for $\log_{10}\tilde{C}_{ab}(t)$. We note that the Fourier coefficients scatter over more than five orders of magnitude. The cutoff at $t=800$ ns is due to noise. The decay in time is strikingly nonexponential, i.e., powerlike, as for isolated resonances (Fig. 9).

The solid lines in Fig. 11 result from fitting Eqs. (75)–(77) of the statistical theory to the data points. The parameters in Eqs. (75)–(77) for the S-matrix autocorrelation function $C_{ab}(\varepsilon)$ are the transmission coefficients T_a with $a=1,2$ for the open antenna channels, T_c, with $c=3,4,\ldots$ for additional fictitious channels modeling Ohmic absorption (Schäfer *et al.*, 2003) in the walls of the normally conducting resonator and the average level spacing d. For $a=1,2$ the transmission coefficients were calculated from $T_a=1-|\langle S_{aa}\rangle|^2$ with data on S_{aa} as input. The average level spacing d was calculated from the Weyl formula (Baltes and Hilf, 1976). The product in Eq. (75) over the ficticious channels was replaced by an exponential function of the sum $\tau_{\rm abs}$ of the transmission coefficients of these channels. This is a good approxima-

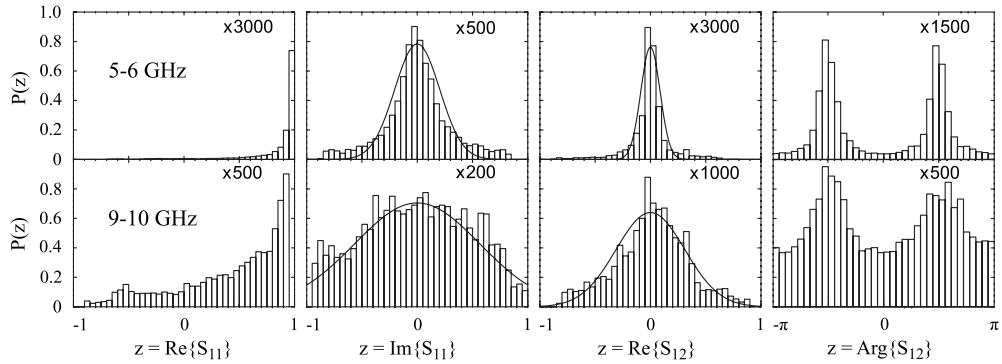

FIG. 12. Distribution of scattering amplitudes. From left to right: Histograms for the scaled distributions of the real and imaginary parts of the reflection amplitude S_{11} and the real part and the phase of the transmission amplitude S_{12}, respectively. The data were taken in the two frequency intervals 5–6 GHz (upper panels) and 9–10 GHz (lower panels). The scaling factors are given in each panel. The solid lines are best fits to Gaussian distributions. From Dietz *et al.*, 2008.

tion when all $T_c \ll 1$ and left $\tau_{\rm abs}$ as the only free parameter in the fit. In order to allow for secular variations of $\tau_{\rm abs}$ the experimental data were analyzed in 1 GHz intervals. It was found that the sum $T_1+T_2+\tau_{\rm abs}$ increases from the value 0.11 in the interval 3–4 GHz to the value 1.15 in the interval 9–10 GHz. (The resulting increase of $\tau_{\rm abs}$ is consistent with conductance properties of copper.) Using these numbers and the Weisskopf estimate $\Gamma \approx (d/2\pi)\Sigma_c T_c$ of Eq. (11) for the correlation width Γ one finds that Γ/d increases from 0.02 to 0.2 over the same frequency range. Thus, the statistical theory of chaotic scattering was indeed experimentally tested in the regime of weakly overlapping resonances. The Fourier coefficients turn out to be uncorrelated, Gaussian-distributed random variables. This fact and the large number of such coefficients (2400 per frequency interval) made it possible to assess the quality of the agreement between data and the fits in terms of a goodness-of-fit test with excellent results (Dietz *et al.*, 2008).

The experiment of Dietz *et al.* (2008) has produced interesting results also on the distribution of moduli and phases of S-matrix elements (see Sec. VI.D) and the elastic enhancement factor (see Secs. VI.A and VI.B.1). Concerning the first point, we expect theoretically that for $\Gamma \ll d$ the distribution of S-matrix elements is non-Gaussian. This is because unitarity constrains the distribution of S-matrix elements. The constraints are strongest for $\Gamma \ll d$ (see Sec. VI.E). Figure 12 shows that the distribution of the real part of S_{11} is strongly peaked near unity, especially for the lower frequency interval from 5 to 6 GHz in which mostly isolated resonances are found. But even in the regime of weakly overlapping resonances, i.e., from 9 to 10 GHz, the distributions of the real and imaginary parts of S_{11} deviate from Gaussians (solid lines). The distributions of the phases (rightmost panels in Fig. 12) are peaked. However, the valley between the two peaks fills up as Γ/d increases. For $\Gamma/d \gg 1$, i.e., in the Ericson regime, the phases are expected to be uniformly distributed and the S-matrix elements to be Gaussian distributed. The elastic enhancement factor, defined as $W=(\langle|S_{11}^{\rm fl}|^2\rangle\langle|S_{22}^{\rm fl}|^2\rangle)^{1/2}/\langle|S_{12}^{\rm fl}|^2\rangle$, is determined from the data as a function of f in two ways. One may use either the autocorrelation functions (Fig. 11) or the widths of the distributions of the imaginary parts of the scattering matrix. Both results agree and yield a smooth decrease of W with f from $W \approx 3.5 \pm 0.7$ for $4 \leqslant f \leqslant 5$ GHz to $W \approx 2.0 \pm 0.7$ for $9 \leqslant f \leqslant 10$ GHz, the errors being finite-range-of-data errors. The calculation of the enhancement factor using Eqs. (75)–(77) gives the values $W=2.8$ and 2.2 for the respective frequency intervals. We return to the determination of W once more in Sec. VIII.C below.

In summary, we have reviewed in this section how a wealth of very precise experimental data on chaotic quantum billiards that mimic the CN and its resonances can be used for a stringent test of the theory of quantum chaotic scattering. Measurements of the phases of the scattering matrix elements provide valuable additional information that is usually not accessible in CN reactions. In the work of Alt *et al.* (1995) on the statistics of partial widths of isolated resonances ($\Gamma \ll d$), all tests applied—the Porter-Thomas distribution, the lack of correlations between partial widths in different scattering channels, the lack of correlations between partial widths and resonance frequencies, the non-Lorentzian decay of the S-matrix autocorrelation function, and the related nonexponential time decay of the chaotic quantum system—are in perfect agreement with GOE predictions for the statistics of eigenfunctions and eigenvalues. In a continuation of this work by Dietz *et al.* (2008) into the regime of weakly overlapping resonances ($\Gamma \approx d$), the distributions of S-matrix elements are found to be non-Gaussian while the Fourier coefficients of these S-matrix elements do have an approximately Gaussian distribution. These data were used for a highly sensitive test of the statistical theory reviewed in Secs. V and VI. In particular, the predicted nonexponential decay in time of isolated and weakly overlapping resonances and the values of the elastic enhancement factors are confirmed. The evidence for nonexponential decay in time, obtained by Fourier-transforming measured S-matrix elements into time space, is still indirect. A direct mea-

surement of the decay time of an excited nucleus might become possible at high-power laser facilities such as the National Ignition Facility where all nuclear resonances (or subsets of them) might be excited simultaneously by a short laser pulse (Moses *et al.*, 2009, Dietz and Weidenmüller, 2010).

B. Strongly overlapping CN resonances: Ericson fluctuations

In the 1960s and 1970s, the newly discovered phenomenon of Ericson fluctuations formed a central part of research in nuclear reactions (see Sec. III.B). Protons, deuterons, and light ions up to oxygen or so and also fast neutrons have been used as projectiles in various CN reactions. The field has been reviewed early (Ericson and Mayer-Kuckuk, 1966) and again later (Richter, 1974). Both articles showed that all of Ericson's predictions were confirmed experimentally. We do not reiterate here what has been known for many years about the cross-section autocorrelation functions, their Lorentzian shape, the mean coherence width Γ, the vanishing of cross-correlation functions between cross sections in different reaction channels in the absence of direct reaction contributions, the Hanbury Brown–Twiss behavior of cross-correlation functions of cross sections measured at different scattering angles, the probability distributions of randomly fluctuating cross sections, and about the interplay between direct and CN reaction processes in general. From the few experiments performed lately in nuclear physics, two are chosen to exemplify over and above what has been stated in Sec. II.D why Ericson fluctuations are now commonly viewed as a paradigm for chaotic behavior of a quantum system.

Recently, a number of mainly neutron-induced CN reactions on medium-heavy nuclei has been studied in the Ericson regime primarily in order to deduce nuclear level densities from the data (Grimes, 2000, and references therein). A striking example, the excitation function for the reaction $^{28}\mathrm{Si}(n,p_{0+1})^{28}\mathrm{Al}$, is shown in Fig. 13 (Bateman *et al.*, 1997). Decay of the CN ^{29}Si populates the ground state and the first-excited state of the final odd-odd nucleus ^{28}Al. The two proton channels p_{0+1} are not resolved. The high-resolution measurement of the CN cross section reveals significant fluctuations with energy. The peaks and minima of the excitation function are not caused by individual, more or less isolated resonances, but instead result from the constructive (or destructive) superposition of many overlapping CN resonances. The amplitudes of the resonances are random variables. Therefore, the curve connecting the measured points in Fig. 13 has the curious feature of being both reproducible and random (Weidenmüller, 1990). A measurement of the same reaction in the same energy interval with the same energy resolution will reproduce Fig. 13. Nonetheless, the energy dependence of the cross section in the figure displays the features of a random process.

The second example for the role of Ericson fluctuations in nuclei is from the field of giant resonances where the question of direct versus statistical decay

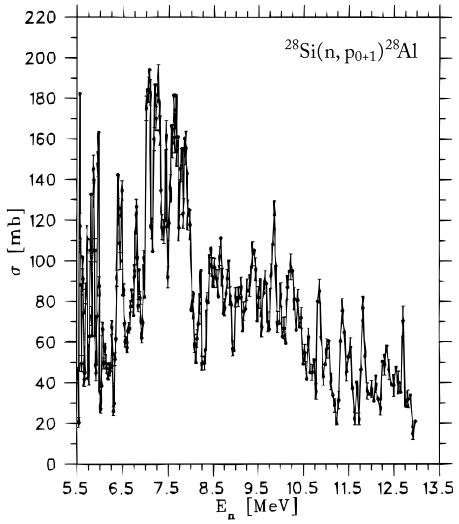

FIG. 13. Fluctuating excitation function of the reaction $^{28}\mathrm{Si}(n,p_{0+1})^{28}\mathrm{Al}$ in the regime of strongly overlapping resonances ($\Gamma \gg d$) for the CN ^{29}Si. The cross sections of proton exit channels p_0 and p_1 leading to the ground and first-excited states in ^{28}Al, respectively, were not resolved. From Bateman *et al.*, 1997.

plays a central role (Bortignon *et al.*, 1998; Harakeh and van der Woude, 2001). The giant resonance is a "distinct" and "simple" mode of excitation of the nuclear ground state whose amplitude is usually spread over many "complicated" states for which the distinct mode acts as a "doorway." The strength function is typically of Breit-Wigner shape (Bohr and Mottelson, 1969). Doorway states were reviewed in Sec. I.II.G. To describe the approach, we have to distinguish several contributions to the total width Γ_0 of the giant resonance. In good approximation (Goeke and Speth, 1982) Γ_0 can be written as $\Gamma_0=\Delta\Gamma+\Gamma^{\uparrow}+\Gamma^{\downarrow}$. Here $\Delta\Gamma$ stands for the Landau damping of the giant resonance. [Electric dipole excitation of the ground state in the first step produces a coherent superposition of one particle–one hole (1p-1h) states that have different single-particle energies.] The 1p-1h states, in turn, couple to the continuum and acquire an escape width $\Gamma^{\uparrow}$ which gives rise to a direct decay contribution into dominant hole states of the daughter nucleus. Finally, $\Gamma^{\downarrow}$ describes the spreading width resulting from mixing the 1p-1h states with more complex 2p-2h and further np-nh configurations until an equilibrated compound nucleus is reached. A primary goal of all giant-resonance high-resolution decay experiments is, thus, to determine the relative contributions of the widths $\Gamma^{\uparrow}$ and $\Gamma^{\downarrow}$ to the total width Γ_0. The experimental signature of direct nuclear decay of a giant resonance in a nucleus with mass number A is the enhanced population of hole states in the daughter nucleus $A-1$. Statistical decay can be identified either by a comparison of the measured decay spectrum with predictions of the Hauser-Feshbach formula (10) or by an Ericson-fluctuation analysis of the fine structure in the decay spectrum measured with high resolution. Here we address the second possibility.

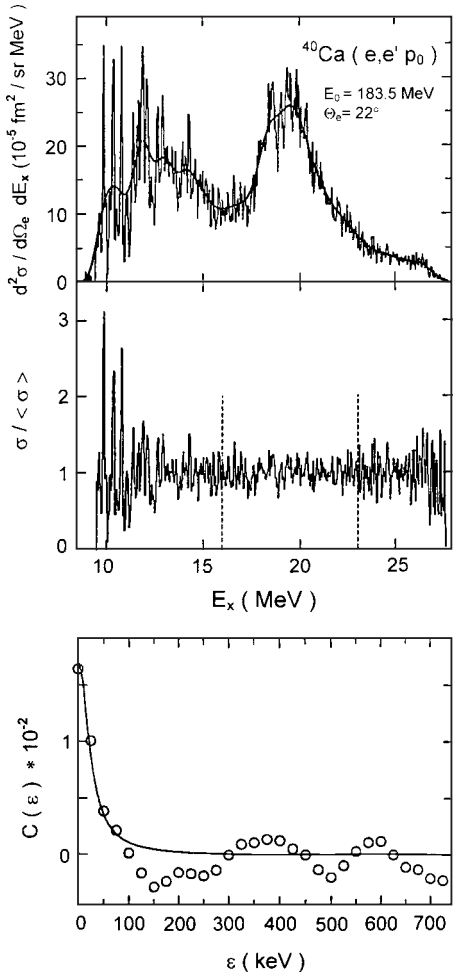

FIG. 14. Ericson fluctuations in the giant dipole resonance. Upper part: Double differential cross section of the ^{40}Ca$(e,e'p_0)$ reaction at an electron energy E_0=183.5 MeV. Middle part: Ratio of the measured cross section and the smoothed cross section. Lower part: Autocorrelation function. From Carter *et al.*, 2001.

Giant-resonance spectroscopy of ^{40}Ca has recently been performed through exclusive electroexcitation experiments of the type ^{40}Ca$(e,e'x)$, where x stands for either protons or alpha particles detected in coincidence with the scattered electron (Carter *et al.*, 2001; Diesener, Helm, Huck, *et al.*, 2001; Diesener, Helm, von Neumann-Cosel, *et al.*, 2001). The description of the $(e,e'x)$ reaction is based on the one-photon-exchange mechanism. The incident electron is inelastically scattered on ^{40}Ca, and a virtual photon with energy E_x and momentum $\vec{q}$ is transferred to the ^{40}Ca nucleus exciting it into the giant-resonance region. The excited nucleus propagates in time and finally decays into a residual nucleus (^{39}K, ^{36}Ar) by emitting particle x. It is assumed that excitation and decay can be treated independently. The upper part of Fig. 14 shows the double-differential cross section for electrons that are scattered inelastically on ^{40}Ca and measured in coincidence with protons that leave the residual nucleus ^{39}K in its ground state. The electrons were detected at an angle Θ_e=22°. The protons were measured under various angles. The total yield (integrated over all angles) was determined. The range of excitation energies E_x in ^{40}Ca is $E_x \approx 10$–27 MeV. For E_x between 10 and 15 MeV, a number of isolated states are observed but the most prominent excitation is the MeV-wide peak at $E_x \approx 19$ MeV. It is the electric giant dipole resonance in ^{40}Ca. Superposed upon the peak is considerable fine structure due to Ericson fluctuations of the underlying overlapping CN resonances. Such fluctuations have been seen already some time ago (Diener *et al.*, 1973) in the reaction ^{39}K$(p,\gamma_0)^{40}$Ca. The original spectrum has been smoothed with a Gaussian of full width at half maximum=800 keV (continuous solid line). The middle panel shows the ratio of the actual cross section and the smoothed one. The data fluctuate around the value unity. The autocorrelation function shown in the lower part was computed from the fluctuating cross section within $16 \leqslant E_x \leqslant 23$ MeV (dashed lines in the middle part of the figure). The Lorentzian predicted by Ericson, $C(\varepsilon)=C(0)(\Gamma^{\downarrow})^2/[(\Gamma^{\downarrow})^2+\varepsilon^2]$, was fitted to the experimental points (open circles). This determines the spreading width with a value between about 15 and 30 keV, depending on the method of averaging (Diener *et al.*, 1973; Carter *et al.*, 2001). The scatter of the points results from the finite range of the data (Richter, 1974).

The value of $C(\varepsilon)$ at $\varepsilon=0$, i.e., the normalized variance $C(0)=\langle\sigma^2\rangle/\langle\sigma\rangle^2-1$, is related to the direct part $y_d=|\langle S\rangle|^2/\langle|\langle S\rangle+S^{\mathrm{fl}}|^2\rangle$ for the reaction feeding the proton decay channel (with $S=\langle S\rangle+S^{\mathrm{fl}}$) through $C(0)=(1/nN)(1-y_d^2)$. Here N corresponds to the effective number of spin channels contributing to the reaction, and n describes a damping factor due to the finite experimental energy resolution. The detailed analysis of the fluctuating cross sections in the ^{40}Ca$(e,e'p)^{39}$K reaction yields as a fraction y_d of the direct cross section a value between about 85% and 95% for the p_0 and p_1 decay into the ground and first-excited states in ^{39}K, respectively. From the point of view of the shell model, these states are dominated by the $1d_{3/2}^{-1}$ and $2s_{1/2}^{-1}$ single-particle configurations, respectively. Furthermore, the ratio of the cross sections for these two decay channels is close to the ratio of the single-nucleon transfer spectroscopic factors from the ^{40}Ca$(d,^3\mathrm{He})^{39}$K reaction (Doll *et al.*, 1976). Thus, the analysis of Ericson fluctuations (Carter *et al.*, 2001) has shown that in ^{40}Ca the escape width $\Gamma^{\uparrow}$ for direct proton emission of the electric giant dipole resonance feeding low-lying states of ^{39}K is considerably larger than the spreading width $\Gamma^{\downarrow}$. We note that, for the nuclear giant dipole resonance, the ratio $\Gamma^{\downarrow}/\Gamma^{\uparrow}$ strongly increases with mass number so that $\Gamma^{\downarrow}$ dominates in heavy nuclei.

We return once more to the analogy between a flat chaotic microwave resonator—a quantum billiard—and a CN. The data on billiards described so far relate to the cases of isolated or weakly overlapping resonances. An extension of the measurements with the chaotic tilted stadium billiard (inset of Fig. 10) into the Ericson regime

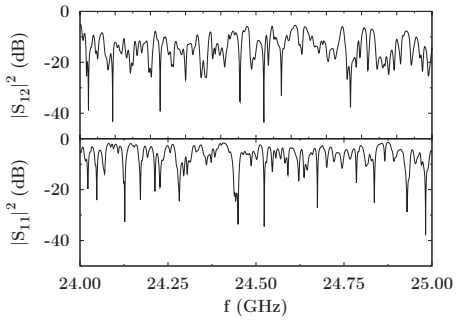

FIG. 15. Same as in Fig. 10 but in the Ericson regime of overlapping resonances. From Schäfer, 2009.

($\Gamma > d$) was reported by Dietz, Friedrich, *et al.* (2010). The absolute squares of the strongly fluctuating matrix elements S_{12} and S_{11}, taken at high excitation frequencies, are plotted versus frequency in Fig. 15. The autocorrelation functions and their Fourier transforms are shown in Fig. 16. The data show that already for a value of $\Gamma/D \approx 1.06$ the system decays exponentially in time. Again, the decay pattern and the autocorrelation functions of the S-matrix elements in Fig. 16 are well described by the statistical theory. Furthermore, as shown in Fig. 17 for S_{12}, the S-matrix elements have a Gaussian distribution, and the phases are uniformly distributed in the interval $\{0, 2\pi\}$ (Dietz, Friedrich, *et al.*, 2010). We note that the doorway-state phenomenon can also be

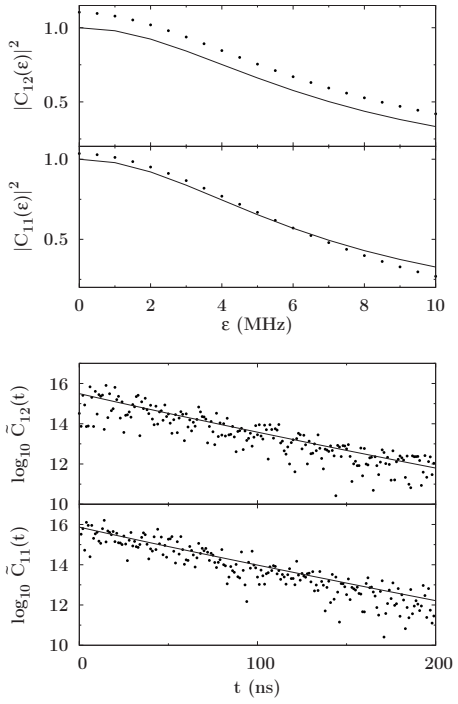

FIG. 16. Autocorrelation function in the Ericson regime. Autocorrelation functions (upper part) and Fourier coefficients (lower part) with a fit of Eqs. (75)–(77) of the statistical theory. Same as in Fig. 11 but for the Ericson regime. The exponential decay in time in the region of overlapping resonances ($\Gamma/D \approx 1.06$) is striking. From Schäfer, 2009.

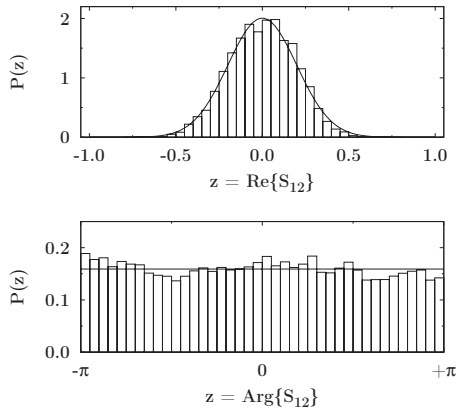

FIG. 17. Distribution of transmission amplitudes. Upper part: Histogram for the distribution of the real part of the matrix element S_{12}. Lower part: Histogram for the distribution of the phase of S_{12}. The data are taken in the Ericson regime ($\Gamma/D \approx 1.06$). From Schäfer, 2009.

modeled in terms of a microwave billiard (Åberg *et al.*, 2008).

Kuhl *et al.* (2008) have taken a different approach to chaotic scattering in microwave cavities in the Ericson regime. They used the method of harmonic analysis to determine the locations of the poles of S in the complex energy plane. The resulting width distribution was compared with theoretical results by Sommers *et al.* (1999).

These examples from recent experiments together with the many others summarized in the earlier reviews (Ericson and Mayer-Kuckuk, 1966; Richter, 1974) should suffice to demonstrate the importance of Ericson fluctuations in nuclei. The phenomenon occurs, however, also in other quantum systems. Blümel and Smilansky (1988) analyzed numerically the effect of irregular classical scattering on the corresponding quantum-mechanical scattering matrix. Using semiclassical arguments they showed that the fluctuations of the S matrix and of the cross section are consistent with Ericson fluctuations. Weidenmüller (1990) and Sorathia *et al.* (2009) compared universal conductance fluctuations of mesoscopic systems in the metallic regime with Ericson fluctuations of CN cross sections and pointed out not only the common stochastic features of the resonances in both phenomena but also the differences. These arise because the conductance is a sum over many channels and because the length of the mesoscopic system can be varied continuously. Main and Wunner (1992) reported exact quantum calculations for the photoionization cross sections of the hydrogen atom in crossed magnetic and electric fields and found strong Ericson fluctuations as a characteristic feature of chaotic scattering. A featured article in physical chemistry by Reid and Reisler (1996) emphasized the manifestation of interfering overlapping resonances and Ericson fluctuations in the unimolecular dissociation reaction of NO_2 molecules into NO + O final states. They treated this process as resonance scattering within the formalism of random-matrix theory. In a pioneering work, Stania and Walther (2005) reported the first experimental observation of Ericson fluctuations in

atomic and molecular systems. Quantum chaotic scattering was studied in ^{85}Rb in strong crossed magnetic and electric fields in an energy regime beyond the ionization threshold. The impressive experimental results of photoexcitation cross sections were later supported by exact numerical calculations (Madroñero and Buchleitner, 2005). Very recently, Ericson fluctuations have also been predicted for the inelastic electron-scattering cross section on a helium atom near the double-ionization threshold (Xu *et al.*, 2008). The universality of Ericson fluctuations in quantum chaotic scattering is, thus, very well established.

VIII. VIOLATION OF SYMMETRY OR INVARIANCE

As mentioned toward the end of Sec. IV.B, the theoretical framework of Eqs. (40)–(42) and (47) is quite flexible and allows for extensions of the theory that describe violation of isospin symmetry, of parity, or of time-reversal invariance in CN reactions. These are reviewed in turn. In the case of both isospin and parity violation, the statistical theory is taken for granted and used as a means to analyze the data. The same is true for tests of time-reversal invariance in nuclear reactions. But in experiments on induced violation of time-reversal symmetry in microwave billiards, the underlying theoretical framework has been thoroughly tested.

A. Isospin

Violation of isospin symmetry has a number of causes: The Coulomb interaction between protons, the mass difference between neutron and proton (or between u quark and d quark), etc. (see Sec. I.III.D.1). All these are treated summarily by replacing H^{GOE} in Eq. (47) by a Hamiltonian H with block structure (Rosenzweig and Porter, 1960) as done in Eq. (I.30). We simplify the presentation and consider only two classes of states with different isospins T_1 and T_2 (where typically we have $T_2=T_1+1$) containing N_1 and N_2 elements, respectively. The generalization to more classes with different isospins is straightforward but is not needed in practice. The matrix representation of H has the form

$$\begin{pmatrix} H^{(1)}_{\mu\nu} & V_{\mu\sigma} \\ V_{\rho\nu} & H^{(2)}_{\rho\sigma} \end{pmatrix}. \tag{98}$$

Here $H^{(1)}$ and $H^{(2)}$ are the Hamiltonian matrices acting on states that carry the isospin quantum numbers T_1 and T_2, respectively; each is taken from the GOE. The isospin-breaking interaction is represented by the rectangular matrix V residing in the nondiagonal blocks. The elements of V represent all isospin-breaking effects and are typically small compared to those of $H^{(1)}$ and $H^{(2)}$. A similar model is also used to describe parity mixing, with $H^{(1)}$ and $H^{(2)}$ now denoting the Hamiltonian matrices of states of positive and negative parity, respectively, and V denoting the induced parity-violating nucleon-nucleon interaction. In both cases, RMT predicts only fluctuations of the relevant observable. The mean-square value of the matrix elements of V serves as an input parameter and must be either calculated dynamically or inferred from the statistical analysis of the data. Within an RMT approach it is, thus, inherently impossible to shed light on the dynamical origin of the different sources of isospin violation or of the parity-breaking part of the nuclear Hamiltonian. The dynamical aspects of isospin violation have been reviewed, for instance, in Steiner *et al.* (2005), Miller *et al.* (2006), and Londergan *et al.* (2010).

The density of states with isospin T_1 is usually considerably larger than that of states with isospin $T_2=T_1+1$. Isospin mixing has been extensively investigated for two cases: (i) In the Ericson regime. For both isospin classes the resonances overlap strongly. (ii) For isobaric analog resonances. Resonances with isospin T_2 are well separated. Because of isospin mixing, each acts as a doorway for the weakly overlapping resonances with isospin T_1. We deal with both cases in turn.

1. Ericson regime

Isospin violation in the Ericson regime (strongly overlapping resonances for both values T_1 and T_2 of isospin) was extensively reviewed in Harney *et al.* (1986). Since then, essential new developments have not occurred either in theory or in experiment. We confine ourselves here to a brief summary. The only recent experimental information on isospin mixing in very highly excited CN is from measurements of γ-ray spectra in heavy-ion fusion reactions which we address below. We first sketch the modifications of the general framework of Secs. IV.B, V, and VI that are required if two values of isospin contribute to the reaction. We then turn to a summary of the main experimental results.

In order to model isospin violation theoretically in the Ericson regime one must, in addition to Eq. (98) for the Hamiltonian, also specify the isospin properties of the channels. The physical channels labeled (at) carry the quantum number t. It is given by the projection of total isospin onto some axis and equals half the difference of neutron and proton numbers in both fragments (projectile plus target). The background matrix $S^{(0)}$ that describes scattering in the absence of resonances and is given by Eq. (40) as $S^{(0)}=UU^T$ is assumed to be diagonal with respect to the physical channels, $S^{(0)}_{at,bt'}=\delta_{ab}\delta_{tt'}\exp\{2i\delta^{(0)}_{at}\}$. In other words, in Eq. (39) we put both $\mathcal{O}^{(0)}$ and $\mathcal{O}^{\mathrm{CN}}$ equal to unit matrices. Then, the physical S matrix differs from the matrix S^{CN} in Eq. (41) only by phase factors; these are suppressed in what follows. Our assumption neglects direct transitions between "mirror" channels that are related by neutron-proton symmetry; Harney *et al.* (1986) showed that in the Ericson regime this neglect is irrelevant.

Although the theory (Harney *et al.*, 1986) is more general, we focus attention here on the main mechanism of isospin mixing. It is due to "internal mixing" induced by the matrix elements of V in Eq. (98). Because of charge effects, isospin mixing also occurs in the channels but is

negligible. The coupling matrix elements $W^T_{a\mu}$ in Eq. (41) carry the additional isospin quantum number T and so do the transmission coefficients labeled τ_{aT} (we deviate here from our standard notation to distinguish the transmission coefficients from the isospin quantum number). In the physical channels the transmission coefficients $\tau^{tt'}_{aT}$ are not diagonal and are given by projecting (with the help of angular-momentum coupling coefficients $\langle aT|at\rangle$) the transmission coefficient τ_{aT} onto t,t' by $\tau^{tt'}_{aT}=\langle aT|at\rangle\langle aT|at'\rangle\tau_{aT}$. The autocorrelation function of $S^{\rm fl}$ is then given by

$$\langle S^{\rm fl}_{at,bt'}(E_1)(S^{\rm fl}_{ct'',dt'''}(E_2))^*\rangle = \delta_{ac}\delta_{bd}\sum_{mn}\tau^{tt''}_{am}\Pi_{mn}\tau^{t't'''}_{bn} + \delta_{ad}\delta_{bc}\sum_{mn}\tau^{tt'''}_{am}\Pi_{mn}\tau^{t't''}_{bn}. \tag{99}$$

Here Π_{mn} is a 2×2 matrix in isospin space. With $\varepsilon=E_2-E_1$, the inverse of Π is given by

$$\Pi^{-1}=\begin{pmatrix}\mathcal{N}_1+z+2i\pi\varepsilon/d_1 & -z\\ -z & \mathcal{N}_2+z+2i\pi\varepsilon/d_1\end{pmatrix}. \tag{100}$$

The average level spacing for the states with isospin T_m, $m=1,2$, is denoted by d_m, and $\mathcal{N}_m=\Sigma_a\tau_{aT_m}$. Equations (99) and (100) generalize Eq. (67) for the Ericson regime to the case of isospin mixing. The strength of isospin mixing is characterized by a single dimensionless parameter z given by

$$z=4\pi^2\langle V^2\rangle/(d_1d_2). \tag{101}$$

The parameter z bears an obvious close analogy to the spreading width $\Gamma^{\downarrow}$ introduced in Sec. I.II.G. The matrix (100) becomes diagonal if $z=0$. In the full theory not reviewed here, the parameter z comprises both internal isospin mixing (via the Coulomb interaction) and external mixing (via the reaction channels). The theory contains also both the predictions from the static criterion and the dynamic criterion for isospin symmetry breaking: The effect is large when either the Coulomb mixing matrix elements are of the order of the mean level spacing (so that $z\approx 1$) or when the spreading widths zd_1 (zd_2) are comparable to the decay widths $2\pi\mathcal{N}_1/d_1$ ($2\pi\mathcal{N}_2/d_2$).

Harney *et al.* (1986) applied the theory to a number of experimental examples of isospin mixing from which z was determined. The examples can be divided into four classes. In the first class, the average cross section of a reaction forbidden by an isospin selection rule is compared to the average cross section of an isospin-allowed reaction. The resulting suppression factor f is related to the mixing parameter z and is a measure of the average mixing probability of the CN levels with isospin T_2 with those that have isospin T_1. Nuclear reactions in this first category use self-conjugate target nuclei (i.e., nuclei with equal neutron and proton numbers) and are of the type $(d,\alpha),(d,d'),(\alpha,\alpha'),(^6\mathrm{Li},\alpha),\ldots$. For CN excitation energies close to neutron threshold one finds suppression factors f around 0.3–0.5. These decrease to values of only a few percent at high excitation energies suggesting that at those energies isospin symmetry is restored. The detection of isospin-forbidden dipole radiation from alpha and heavy-ion capture reactions supports the observation. While the former yields suppression factors $f\approx 0.15$ for compound nuclei in the *sd*-shell nuclei at about 14 MeV excitation energy, in the fusion reaction $^{12}\mathrm{C}+^{16}\mathrm{O}$ populating the CN $^{28}\mathrm{Si}$ at $E_x=34$ MeV, f was found to be $\lesssim 0.05$. Since the early experiments (Snover, 1984; Harakeh *et al.*, 1986) several more heavy-ion fusion reactions were studied. Kicińska-Habior *et al.* (1994) investigated isospin mixing in the CN $^{26}\mathrm{Al}$ and $^{28}\mathrm{Si}$ up to excitation energies $E_x\approx 63$ MeV, Di Pietro *et al.* (2001) in $^{24}\mathrm{Mg}$ up to $E_x\approx 47$ MeV, Kicińska-Habior (2005) in $^{32}\mathrm{S}$ and $^{36}\mathrm{Ar}$, and lately Wójcik *et al.* (2007) also in $^{44}\mathrm{Ti}$ and $^{60}\mathrm{Zn}$ at $E_x\approx 50$ MeV. [The isospin mixing parameter α^2 determined in these heavy-ion capture γ-ray reactions is directly related to the parameter f introduced in Harney *et al.* (1986).] The emerging systematics on the very small suppression factors f supports the statement that isospin is quite pure at high excitation energies (several tens of MeV) of the CN. Other experiments on isospin mixing in the Ericson regime that belong to the first category are measurements of the isospin-forbidden neutron decay of the giant dipole resonance in medium-heavy ($^{60}\mathrm{Ni}$) to heavy nuclei ($^{88}\mathrm{Sr}$, $^{89}\mathrm{Y}$, $^{90}\mathrm{Zr}$). One finds suppression factors ranging from $f=0.48$ to 0.84 which indicate a fairly sizable isospin mixing at nuclear excitation energies of $E_x\approx 20$ MeV. Information on isospin mixing in highly excited compound nuclei is also deduced from evaporation spectra in (α,α'), (p,p'), (p,α'), and (α,p') reactions. In short, if the cross-section ratio $R=\sigma_{\alpha\alpha'}\sigma_{pp'}/\sigma_{\alpha p'}\sigma_{p\alpha'}$ is approximately equal to unity, then the isospin selection rule does not play any role. This follows from the Bohr hypothesis (independence of formation and decay of the CN). More generally, an expression for R can be obtained and compared with the experimental results for any degree of isospin mixing from the generalized Hauser-Feshbach expression (99) (Harney *et al.*, 1986).

Another highly sensitive test of isospin violation is provided by a comparison of cross-section fluctuations in the Ericson regime for pairs of isobaric mirror channels (channels that are linked by the neutron↔proton transformation). Such reactions were studied by Simpson *et al.* (1978) and form the second class of nuclear reactions that test isospin violation. An example is the reaction $^{14}\mathrm{N}+^{12}\mathrm{C}$ leading to the highly excited CN $^{26}\mathrm{Al}^*$ which subsequently decays into $^{23}\mathrm{Mg}+^{3}\mathrm{H}$ or into the mirror channel $^{23}\mathrm{Na}+^{3}\mathrm{He}$. The most sensitive test for isospin violation is provided by the value of the cross-correlation function $C_{tt'}(\varepsilon)$ at $\varepsilon=0$ for the two mirror channels t and t'. If isospin is a good quantum number (so that the mixing parameter $z=0$), the cross sections in the mirror channels are strongly correlated. If isospin mixing is complete (so that $z/\mathcal{N}_2\to\infty$), the two cross sections should fluctuate in an uncorrelated way, as does any pair of cross sections pertaining to different final states (Ericson and Mayer-Kuckuk, 1966; Richter, 1974).

In several pairs of mirror channels the measured cross correlations are significantly larger than for arbitrary pairs of cross sections.

In the third class of CN reactions sensitive to isospin mixing, the shape of the cross-section autocorrelation function in the Ericson regime is used as a test. The relevant observable is the correlation width Γ. The Lorentzian form of the autocorrelation function is obtained only for very strong isospin mixing. In the case of strict isospin conservation, a superposition of two Lorentzians is expected. The theoretical expressions for the case of partial isospin symmetry breaking obtained from Eq. (99) (Harney *et al.*, 1986) have been compared with very precise cross-section fluctuation data mainly from the $^{32}\mathrm{Si}(d,\alpha)^{30}\mathrm{P}$ reaction (Spijkervet, 1978), leading to final states with isospins $T=0$ and 1.

Charge-exchange reactions, such as (p,n) or (n,p), that populate the isobaric analog state of the target (see Sec. VIII.A.2), form the fourth class of CN reactions sensitive to isospin effects. If isospin were totally conserved, such reactions could be viewed as elastic-scattering processes in isospin space. In the Ericson regime, the elastic enhancement factor has the value $W=2$ [see Eq. (67)]. This same value for W is expected for a charge-exchange reaction if isospin is conserved while $W=1$ for strong isospin mixing. It seems that this interesting test has not been used so far.

We have briefly summarized what is known about isospin-symmetry breaking in CN reactions (Harney *et al.*, 1986). The data show that in the Ericson regime isospin-symmetry breaking is neither so weak as to be altogether negligible nor so strong as to reduce CN scattering to a Hauser-Feshbach situation without any reference to the isospin quantum number. Isospin mixing is expected to become weaker with increasing excitation energy [see Sokolov and Zelevinsky (1997), and references therein]. As shown in Harney *et al.* (1986), data in the Ericson regime can be used to determine the average Coulomb matrix elements $\langle V^2\rangle^{1/2}$ and spreading widths $\Gamma_1^{\downarrow}=z^2d_2/(2\pi)$ or $\Gamma_2^{\downarrow}=z^2d_1/(2\pi)$ for isospin violation in nuclei. While the values of the average Coulomb matrix elements vary over many orders of magnitude, the values of the spreading widths are nearly constant versus excitation energy and mass number [see Fig. 15 in Harney *et al.* (1986)]. This fact provides a meaningful consistency check on both theory and data analysis. Similarly to the experiments reviewed in Sec. VII.A and the study of symmetry breaking in the regime of isolated resonances (Alt *et al.*, 1998; Dietz *et al.*, 2006), further subtle aspects of the theory in the regime $\Gamma \gg d$ might be tested with the help of experiments on two coupled microwave billiards.

2. Fine structure of isobaric analog resonances

If isospin T were a good quantum number, isospin multiplets consisting of degenerate states with fixed T but with different z-quantum number T_z ("isobaric analog states") would exist in nuclei with the same mass number A but different neutron and proton numbers.

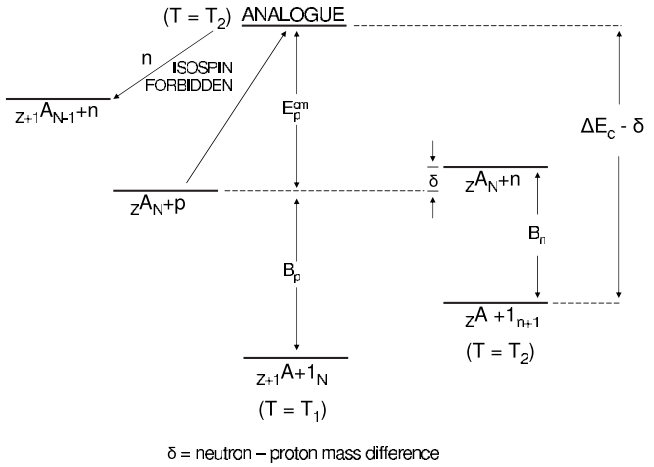

FIG. 18. Level scheme showing the parent nucleus, the isobaric analog state, and a state of lower isospin (schematic). Adapted from Bilpuch *et al.*, 1976.

The degeneracy is lifted by the isospin-breaking interaction (mainly the Coulomb interaction between protons), and the energies of the members of a multiplet increase with increasing proton number. For proton numbers $Z\approx 20$, the energy difference between neighboring members of a multiplet is of the order of 10 MeV. In a medium-weight nucleus with ground-state isospin T_1, the lowest state with next-higher isospin $T_2=T_1+1$ (an isobaric analog state of the "parent state," here the ground state of a nucleus with the same mass number but one proton replaced by a neutron) typically has an excitation energy of several MeV. Higher-lying states with isospin T_2 follow with typical spacings of several hundreds of keV. These states may be unstable against proton decay. The resulting resonances ["isobaric analog resonances" (IARs)] are then observed in elastic proton scattering. The proton channel does not have good isospin and couples to both the IARs and the numerous background states with isospin T_1. The situation is shown schematically in Fig. 18. The parent state is the ground state of the nucleus $Z^{(A+1)}{}_{N+1}$ with isospin T_2. In its ground state the CN nucleus $Z+1^{(A+1)}{}_N$ has isospin T_1. The isobaric analog state in the nucleus occurs at an excitation energy of several MeV.

Low-lying IARs correspond to simple states of the shell model. Therefore, their elastic widths (typically several keV) are much larger than those of the complicated CN background states. On the other hand, the elastic width of the IAR is typically small compared to the average spacing between IARs which will thus be considered as isolated. The isospin-breaking interaction mixes each IAR with CN background resonances. The mixing strongly enhances the elastic widths of all CN resonances that occur in the vicinity of the IAR. The mechanism is similar to that of a doorway state (see Sec. I.II.G), except that now all states are resonances and the mixing mechanism is rather special. The resulting "fine structure" of an IAR is a topic of special interest. While it is sometimes possible to apply nuclear-structure theory to individual IARs, the background states are too

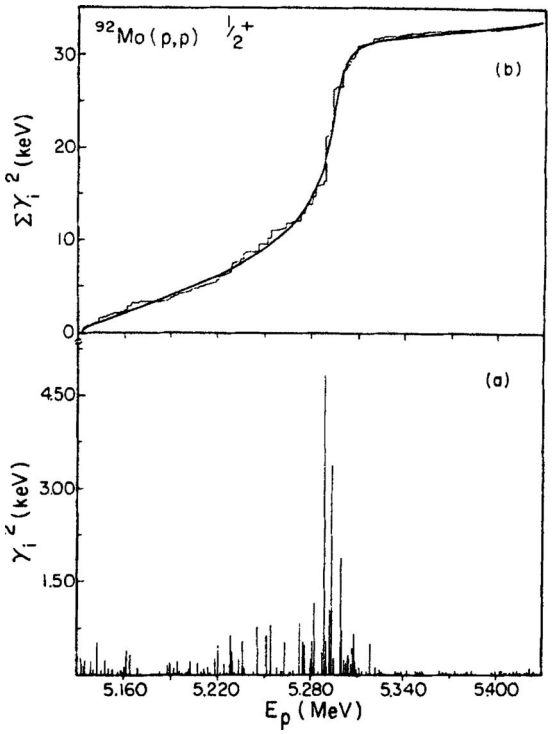

FIG. 19. Partial widths of individual resonances (lower panel) and their integral (upper panel) vs proton bombarding energy E_p in the elastic proton scattering on ^{92}Mo. From Bilpuch *et al.*, 1974.

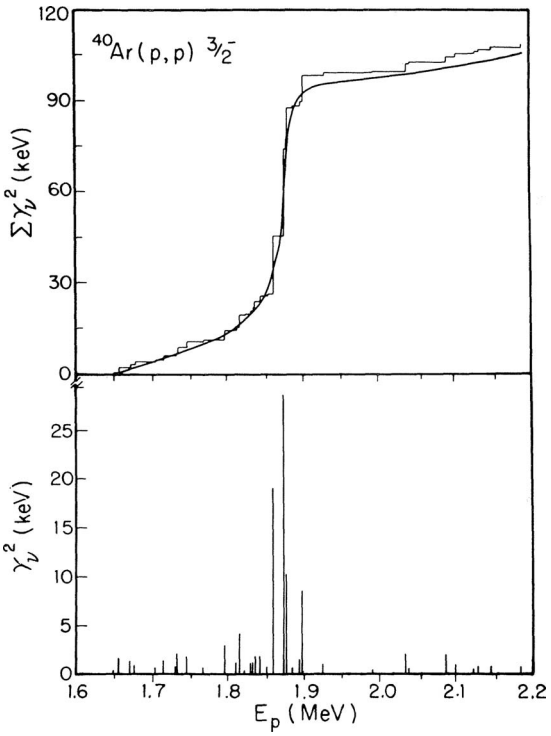

FIG. 20. Same as in Fig. 19 but for the target nucleus ^{40}Ar. From Bilpuch *et al.*, 1976. Adapted from Keyworth *et al.*, 1966.

numerous and too highly excited to allow for anything but a random-matrix approach. Thus, the theoretical description uses for the Hamiltonian the matrix (98) with the proviso that the submatrix $H^{(1)}$ is taken from the GOE while the submatrix $H^{(2)}$ has dimension 1.

IARs as resonances in the CN were discovered by the Florida State group which partially resolved a proton s-wave IAR in ^{92}Mo(p,p) (Richard *et al.*, 1964). If the CN background resonances overlap only weakly, the excitation curves fluctuate strongly, and the fine structure of an IAR can be completely resolved experimentally. This is possible mainly in the nuclear $1f$-$2p$ shell (see Sec. I.IV.A). The fine structure is investigated in elastic and inelastic proton scattering and sometimes in the (p,n) reaction. The latter is isospin forbidden and gives direct evidence for symmetry breaking. Depending on the mean level spacing d of the background states, we distinguish three cases: almost all of the original proton strength is retained by the analog state (weak mixing), the strength is spread among many states with no state being dominant (strong mixing), and cases between these extremes (intermediate mixing). The background states have their own (small) proton widths. Thus, the observed fine structure is the combination of two amplitudes which may display interference effects. Special interest was shown in the resulting asymmetry (Robson, 1965) that is found in many fine-structure distributions. Another phenomenon in nuclear physics with similar mixing patterns is that of fission doorways (Lynn, 1969).

The observation of fine structure of IARs requires excellent energy resolution for the incident-proton beam. Since most of the fine-structure data were obtained by the Triangle Universities' Nuclear Laboratory (TUNL) group, we limit discussion of the experimental techniques to a brief description of their method. The requirements of very good beam-energy resolution (needed to resolve the fine structure) and high beam intensity (needed to have good statistics) seem contradictory particularly because of the time-dependent fluctuations in beam energy. The method adopted by the TUNL group to resolve the resolution-intensity problem uses two beams. One high-intensity (H^+) beam is used to perform the experiment, while the other (HH^+) beam is used to generate a feedback signal that follows the beam-energy fluctuations. This signal generates a voltage difference which is applied to the target, thus canceling the time-dependent energy fluctuations. The experimental details are covered in the review by Bilpuch *et al.* (1976).

After early work by the Florida State group on an s-wave IAR in ^{92}Mo(p,p) (Richard *et al.*, 1964), later measurements on this analog with better resolution (Bilpuch *et al.*, 1974) provided the fine-structure pattern with the largest number of individual states ever (see Fig. 19). Prior to these data the existence of fine structure was most clearly shown by Keyworth *et al.* (1966) who used a windowless gas target (see Fig. 20). Their data definitively established the essential correctness of the view that in the $A \approx 40$ mass region the analog (doorway) state is mixed into the CN background states with a spreading width (see Sec. I.II.G) of the order of 10 keV.

The bulk of the fine-structure data consists of 15 elastic proton scattering excitation functions on thin solid targets (of order 1 μg) in the mass region $40<A<64$. There are also some data on other channels, including the (p,p'), (p,γ), and (p,n) reactions. Almost all of these results are included in the review by Bilpuch *et al.* (1976).

Many data on strength functions of IAR display the "Robson asymmetry" (Robson, 1965), characterized by a dip in the strength function located above the energy of the resonance maximum. For simplicity, we illustrate the origin of the asymmetry for the case of a single open channel (the proton channel). This case suffices to display the very peculiar nature of the doorway mechanism in IARs. The IAR is mixed with the background states by two mechanisms: the matrix elements of the Coulomb interaction V appearing in the nondiagonal blocks of expression (98), and the elements $F_{\mu\nu}$ of the matrix (44) connecting IAR and background states. The latter do not vanish automatically because isospin is not a good quantum number in the proton channel. Moreover, in contrast to most other applications of the statistical theory reviewed in this paper, the elements of the shift matrix are not small, and the characteristic features of the IARs are, in fact, due to the real part of $F_{\mu\nu}$. This is because IARs occur below or at the Coulomb barrier where the energy dependence of the matrix elements $W_{\mu c}(E)$ cannot be neglected. To display the effect most clearly we follow Robson, neglect V (this approximation is often referred to as "no internal mixing"), and consider only mixing due to $F_{\mu\nu}$ ("purely external mixing"). In other words, isospin mixing is solely due to the proton channel to which both the IAR and the background states are coupled.

We omit the channel index and express the scattering function $S(E)$ in terms of the K function [see Eqs. (34) and (35)]. We replace $\sqrt{2\pi}W_\mu$ by γ_μ and have

$$K(E)=\frac{1}{2}\sum_\mu \frac{\gamma_\mu^2}{E-E_\mu}. \tag{102}$$

The parameters γ_μ and E_μ of the K function are experimentally obtained by a multilevel R-matrix fit to fine-structure data (see Sec. IV.C). The object of interest is the strength function $\langle\gamma_\mu^2\rangle/d$ obtained as an average over a number of neighboring resonances (see Figs. 19 and 20). We replace in Eq. (102) E by $E+iI$ and obtain $-(1/\pi)\mathrm{Im}\,K(E+iI)\approx\langle\gamma_\mu^2\rangle/d$ (see Sec. V.A). The averaging interval I should contain many CN resonances (to reduce the statistical error), but be small compared to the spreading width of the IAR defined below (to display the resonance enhancement and asymmetry). In the analysis of actual data it may be hard to meet both requirements. To calculate $K(E)$ we drop V in Eq. (98) and use Eqs. (41) and (42) keeping the shift function F. After a little algebra we obtain

$$K(E)=\pi\sum_{ij} W_i(\mathcal{B}^{-1})_{ij}W_j. \tag{103}$$

The matrix $\mathcal{B}$ has the same form as Eq. (98). The indices (i,j) take the values 1 to N (for the background states) and 0 (for the analog state) while μ and ν run from 1 to N as before. Explicitly, we have

$$\mathcal{B}=\begin{pmatrix}(E-\varepsilon_\mu)\delta_{\mu\nu} & -\mathrm{Re}\,F_{\mu 0}\\ -\mathrm{Re}\,F_{0\nu} & (E-E_0-F_{00})\end{pmatrix}. \tag{104}$$

We have assumed that the matrix $H^{(1)}_{\mu\nu}+\mathrm{Re}\,F_{\mu\nu}$ has been diagonalized. The resulting eigenvalues are denoted by ε_μ but the notation on the transformed matrix elements W_μ and $\mathrm{Re}\,F_{\mu 0}$ has not been changed. The W_μ are random Gaussian variables which also appear as arguments of the integrals defining the matrix elements $\mathrm{Re}\,F_{\mu 0}$. Thus, W_μ and $\mathrm{Re}\,F_{\nu 0}$ are correlated for $\mu=\nu$. The energy of the unperturbed IAR is denoted by E_0. The matrix element W_0 is not random.

For a common doorway state, the spreading width $\Gamma^\downarrow$ is defined as $\Gamma^\downarrow=2\pi v^2/d$ [see Eq. (I.26)]. Here d is the mean spacing of the background states and v^2 is the average squared coupling matrix element. Using the analogy between Eq. (104) and the matrix description Eq. (I.24) for a doorway state, we define the spreading width of an IAR as

$$\Gamma^\downarrow=2\pi\langle(\mathrm{Re}\,F_{0\mu})^2\rangle/d. \tag{105}$$

This equation shows once again that isospin mixing is due to the proton channel.

The strength function is obtained from Eq. (103) by replacing E by $E+iI$ and assuming $d\ll I\ll\Gamma^\downarrow$. The explicit calculation uses the statistical assumptions mentioned above and may, for instance, be found in Chap. 13 of Mahaux and Weidenmüller (1969). The result is

$$\frac{\langle\gamma_\mu^2\rangle}{d}=s^{\mathrm{bg}}\frac{(E-E_0)^2}{(E-E_0-\mathrm{Re}\,F_{00})^2+(1/4)(\Gamma^\downarrow)^2}. \tag{106}$$

Here s^{bg} is the strength function of the background states in the absence of the IAR. The IAR enhances the strength function in the vicinity of the analog state. Since $\Gamma^\downarrow\gg d$, the resonance is completely mixed with the background states and is seen only through the enhancement factor in Eq. (106). The factor has the shape of an asymmetric Lorentzian and approaches the value unity far from the resonance. The width of the Lorentzian is given by the spreading width. The strength function vanishes at $E=E_0$ where there is no isospin mixing. The zero occurs above the resonance energy $E_0+\mathrm{Re}\,F_{00}$: Because of the Coulomb barrier, the main contribution to the integral defining $\mathrm{Re}\,F_{00}$ stems from states with energies larger than E_0 and $\mathrm{Re}\,F_{00}$ is, therefore, negative.

In general (several open channels, both external and internal mixing), the asymmetry of the strength function in channel c in the vicinity of an analog state is reduced. For purposes of fitting data the expression given, for instance, by Lane (1969) can be written in the form (Bilpuch *et al.*, 1976)

$$\frac{\langle \gamma_{c\mu}^2 \rangle}{d} = s_c^{\mathrm{bg}} + \frac{2 s_c^{\mathrm{bg}} \Delta_c (\varepsilon_0 - E)}{(\varepsilon_0 - E)^2 + (1/4)(\Gamma^{\downarrow})^2} + \frac{\gamma_c^2 \Gamma^{\downarrow}/(2\pi)}{(\varepsilon_0 - E)^2 + (1/4)(\Gamma^{\downarrow})^2}. \quad (107)$$

Here s_c^{bg} is the background strength function in channel c, ε_0 is the resonance energy, Δ_c is the asymmetry parameter in channel c, and γ_c^2 is the total reduced width of the analog state in channel c, i.e., the sum over the fine-structure contributions.

Equation (107) was originally derived under the assumption of strong mixing, $\Gamma^{\downarrow} \gg d$. However, the experimental data indicate intermediate or weak mixing in essentially all cases. This case was theoretically considered by Lane *et al.* (1974). It was shown that the form of Eq. (107) remains unchanged and that $\langle \gamma_{c\mu}^2 \rangle / d$ as given by Eq. (107) must be considered an ensemble average of the strength function, all members of the ensemble having the same physical parameters. To analyze the data one avoids the need of using energy-averaging intervals and fits the accumulated strength to its ensemble average $\int^E \langle \gamma_{c\mu}^2 \rangle / d$.

Due to the limited number of fine-structure states and to the width fluctuations [we recall that the latter follow the Porter-Thomas distribution (see Sec. I.II.D.1)], the extracted parameters have rather large uncertainties. The general status of these parameters is as follows: The best-fit values for the background strength function $s_c^{\mathrm{bg}}(E)$ are generally in agreement with those expected from systematics. The values of the energy ε_0 of the analog resonance agree with systematics on shifts between analog state and parent state [see Jänecke (1969)]. The values of the reduced widths γ_c^2 can be used to calculate the proton spectroscopic factors S_p. The latter essentially measure the probability to find a proton of fixed angular momentum in the projection of the resonance wave function onto the target nucleus. When compared with the neutron spectroscopic factors S_n of the parent states, the analog spectroscopic factors are significantly lower (30–50 %) than expected, even after Coulomb corrections. To the best of our knowledge, the discrepancy has never been satisfactorily resolved. The statistically significant best-fit values for the asymmetry parameter Δ_c are all negative and usually agree (within a factor of 2) with the values predicted by Robson (1965). More detailed analysis indicated that the effects of the inelastic channels do not dominate the elastic channel but are not negligible either (as assumed by the Robson model). Instead, these effects are comparable to that of the elastic channel for most analogs. The best-fit values of the spreading width $\Gamma^{\downarrow}$ agree rather well with the Robson model (only external mixing that occurs only in the elastic channel). There is evidence that the inelastic channels contribute significantly to $\Gamma^{\downarrow}$ in some cases.

The analog state can decay via several inelastic and/or capture-gamma channels and is then a doorway common to these channels. Such decay processes provide unique information on the analog state. For an isolated doorway common to two channels c and c', Lane (1971) predicted that the reduced width amplitudes $\gamma_{c\mu}$ and $\gamma_{c'\mu}$ of the fine-structure resonances labeled μ should be maximally correlated. More precisely, the normalized linear correlation coefficient $\rho(\gamma_c, \gamma_{c'})$ defined in Eq. (I.29) should be equal to unity and the product $\gamma_{c\mu}\gamma_{c'\mu}$ should have the same sign for all fine-structure resonances μ. Graw *et al.* (1974) and Davis *et al.* (1975) indirectly showed the expected constancy of the relative phase. The two predictions were proved directly by Mitchell *et al.* (1985). We consider the fragmented $3/2^-$ analog state at proton bombarding energy $E_p = 2.62$ MeV in ^{45}Sc as an example.

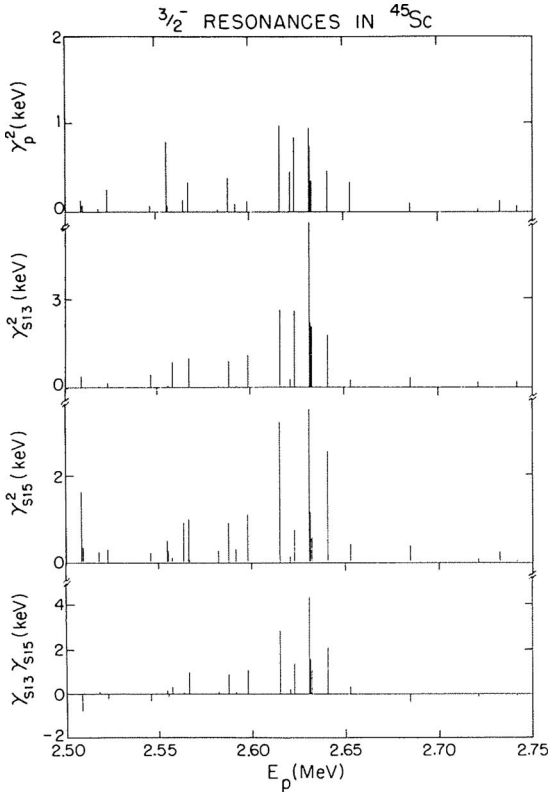

FIG. 21. Fine structure of the analog resonance with spin 3/2 in the CN ^{45}Sc. The partial width amplitudes γ are indexed by the channel angular momentum and spin. The Robson asymmetry is clearly displayed. From Mitchell *et al.*, 1985.

The state has a strong decay to the 2^+ first-excited state in ^{44}Ca. In the channel-spin representation, the two p-wave proton inelastic decay channels have spins $s = 3/2$ and $5/2$. These two channels also display a well-developed fine-structure pattern (see Fig. 21); both show clearly the Robson asymmetry. With the method described by Mitchell *et al.* (1985), one can determine the correlation between the decay amplitudes. The measured value $\rho(\gamma_{s=3/2}, \gamma_{s=5/2}) = 0.93$ is in agreement with the predicted value of unity. The relative sign of the decay amplitudes is the same for the 15 consecutive resonances that make up the analog. To quote Mahaux and Weidenmüller (1979), "isobaric analog resonances provide the best-understood example of isolated doorway states."

B. Parity

In this section we discuss data on parity violation obtained by low-energy neutron scattering and their statistical analysis. We keep the discussion short since a general survey of experiments on parity violation with neutrons and their analysis was given by Mitchell *et al.* (1999). A comprehensive review of the experiments and analysis of the time-reversal invariance and parity violation at low energies (TRIPLE) collaboration was presented by Mitchell *et al.* (2001). For the theoretical analysis we use the model of Eq. (98) where the two classes now comprise states of opposite parity and where V denotes the effective parity-violating interaction. For the connection between V and the basic parity-violating weak interaction, see Desplanques *et al.* (1980) and Zhu *et al.* (2005), and references therein.

The study of parity violation in nuclei has a long history. Following the initial discovery of parity violation in beta decay, efforts toward detecting and understanding the induced parity-violating nucleon-nucleon interaction focused on precise measurements of observables indicating parity violation. Most of these involved electromagnetic transitions between nuclear states at excitation energies of a few MeV. In spite of many efforts and elegant experimental results, the work has been only partially successful. The difficulty is in the theoretical analysis: Calculating the induced effective parity-violating interaction required a more precise knowledge of the wave functions of the nuclear states involved than can be attained with present-day nuclear theory (Adelberger and Haxton, 1985). The situation changed when Sushkov and Flambaum (1980) predicted two enhancement factors which together would lead to large parity-violating effects in the CN scattering of low-energy neutrons and when statistical concepts were used to analyze the data.

The two enhancement factors are usually referred to as dynamical enhancement and kinematical enhancement. Dynamical enhancement (Blin-Stoyle, 1960; Sushkov and Flambaum, 1980) arises because in heavy nuclei the average spacing of neutron resonances of opposite parity is small and typically 10 eV or so. With V the parity-violating part of the nucleon-nucleon interaction and E_1 and E_2 the energies of two levels, $|1\rangle$ and $|2\rangle$, of opposite parity, the mixing of the two states is given by $\langle 1|V|2\rangle/(E_1-E_2)$. The mixing obviously increases with decreasing spacing (E_1-E_2). The increase is not inversely proportional to the spacing, however, because the complexity of the wave functions of the states $|1\rangle$ and $|2\rangle$ also increases with increasing level density, reducing the overlap in $\langle 1|V|2\rangle$. The result is an increase of the mixing that is inversely proportional to the square root of the spacing (Sushkov and Flambaum, 1982; French *et al.*, 1988a, 1988b). With typical spacings of states of opposite parity in the ground-state domain around 100 keV, the resulting enhancement factor is $\approx 10^2$ and does not change rapidly with excitation energy. Kinematical enhancement arises because of the unequal resonance strength of the states mixed by the parity-violating interaction. At low neutron energies only resonances with orbital angular momentum 0 or 1 are populated. Because of the angular-momentum barrier, the s-wave resonances have much larger widths than the p-wave resonances. Thus, s-wave decay of a p-wave resonance with an s-wave resonance admixture is enhanced over the regular p-wave decay of that resonance by a factor given by the ratio of the two barrier penetrabilities—approximately $(kR)^{-1}$. Here R is the nuclear radius and k is the wave number. The factor $(kR)^{-1}$ is strongly energy dependent; significant enhancement occurs only near neutron threshold. The product of the two enhancement factors is about 10^5. Since the weak interaction is approximately a factor of 10^7 smaller than the strong interaction, the total enhancement leads to expected parity-violating effects on the order of percent. The prediction of Sushkov and Flambaum (1980) was confirmed shortly afterward at Dubna (Alfimenkov *et al.*, 1983, 1984). The results at Dubna were extremely interesting. However, there were both experimental and theoretical limitations.

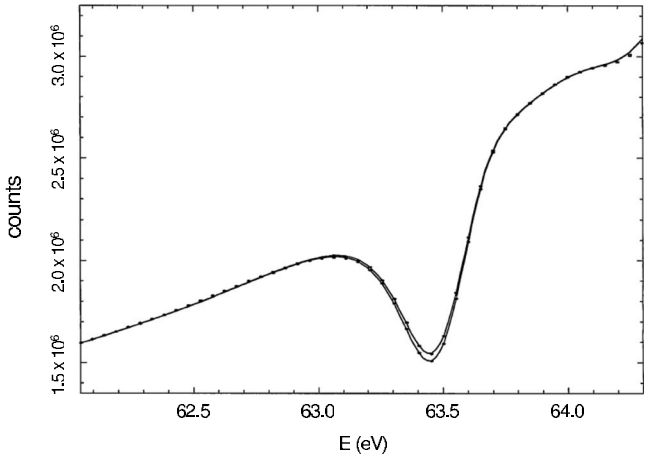

FIG. 22. Neutron transmission spectra for two helicity states near the 63 eV resonance in ^{238}U. The resonance appears as a dip in the transmission curve. The transmission at the resonance differs significantly for the two helicity states and parity violation is apparent by inspection. From Mitchell *et al.*, 1999.

The experimental limitations at the Dubna facility were severe: the neutron flux dropped dramatically above a few tens of eV, limiting the experiments on parity violation to neutron energies below 20 or 30 eV. Subsequently, the TRIPLE Collaboration was formed to extend the experiments on parity violation to higher energies. These experiments were performed at the Los Alamos Neutron Science Center. A moderated and collimated beam of neutrons is produced by spallation. A beam of longitudinally polarized protons is produced by scattering from a longitudinally polarized proton target. The neutron spin direction is reversed by a system of magnetic fields. The neutrons pass through the target and are detected in a highly segmented system of liquid detectors located at a distance of approximately 57 m. CN resonance energies are determined by the time-of-flight method. A sample result is shown in Fig. 22. The

details of the experimental system are given in the review by Mitchell *et al.* (2001).

Although the observation of large parity violation in neutron resonances was certainly very impressive, the Dubna results were first considered of only anecdotal interest since the resonance wave functions were too complicated to be theoretically accessible. This problem was overcome by the statistical approach. Since *s*-wave neutron resonances obey GOE statistics, it is safe to assume that *p*-wave resonances do too. Then, the matrix elements of the parity-violating interaction connecting *s*- and *p*-wave resonances have a Gaussian distribution with mean value zero. The variance of the distribution (or the mean-squared matrix element $\overline{v^2}$ for parity violation) can be determined from a set of *p*-wave resonances with parity violation in a given nuclide. This is described below. However, $\overline{v^2}$ is not a good measure for the strength of the parity-violating interaction since it decreases rapidly with increasing complexity of the wave functions and, thus, with increasing mean level density. A measure that is roughly independent of excitation energy and mass number is the spreading width $\Gamma^{\downarrow}=2\pi\overline{v^2}/d$ (see Secs. I.II.G and VIII.A). The convention is to adopt for d the mean spacing of the *s*-wave resonances. The expected size of the weak spreading width can be estimated from the spreading width for the strong interaction (which is experimentally of order MeV) and by adopting for the ratio of the square of the strength of the weak interaction to the strength of the strong interaction the value 10^{-13}. Thus, one expects $\Gamma^{\downarrow}\approx 10^{-6}$ eV.

The observable for parity violation is the longitudinal asymmetry (often simply referred to as "asymmetry")

$$P=\frac{\sigma_+^p-\sigma_-^p}{\sigma_+^p+\sigma_-^p}, \tag{108}$$

where $\sigma_{\pm}^p$ is the total *p*-wave cross section for neutrons with helicities $\pm$. Clearly, we have $P=0$ if parity is conserved. Asymmetries for a set of resonances were determined separately for each run of approximately 30 min and a histogram created for each nuclide and each resonance measured. The mean of this histogram was the value adopted for P.

We illustrate the analysis that determines $\overline{v^2}$ and the weak spreading width $\Gamma^{\downarrow}$ by considering a target nucleus with spin $I=0$ and positive parity. This case illustrates most of the principles involved. The *s*-wave resonances have spin and parity $1/2^+$ and the *p*-wave resonances $1/2^-$ or $3/2^-$. Only the $1/2^-$ resonances are considered as only these are mixed with the $1/2^+$ resonances by the parity-violating interaction. We use the formalism of Sec. IV.B. We neglect direct reactions, use the scattering matrix as given by Eqs. (41) and (42), and replace the Hamiltonian H^{GOE} in Eq. (47) by an expression of the form (98). The upper indices 1 and 2 now stand for states with positive and negative parity, respectively, and V denotes the induced parity-violating nucleon-nucleon interaction. We use the diagonal representation of $H^{(1)}$ and $H^{(2)}$ and denote the eigenvalues by $E_\mu^{(1)}$ and $E_\nu^{(2)}$ and the eigenfunctions by $|1\mu\rangle$ and $|2\nu\rangle$, respectively. The matrix (98) takes the form

$$\begin{pmatrix} E_\mu^{(1)}\delta_{\mu\nu} & \langle 1\mu|V|2\rho\rangle \\ \langle 2\sigma|V|1\nu\rangle & E_\rho^{(2)}\delta_{\rho\sigma}\end{pmatrix}. \tag{109}$$

In the diagonal representation of $H^{(1)}$ and $H^{(2)}$, the partial width amplitudes of the states with positive and negative parity are denoted by $g_\mu^{(1)}$ and $g_\rho^{(2)}$, respectively. We assume that the *p*-wave resonances are isolated and focus attention on a single one. We take the bombarding energy E in the center of that resonance, $E=E_\rho^{(2)}$. We neglect the total width of the resonance and of the admixed *s*-wave resonances since in all cases investigated so far the spacings $|E_\mu^{(1)}-E_\rho^{(2)}|$ are large compared to the total widths. This yields (Sushkov and Flambaum, 1980; Bunakov and Gudkov, 1981)

$$P_\rho=2\sum_\mu \frac{\langle 1\mu|V|2\rho\rangle}{E_\mu^{(1)}-E_\rho^{(2)}}\frac{g_\mu^{(1)}g_\rho^{(2)}}{\Gamma_\rho^{(n)}}, \tag{110}$$

where $\Gamma_\rho^{(n)}=(g_\rho^{(2)})^2$ is the partial width for neutron decay of the *p*-wave resonance with label ρ. The ratio $g_\mu^{(1)}g_\rho^{(2)}/\Gamma_\rho^{(n)}=g_\mu^{(1)}/g_\rho^{(2)}$ contains the kinematical enhancement factor and the first term on the right-hand side, the dynamical enhancement factor.

For spin-zero target nuclei, the resonance parameters are usually known. For the *s*-wave resonances, the information is available from previous work on *s*-wave neutron scattering. For the *p*-wave resonances, most of the information was obtained in the framework of the TRIPLE experiments. In practice one may assign the spin value of 1/2 to a *p*-wave resonance by the presence of parity violation. Unfortunately, one cannot determine the individual matrix elements $\langle 1\mu|V|2\rho\rangle$ since there are too few equations and too many unknowns. But using the fact that the matrix elements $\langle 1\mu|V|2\rho\rangle$ have a Gaussian distribution with mean value zero and a second moment given by $\overline{v^2}$, we write Eq. (110) in the form $P_\rho=\Sigma_\mu A_{\mu\rho}\langle 1\mu|V|2\rho\rangle$, with coefficients $A_{\mu\rho}=[2/(E_\mu^{(1)}-E_\rho^{(2)})](g_\mu^{(1)}/g_\rho^{(2)})$. Then, P_ρ is a linear combination of equally distributed Gaussian random variables and, therefore, is itself a Gaussian random variable with mean value zero. The variance of P_μ with respect to both μ and the ensemble generated by a sequence of runs is given by $A^2\overline{v^2}$, where $A^2=(1/N)\Sigma_{\mu\rho}A_{\mu\rho}^2$ and N is the number of *p*-wave resonances. It follows that

$$\overline{v^2}=\mathrm{var}(P_\mu)/A^2. \tag{111}$$

Equation (111) is the central result of the statistical approach. It yields $\overline{v^2}$ from the data in spite of the fact that the signs of the partial width amplitudes in Eq. (110) are usually not known. The analysis is more difficult for target nuclei with nonzero spin values. Moreover, usually some but not all spectroscopic information is available. Suitable methods of analysis were developed for all such cases (Mitchell *et al.*, 2001), but the spirit of the approach is the same. It yields the values of $\overline{v^2}$ and of $\Gamma^{\downarrow}$

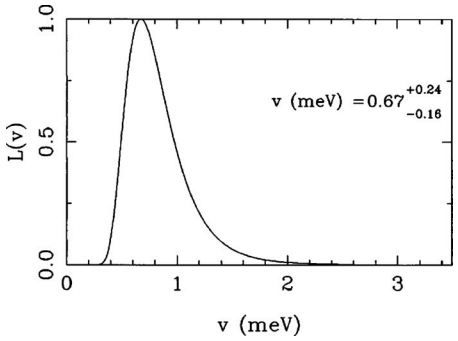

FIG. 23. Plot of the maximum-likelihood function $L(\nu)$ vs the root-mean-square matrix element ν for ^{238}U. The spins of all the p-wave resonances are known. From Mitchell *et al.*, 1999.

although the wave functions of the individual nuclear states are not known.

For the actual determination of $\overline{\nu^2}$, a maximum-likelihood approach was adopted. The value of P_ρ is a realization of a random variable. For a number of independent resonances the likelihood function is the product of the functions for the individual resonances. One inserts the values of the experimental asymmetries and their errors, determines the spectroscopic term A from the known resonance parameters, and calculates the likelihood function. The location of the maximum gives the most likely value ν_L of the root-mean-square matrix element $\nu=(\overline{\nu^2})^{1/2}$. A maximum-likelihood plot for ^{238}U is shown in Fig. 23. The likelihood function is found to have a well-defined maximum so that ν is rather well determined. When the analysis was applied to ^{232}Th, the mean value of $\langle 1\mu|V|2\rho\rangle$ was found to differ from zero, and a Gaussian with nonzero mean value was required to fit the data—all parity violations had the same sign. This result raised serious questions about the statistical approach and led to much theoretical activity. However, the anomaly only occurred in Thorium, and subsequent studies at higher energies in ^{232}Th revealed parity violations of opposite sign (Sharapov *et al.*, 2000). It was concluded that this "sign effect" was due to a local doorway state (see Sec. I.II.G).

Parity violation was studied in 20 nuclides—especially in those regions of mass number A where the p-wave strength function has maxima. (The strength function is defined and discussed in Secs. V.D and VII.A.) Maxima occur near $A=238$, i.e., for ^{232}Th and ^{238}U (maximum of the $4p$ strength function), and near $A=100$ where most of the other nuclides were studied (maximum of the $3p$ strength function). Parity violation was observed in all but one of these targets (^{93}Nb). For 15 nuclei sufficiently many resonances with parity violation were observed to determine the weak spreading width; for the other nuclides only very approximate values or limits could be determined. The values of $\Gamma^{\downarrow}$ lie around 10^{-6} eV as expected and are approximately independent of A, with some indications of local fluctuations. Such fluctuations have been observed in the spreading width for isospin mixing (Sec. VIII.A and Harney *et al.*, 1986).

In summary, except for the Thorium anomaly, the data are consistent with the statistical model. With the help of a statistical analysis, it is possible to determine the root-mean-square matrix element ν for parity violation and the weak spreading width $\Gamma^{\downarrow}$ without knowledge of the wave functions of individual nuclear states. The values found for $\Gamma^{\downarrow}$ are consistent with expectations based on the strength of the weak interaction [see Tomsovic *et al.* (2000) for an analysis]. For lack of space we have not discussed experiments on parity violation in fission (Kötzle *et al.*, 2000).

C. Time reversal

Time-reversal ($\mathcal{T}$) invariance implies symmetry of the S matrix, $S_{ab}=S_{ba}$, and, hence, detailed balance, $|S_{ab}|^2=|S_{ba}|^2$. Tests of $\mathcal{T}$ invariance compare resonance-scattering cross sections for the two-fragment reactions $a\to b$ and $b\to a$ at the same center-of-mass energy and aim at establishing an upper bound on the strength of the $\mathcal{T}$-invariance violating interaction in nuclei. Such experiments have been performed both for isolated and for strongly overlapping resonances more than 20 years ago and are well documented in the literature. Thus, we will be brief.

To test detailed balance, one compares the reaction rates $A_1+A_2\rightleftharpoons B_1+B_2$. The fragments A_1,A_2,B_1,B_2 are in their ground states and unpolarized. A difference in the rates $a\to b$ and $b\to a$ indicates a violation of $\mathcal{T}$ invariance. Detailed balance was tested by Driller *et al.* (1979) in the reactions $^{27}\mathrm{Al}+p\rightleftharpoons{}^{24}\mathrm{Mg}+\alpha$ populating an isolated $J^\pi=2^+$ resonance at an excitation energy $E_x=12.901$ MeV in the CN ^{28}Si. For a reaction through an isolated resonance, detailed balance would normally hold automatically (Henley and Jacobsohn, 1959). The present case is different because for the fragmentation $^{27}\mathrm{Al}+p$, the partial waves with angular momenta $l=0$ and $l=2$ and channel spin $s=2$ interfere (Pearson and Richter, 1975). The cross sections for the reactions $a\to b$ and $b\to a$ were found to agree within $\delta=0.0025\pm0.0192\%$. This result is consistent with $\delta=0$ and, thus, with $\mathcal{T}$ invariance.

Bunakov and Weidenmüller (1989) pointed out that in detailed-balance tests that use two close-lying CN resonances in the regime $\Gamma\ll d$, large enhancement factors amounting to several orders of magnitude for $\mathcal{T}$-invariance violation may arise. Mitchell *et al.* (1993) investigated specific experimental possibilities and showed that the difference δ of the two reaction cross sections depends sensitively on energy, angle, and the parameters of both resonances and may vary by many orders of magnitude. These theoretical predictions have been partially tested experimentally in billiards (Dietz *et al.*, 2007).

In the most precise test of detailed balance in CN reactions so far, the reactions $^{27}\mathrm{Al}(p,\alpha_0)^{24}\mathrm{Mg}$ and $^{24}\mathrm{Mg}(\alpha,p_0)^{27}\mathrm{Al}$ were compared in the Ericson regime $\Gamma\gg d$ (Blanke *et al.*, 1983). As in a predecessor of this experiment (von Witsch *et al.*, 1968), both reaction rates

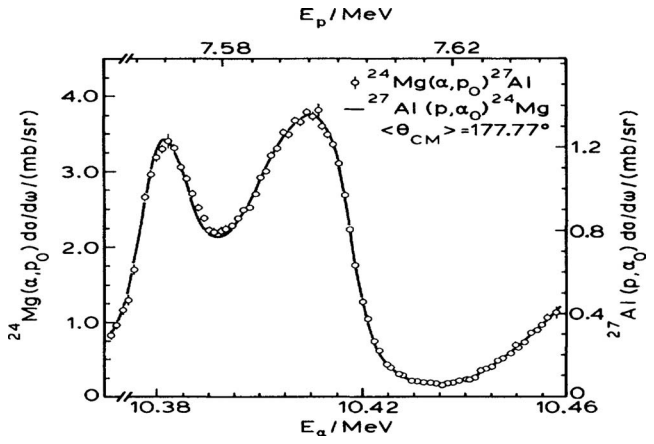

FIG. 24. Normalized cross sections for the reaction $^{27}\mathrm{Al}(p,\alpha_0)^{24}\mathrm{Mg}$ (solid line) and for the inverse reaction $^{24}\mathrm{Mg}(\alpha,p_0)^{27}\mathrm{Al}$ (open circles) near and at a deep minimum. The two cross sections are equal and detailed balance holds. From Blanke *et al.*, 1983.

were measured at a scattering angle of $\Theta \approx 180^\circ$ and normalized at a suitable cross-section maximum. The results were then compared at a cross-section minimum. This was done in order to maximize the sensitivity for $\mathcal{T}$-invariance violation. The result is shown in Fig. 24. The measured relative differential cross sections agree within the experimental uncertainty $\delta = \pm 0.51\%$ and are, thus, consistent with $\mathcal{T}$ invariance. From this result an upper bound $\xi \leqslant 5 \times 10^{-4}$ (80% confidence) for a possible $\mathcal{T}$-noninvariant amplitude in the CN reaction was derived.

At the time of the experiment, there was no adequate theoretical framework to interpret that upper bound. The development of the statistical theory made such an interpretation possible (Boosé *et al.*, 1986a, 1986b) and yielded upper bounds for both the strength of and the spreading width $\Gamma^{\downarrow}$ for the $\mathcal{T}$-invariance violating part of the nuclear Hamiltonian. Both bounds compare favorably with those derived from an analysis of spectral fluctuations [see Sec. I.III.D.4 and French *et al.* (1985, 1988b)]. As in the cases of violation of isospin and parity in Secs. VIII.A and VIII.B, the fundamental parameter is the spreading width, and the upper bound on this quantity is $\Gamma^{\downarrow} \leqslant 9 \times 10^{-2}$ eV. The upper bound from the detailed balance experiment of Blanke *et al.* (1983) has been improved by two orders of magnitude in an experiment on polarized neutron transmission through nuclear-spin-aligned Holmium (Huffmann *et al.*, 1997). The measurements test reciprocity and could possibly be improved by another order of magnitude with more intense neutron beams at new spallation sources and with other targets (Barabanov and Beda, 2005). The expected upper bounds for the strength of possible parity-conserving time-reversal-violating interactions will, however, still be several orders of magnitude larger than the ones provided by the upper limit on the electric dipole moment of the neutron for parity and time-reversal violating interactions (Baker *et al.*, 2006; Harris, 2007).

To include violation of $\mathcal{T}$ invariance in the statistical theory, the $\mathcal{T}$-invariant Hamiltonian ensemble H^{GOE} on the right-hand side of Eq. (47) is generalized (see Sec. I.III.D.4),

$$H^{\mathrm{GOE}} \to H = \frac{1}{\sqrt{1+(1/N)\alpha^2}}\left(H^{\mathrm{GOE}} + i\frac{\alpha}{\sqrt{N}}A\right). \quad (112)$$

The independent elements of the real, antisymmetric, N-dimensional matrix A are uncorrelated Gaussian-distributed random variables with zero mean values and second moments given by $\overline{A_{\mu\nu}A_{\rho\sigma}} = (\lambda^2/N)(\delta_{\mu\rho}\delta_{\nu\sigma} - \delta_{\mu\sigma}\delta_{\nu\rho})$. The parameter α measures the strength of $\mathcal{T}$-invariance violation. As explained in Sec. I.III.D.4, the normalization factor $N^{-1/2}$ is chosen so that significant invariance violation on the scale of the mean level spacing occurs for $\alpha \sim 1$. With the replacement (112) in Eq. (47), the calculation of measures for $\mathcal{T}$-invariance violation in the statistical theory is a formidable task. In the Ericson regime, Boosé *et al.* (1986a, 1986b) solved the problem by combining a perturbative treatment of A with an asymptotic expansion in powers of d/Γ. A treatment valid for all values of Γ/d was given by Pluhar *et al.* (1995) and Gerland and Weidenmüller (1996) and further developed for the analysis of scattering data on microwave resonators with induced violation of $\mathcal{T}$ invariance by Dietz *et al.* (2009). These results were based on progress in understanding the GOE→GUE crossover transition in spectra (Altland *et al.*, 1992, 1993). Dietz *et al.* (2009) replaced the parameter α by $\pi\xi$. The resulting expressions for measures of $\mathcal{T}$-invariance violation are complex and not reproduced here. We confine ourselves to a discussion of the results.

In Secs. VII.A and VII.B it was shown that many properties of chaotic scattering can be studied with the help of microwave resonators. This statement applies also to the violation of $\mathcal{T}$ invariance. In a flat chaotic microwave resonator—a quantum billiard—shown schematically in Fig. 14, $\mathcal{T}$-invariance violation can be induced by placing a ferrite (magnetized by an external field) into the resonator. The spins within the ferrite precess with their Larmor frequency about the magnetic field. This induces a chirality into the system. The magnetic-field component of the radio frequency (rf) field in the resonator can be split into two circularly polarized fields rotating in opposite directions with regard to that static magnetic field. The component that has the same rotational direction and frequency as the rotating spins is attenuated by the ferrite. This causes $\mathcal{T}$-invariance violation. The strongest effect is expected to occur when Larmor frequency and rf frequency coincide. Connecting the resonator to two antennas, one defines a scattering system. The violation of $\mathcal{T}$ invariance then causes the scattering amplitudes S_{12} and S_{21} to differ.

Experiments on induced $\mathcal{T}$-reversal invariance violation in microwave billiards offer two advantages. First, by a measurement of phases and amplitudes of the reflected and transmitted rf signals, it is possible to test the reciprocity relation $S_{ab} = S_{ba}$ while experiments with

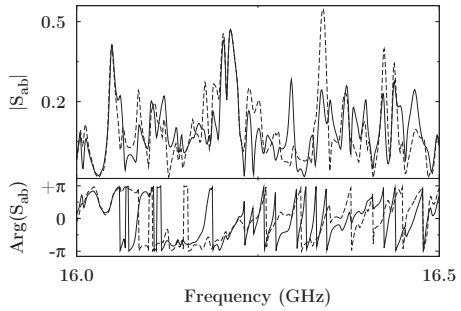

FIG. 25. Magnitude and phase of S_{12} (solid lines) and S_{21} (dashed lines) measured in the frequency interval from 16 to 16.5 GHz for a fixed magnetization of the ferrite. From Dietz *et al.*, 2009.

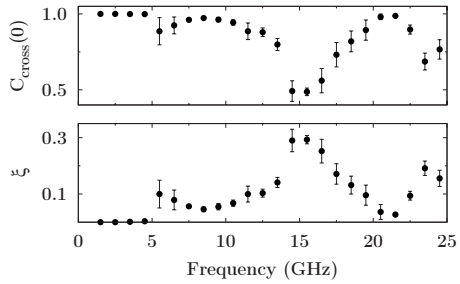

FIG. 26. Cross-correlation coefficient. Upper panel: Values of $C_{\mathrm{cross}}(0)$ calculated from the fluctuating matrix elements S_{12} and S_{21} of Fig. 25. Lower panel: The parameter ξ vs frequency as deduced from the data. From Dietz *et al.*, 2009.

nuclear reactions typically test only the weaker detailed-balance relation $|S_{ab}|^2=|S_{ba}|^2$. Second, such experiments offer the unique chance of a stringent and detailed test of the statistical theory that is otherwise often taken for granted and used to analyze data on CN reactions.

Induced violation of $\mathcal{T}$ invariance in microwave billiards has so far been studied in two scattering experiments. In the first one (Dietz *et al.*, 2007), a vector network analyzer was used to measure magnitudes and phases of S-matrix elements in a fully chaotic "annular" billiard (Dembowski *et al.*, 2000; Hofferbert *et al.*, 2005) in the regime $\Gamma \ll d$. By interchanging input and output antennas, both S_{12} and S_{21} were measured. For all eight isolated resonances (singlets) that were investigated, the complex element S_{12} agrees with S_{21}, i.e., reciprocity holds, in agreement with Henley and Jacobsohn (1959). For the three pairs of partially overlapping resonances (doublets) that were studied reciprocity was found to be violated. The dependence of the $\mathcal{T}$-violating matrix elements of the effective Hamiltonian for the microwave billiard on the magnetization of the ferrite could be determined with the help of Eqs. (112), (41), and (47).

In the second experiment (Dietz *et al.*, 2009), induced violation of $\mathcal{T}$ invariance was investigated in the regime of weakly overlapping resonances. A small cylindrical ferrite was placed within the fully chaotic tilted-stadium billiard shown in the inset of Fig. 10. The ferrite was magnetized by an external magnetic field. Again the elements S_{12} and S_{21} of the complex-valued S matrix were measured versus resonance frequency. Figure 25 shows that magnitude and phase of the S-matrix elements fluctuate strongly and reciprocity is violated. The value of the normalized cross-correlation coefficient

$$C_{\mathrm{cross}}(0) = \mathrm{Re}\,\frac{S_{12}(f)S_{21}^*(f)}{[|S_{12}|^2|S_{21}|^2]^{1/2}} \tag{113}$$

serves as a measure of the strength of $\mathcal{T}$-invariance violation. $\mathcal{T}$ invariance holds (is completely violated) for $C_{\mathrm{cross}}(0)=1$ $[C_{\mathrm{cross}}(0)=0]$. The upper panel of Fig. 26 shows that $C_{\mathrm{cross}}(0)$ depends strongly on frequency. Complete violation of $\mathcal{T}$ invariance is never attained. The lower panel shows the value of the parameter $\xi = \alpha/\pi$ for $\mathcal{T}$-invariance violation deduced from the data.

The data were used for a thorough test of the underlying theory (Dietz *et al.*, 2009). The parameters of the theory (the transmission coefficients T_1 and T_2 in the two antenna channels, a parameter describing Ohmic absorption by the walls of resonator and ferrite, and ξ) were fitted to the Fourier-transformed S-matrix elements. As in Sec. VII.A, a goodness-of-fit test was used to establish the quality of the fit, with excellent results. Moreover, values of the elastic enhancement factor versus frequency were predicted correctly by the theory without further fit parameters. We recall that for $\mathcal{T}$-invariant systems the factor takes values between 2 and 3 [see the remarks below Eq. (65)]. Experimentally, values well below 2 were found in some frequency intervals. These are possible only if $\mathcal{T}$ invariance is violated.

IX. SUMMARY AND CONCLUSIONS

The Bohr assumption on independence of formation and decay of the CN was the first of several insightful conjectures concerning compound-nucleus scattering. It laid the ground for all later developments and was followed by the Hauser-Feshbach formula, the Weisskopf estimate, Ericson's idea of random fluctuations of nuclear cross sections, and the generalization of the Hauser-Feshbach formula for the case of direct reactions. By way of justification, all of these developments referred to the fact that the resonances that dominate compound-nucleus reactions have statistical properties. The work anticipated general features of quantum chaotic scattering discovered only many years later.

The challenge to actually derive these conjectures from the statistical properties of resonances was taken up early. But it took several decades and the efforts of many people until a comprehensive theory of compound-nucleus scattering was established. The theory is based on a description of the statistics of resonances in terms of Wigner's random matrices. The description applies generically to resonances in chaotic quantum systems. As a result, the statistical theory of nuclear reactions is, at the same time, a generic random-matrix theory of quantum chaotic scattering. For systems with few degrees of freedom, it competes with the semiclassical approach to chaotic scattering. The latter incorporates system-specific features in the form of short

periodic orbits. In the statistical theory, such features enter as input parameters. Unfortunately, the semiclassical approach has so far not been extended to many-body systems.

The development of the theory posed essentially two major challenges: (i) How to incorporate random-matrix theory into scattering theory and (ii) how to calculate moments and correlation functions of S-matrix elements from that input. The first problem required a formulation of scattering theory in terms of the Hamiltonian governing the quasibound states that turn into resonances as the coupling to the channels is taken into account. The second problem was solved with the help of methods adopted from quantum field theory. Such methods have found wide application in condensed-matter theory. The connection to this area of physics is not one of technicalities only. It actually connects the statistical theory of nuclei with the statistical mechanics of many-body systems. Conceptually, it shows how a separation of scales is achieved in the limit of large matrix dimension N: Universal features govern the system on an energy scale given by the mean level spacing d. The unphysical properties of random-matrix theory (i.e., the shape of the average spectrum) matter on the scale Nd.

The ensuing statistical theory is a complete theory that uses the minimum number of input parameters and has predictive power. As is typical for many applications of random-matrix theory, the statistical theory predicts fluctuations in terms of mean values. The latter comprise the values of the energy-averaged elements of the scattering matrix and, in the case of correlation functions, the mean level spacing d. It is here that system-specific features enter. Examples are the optical model and the strength function which reflect properties of the nuclear shell model. The theory predicts the values of moments and correlation functions of S-matrix elements. These determine mean values and fluctuation properties of cross sections and other observables. The resulting expressions vindicate the early conjectures, define the limits of their applicability, and yield expressions that hold under more general circumstances. The S-matrix autocorrelation function is a case in point. In nuclei, the range of energies where the statistical theory applies is limited by the underlying assumption that random-matrix theory correctly describes the statistical properties of resonances. This is true only when the nuclear equilibration time is shorter than the average lifetime of the compound nucleus and holds for bombarding energies up to 20 MeV or so. Beyond this range, precompound processes modify the reaction dynamics.

The theory has been the object of stringent tests, largely performed with the help of microwave billiards. These have been extremely successful. There is no reason to doubt that the theory adequately accounts for all aspects of chaotic scattering even though one aspect of the theory has received little attention so far and has not been seriously tested: the unitary transformation in channel space that takes into account the direct reactions. The reason is that direct reactions and CN processes are almost mutually exclusive. When one is important, the other one typically is not and vice versa.

The theory has found numerous applications both within and outside the field of nuclear physics. These have only partly been reviewed. We have paid special attention to violations of parity, isospin, and time-reversal invariance. In the first two cases, the theory allows for the determination of the strength of the symmetry-violating interaction. In the case of time reversal, it yields an upper bound on this strength.

The calculation of moments and correlation functions of the S matrix from the statistical theory is not as complete as one may wish. It would perhaps be unrealistic to expect complete knowledge of all moments and all correlation functions. The theoretical effort grows immensely with increasing order of such expressions. Moreover, moments and correlation functions of low order only can reliably be determined from the finite range of data typically available in experiments. But it would be desirable to have theoretical expressions for cross-section correlation functions even though approximate expressions are available. This poses a continuing challenge for theorists.

ACKNOWLEDGMENTS

We are indebted to many colleagues from whom we have learned much about nuclear reactions and stochastic scattering. We are especially grateful to Y. Alhassid, Y. Fyodorov, G. Garvey, S. Grimes, H. L. Harney, S. Tomsovic, and V. Zelevinsky for critical reading of the paper and for many valuable comments and suggestions, to T. Ericson, K. Jungmann, N. Severijns, H.-J. Stöckmann, and W. Wilschut, for discussions, and to H. Schomerus for correspondence. We also thank S. Bittner and F. Schäfer for help in the preparation of the paper. A.R. is much indebted to B. Dietz and the other members of the Quantum Chaos Group in Darmstadt for the long and intense collaboration in the experiments with microwave billiards. G.E.M. and H.A.W. thank the Institute for Nuclear Theory for its hospitality during the completion of this paper. This work was supported in part by the U.S. Department of Energy Grant No. DE-FG02-97ER41042 and by the DFG within Grant No. SFB 634.

REFERENCES

Åberg, S., T. Guhr, M. Miski-Oglu, and A. Richter, 2008, Phys. Rev. Lett. **100**, 204101.

Adelberger, E. G., and W. C. Haxton, 1985, Annu. Rev. Nucl. Part. Sci. **35**, 501.

Agassi, D., H. A. Weidenmüller, and G. Mantzouranis, 1975, Phys. Rep. **22**, 145.

Alfimenkov, V. P., S. B. Borzakov, Vo Van Thuan, Yu. D. Mareev, L. B. Pikelner, A. S. Khrykin, and E. I. Sharapov, 1983, Nucl. Phys. A **398**, 93.

Alfimenkov, V. P., S. B. Borzakov, Vo Van Thuan, Yu. D. Mareev, L. B. Pikelner, A. S. Khrykin, and E. I. Sharapov, 1984, JETP Lett. **39**, 416.

Alhassid, Y., 2000, Rev. Mod. Phys. **72**, 895.

Alt, H., C. I. Barbosa, H. D. Gräf, T. Guhr, H. L. Harney, R. Hofferbert, H. Rehfeld, and A. Richter, 1998, Phys. Rev. Lett. **81**, 4847.

Alt, H., H.-D. Gräf, H. L. Harney, R. Hofferbert, H. Lengeler, A. Richter, R. Schardt, and H. A. Weidenmüller, 1995, Phys. Rev. Lett. **74**, 62.

Altland, A., S. Iida, and K. B. Efetov, 1993, J. Phys. A **26**, 3545.

Altland, A., S. Iida, A. Müller-Groeling, and H. A. Weidenmüller, 1992, Ann. Phys. (N.Y.) **219**, 148.

Austern, N. F., 1970, *Direct Nuclear Reaction Theories* (Wiley, New York).

Baker, C. A., D. D. Doyle, P. Geltenbort, K. Green, M. G. D. van der Grinten, P. G. Harris, P. Iaydjiev, S. N. Ivanov, D. J. R. May, J. M. Pendlebury, J. D. Richardson, D. Shiers, and K. F. Smith, 2006, Phys. Rev. Lett. **97**, 131801.

Baltes, H. P., and E. R. Hilf, 1976, *Spectra of Finite Systems* (Wissenschaftsverlag, Mannheim).

Barabanov, A. L., and A. G. Beda, 2005, J. Phys. G **31**, 161.

Bateman, F. B., S. M. Grimes, N. Boukharouba, V. Mishra, C. E. Brient, R. S. Pedroni, T. N. Massey, and R. C. Haight, 1997, Phys. Rev. C **55**, 133.

Beck, F., C. Dembowski, A. Heine, and A. Richter, 2003, Phys. Rev. E **67**, 066208.

Beenakker, C. W., 1997, Rev. Mod. Phys. **69**, 731.

Berezin, F. A., 1986, in *Method of Second Quantization*, 2nd ed., edited by M. K. Polivanov (Nauka, Moscow).

Bethe, H. A., 1937, Rev. Mod. Phys. **9**, 69.

Bilpuch, E. G., A. M. Lane, G. E. Mitchell, and J. D. Moses, 1976, Phys. Rep. **28**, 145.

Bilpuch, E. G., J. D. Moses, F. O. Purser, H. W. Newson, R. O. Nelson, D. Outlaw, and G. E. Mitchell, 1974, Phys. Rev. C **9**, 1589.

Blanke, E., H. Driller, W. Glöckle, H. Genz, A. Richter, and G. Schrieder, 1983, Phys. Rev. Lett. **51**, 355.

Blann, M., 1975, Annu. Rev. Nucl. Sci. **25**, 123.

Blatt, J. M., and L. C. Biedenharn, 1952, Rev. Mod. Phys. **24**, 258.

Blatt, J. M., and V. F. Weisskopf, 1952, *Theoretical Nuclear Physics* (Wiley, New York).

Blin-Stoyle, R. J., 1960, Phys. Rev. **120**, 181.

Blümel, R., and U. Smilansky, 1988, Phys. Rev. Lett. **60**, 477.

Bohigas, O., M. J. Giannoni, and C. Schmit, 1984, Phys. Rev. Lett. **52**, 1.

Bohigas, O., and H. A. Weidenmüller, 1988, Annu. Rev. Nucl. Part. Sci. **38**, 421.

Bohr, A., and B. Mottelson, 1969, *Nuclear Structure* (Benjamin, New York).

Bohr, N., 1936, Nature (London) **137**, 344.

Bohr, N., and J. A. Wheeler, 1939, Phys. Rev. **56**, 426.

Boosé, D., H. L. Harney, and H. A. Weidenmüller, 1986a, Phys. Rev. Lett. **56**, 2012.

Boosé, D., H. L. Harney, and H. A. Weidenmüller, 1986b, Z. Phys. A **325**, 363.

Bortignon, P. F., A. Bracco, and R. A. Broglia, 1998, *Giant Resonances: Nuclear Structure at Finite Temperatures* (Harwood Academic, Amsterdam).

Brink, D. M., and R. O. Stephen, 1963, Phys. Lett. **5**, 77.

Brink, D. M., R. O. Stephen, and N. W. Tanner, 1964, Nucl. Phys. **54**, 577.

Brody, T. A., J. Flores, J. B. French, P. A. Mello, A. Pandey, and S. S. M. Wong, 1981, Rev. Mod. Phys. **53**, 385.

Brouwer, P. W., 1995, Phys. Rev. B **51**, 16878.

Brouwer, P. W., K. M. Frahm, and C. W. J. Beenakker, 1997, Phys. Rev. Lett. **78**, 4737.

Brouwer, P. W., K. M. Frahm, and C. W. J. Beenakker, 1999, Waves Random Media **9**, 91.

Brown, G. E., 1959, Rev. Mod. Phys. **31**, 893.

Bunakov, V. E., and V. P. Gudkov, 1981, Z. Phys. A **303**, 285.

Bunakov, V. E., and H. A. Weidenmüller, 1990, Phys. Rev. C **42**, 1718.

Bunimovich, L. A., 1985, Sov. Phys. JETP **62**, 842.

Carter, J., H. Diesener, U. Helm, G. Herbert, P. von Neumann-Cosel, A. Richter, G. Schrieder, and S. Strauch, 2001, Nucl. Phys. A **696**, 317.

Celardo, G. L., F. M. Izrailev, V. G. Zelevinsky, and G. P. Berman, 2007, Phys. Rev. E **76**, 031119.

Celardo, G. L., F. M. Izrailev, V. G. Zelevinsky, and G. P. Berman, 2008, Phys. Lett. B **659**, 170.

Davis, E. D., and D. Boosé, 1988, Phys. Lett. B **211**, 379.

Davis, E. D., and D. Boosé, 1989, Z. Phys. A **332**, 427.

Davis, S., C. Glashausser, A. B. Robbins, G. Bissinger, R. Albrecht, and J. P. Wurm, 1975, Phys. Rev. Lett. **34**, 215.

Dembowski, C., B. Dietz, T. Friedrich, H.-D. Gräf, H. L. Harney, A. Heine, M. Miski-Oglu, and A. Richter, 2005, Phys. Rev. E **71**, 046202.

Dembowski, C., H.-D. Gräf, A. Heine, R. Hofferbert, H. Rehfeld, and A. Richter, 2000, Phys. Rev. Lett. **84**, 867.

Desplanques, B., J. F. Donoghue, and B. R. Holstein, 1980, Ann. Phys. (N.Y.) **124**, 449.

Dicke, R. H., 1954, Phys. Rev. **93**, 99.

Diener, E. M., J. F. Amann, and P. Paul, 1973, Phys. Rev. C **7**, 695.

Diesener, H., U. Helm, V. Huck, P. von Neumann-Cosel, C. Rangacharyulu, A. Richter, G. Schrieder, A. Stascheck, S. Strauch, J. Rykebusch, and J. Carter, 2001, Nucl. Phys. A **696**, 293.

Diesener, H., U. Helm, P. von Neumann-Cosel, A. Richter, G. Schrieder, A. Stascheck, A. Stiller, and J. Carter, 2001, Nucl. Phys. A **696**, 272.

Dietz, B., T. Friedrich, H. L. Harney, M. Miski-Oglu, A. Richter, F. Schäfer, J. Verbaarschot, and H. A. Weidenmüller, 2009, Phys. Rev. Lett. **103**, 064101.

Dietz, B., T. Friedrich, H. L. Harney, M. Miski-Oglu, A. Richter, F. Schäfer, and H. A. Weidenmüller, 2007, Phys. Rev. Lett. **98**, 074103.

Dietz, B., T. Friedrich, H. L. Harney, M. Miski-Oglu, A. Richter, F. Schäfer, and H. A. Weidenmüller, 2008, Phys. Rev. E **78**, 055204R.

Dietz, B., T. Friedrich, H. L. Harney, M. Miski-Oglu, A. Richter, F. Schäfer, and H. A. Weidenmüller, 2010, Phys. Rev. E **81**, 036205.

Dietz, B., T. Guhr, H. L. Harney, and A. Richter, 2006, Phys. Rev. Lett. **96**, 254101.

Dietz, B., H. L. Harney, A. Richter, F. Schäfer, and H. A. Weidenmüller, 2010, Phys. Lett. B **685**, 263.

Dietz, B., A. Richter, and H. A. Weidenmüller, 2010, private communication.

Dietz, B., and H. A. Weidenmüller, 2010, Phys. Lett. B **693**, 316.

Di Pietro, A., P. Figuera, R. Neal, C. Sükösd, F. Amorini, F. Binon, W. Bradfield-Smith, M. Cabibbo, G. Cardella, R. Coszach, T. Davinson, P. Duhamel, A. Emmi, R. Irvine, P. Leleux, J. Mackenzie, A. Musumarra, A. Ninane, M. Papa, G. Pappalardo, F. Rizzo, A. C. Shotter, S. Tudisco, J. Vanhorenbeeck, and P. J. Woods, 2001, Nucl. Phys. A **689**, 668.

Dirac, P. A. M., 1958, *The Principles of Quantum Mechanics*, 4th ed. (Oxford University Press, New York).
Dittes, F.-M., H. L. Harney, and A. Müller, 1992, Phys. Rev. A **45**, 701.
Doll, P., G. J. Wagner, K. T. Knöpfle, and G. Mairle, 1976, Nucl. Phys. A **263**, 210.
Doron, E., U. Smilansky, and A. Frenkel, 1990, Phys. Rev. Lett. **65**, 3072.
Driller, H., E. Blanke, H. Genz, A. Richter, G. Schrieder, and J. M. Pearson, 1979, Nucl. Phys. A **317**, 300.
Dyson, F. J., 1962a, J. Math. Phys. **3**, 140.
Dyson, F. J., 1962b, J. Math. Phys. **3**, 157.
Dyson, F. J., 1962c, J. Math. Phys. **3**, 166.
Edwards, S. F., and P. W. Anderson, 1975, J. Phys. F: Met. Phys. **5**, 965.
Efetov, K. B., 1983, Adv. Phys. **32**, 53.
Engelbrecht, C., and H. A. Weidenmüller, 1973, Phys. Rev. C **8**, 859.
Ericson, T., 1960, Phys. Rev. Lett. **5**, 430.
Ericson, T., 1963, Ann. Phys. (N.Y.) **23**, 390.
Ericson, T., and T. Mayer-Kuckuk, 1966, Annu. Rev. Nucl. Sci. **16**, 183.
Ericson, T. E. O., 1965, *Nuclear Structure Physics*, Lectures in Theoretical Physics (Cambridge University Press, Boulder, CO), Vol. VIII.
Fano, U., 1961, Phys. Rev. **124**, 1866.
Feshbach, H., 1958, Ann. Phys. (N.Y.) **5**, 357.
Feshbach, H., 1962, Ann. Phys. (N.Y.) **19**, 287.
Feshbach, H., 1964, Rev. Mod. Phys. **36**, 1076.
Feshbach, H., C. E. Porter, and V. F. Weisskopf, 1954, Phys. Rev. **96**, 448.
Frahm, K. M., H. Schomerus, M. Patra, and C. W. J. Beenakker, 2000, Europhys. Lett. **49**, 48.
French, J. B., V. K. B. Kota, A. Pandey, and S. Tomsovic, 1985, Phys. Rev. Lett. **54**, 2313.
French, J. B., V. K. B. Kota, A. Pandey, and S. Tomsovic, 1988a, Ann. Phys. (N.Y.) **181**, 198.
French, J. B., V. K. B. Kota, A. Pandey, and S. Tomsovic, 1988b, Ann. Phys. (N.Y.) **181**, 235.
Friedman, F., and V. F. Weisskopf, 1955, *Niels Bohr and the Development of Physics* (Pergamon, London).
Friedman, W. A., and P. A. Mello, 1985, Ann. Phys. (N.Y.) **161**, 276.
Fyodorov, Y. V., and B. A. Khoruzhenko, 1999, Phys. Rev. Lett. **83**, 65.
Fyodorov, Y. V., B. A. Khoruzhenko, and H. J. Sommers, 1997, Phys. Lett. A **226**, 46.
Fyodorov, Y. V., and D. V. Savin, 2010, *Oxford Handbook on Random-Matrix Theory* (Oxford University Press, New York, in press).
Fyodorov, Y. V., D. V. Savin, and H. J. Sommers, 1997, Phys. Rev. E **55**, R4857.
Fyodorov, Y. V., D. V. Savin, and H. J. Sommers, 2005, J. Phys. A **38**, 10731.
Fyodorov, Y. V., and H. J. Sommers, 1996, JETP Lett. **63**, 1026.
Fyodorov, Y. V., and H. J. Sommers, 1997, J. Math. Phys. **38**, 1918.
Fyodorov, Y. V., and H. J. Sommers, 2003, J. Phys. A **36**, 3303.
Gallmann, A., P. Wagner, G. Franck, D. Wilmore, and P. E. Hodgson, 1966, Nucl. Phys. **88**, 654.
Gaspard, P., 1991, in *Quantum Chaos*, edited by G. Casati *et al.*, Proceedings of the Summer School E. Fermi (North-Holland, Amsterdam), p. 307.
Gaspard, P., and S. Rice, 1989a, J. Chem. Phys. **90**, 2225.
Gaspard, P., and S. Rice, 1989b, J. Chem. Phys. **90**, 2242.
Gerland, U., and H. A. Weidenmüller, 1996, Europhys. Lett. **35**, 701.
Glendenning, N. K., 2004, *Direct Nuclear Reactions* (World Scientific, Hong Kong).
Goeke, K., and J. Speth, 1982, Annu. Rev. Nucl. Part. Sci. **32**, 65.
Gräf, H.-D., H. L. Harney, H. Lengeler, C. H. Lewenkopf, C. Rangacharyulu, A. Richter, P. Schardt, and H. A. Weidenmüller, 1992, Phys. Rev. Lett. **69**, 1296.
Graw, G., H. Clement, J. H. Feist, W. Kretschmer, and P. Pröel, 1974, Phys. Rev. C **10**, 2340.
Grimes, S. M., 2002, J. Nucl. Sci. Technol. **2**, 709.
Gutzwiller, M., 1990, *Chaos in Classical and Quantum Mechanics* (Springer-Verlag, Berlin).
Haake, F., F. Izrailev, N. Lehmann, D. Sabor, and H. J. Sommers, 1992, Z. Phys. B: Condens. Matter **88**, 359.
Hackenbroich, G., and H. A. Weidenmüller, 1995, Phys. Rev. Lett. **74**, 4118.
Harakeh, M. N., D. H. Dowell, G. Feldman, E. F. Garman, R. Loveman, J. L. Osborne, and K. A. Snover, 1986, Phys. Lett. B **176**, 297.
Harakeh, M. N., and A. van der Woude, 2001, *Giant Resonances: Fundamental High-Frequency Modes of Nuclear Excitation* (Oxford University Press, New York).
Harney, H. L., F.-M. Dittes, and A. Müller, 1992, Ann. Phys. (N.Y.) **220**, 159.
Harney, H. L., A. Richter, and H. A. Weidenmüller, 1986, Rev. Mod. Phys. **58**, 607.
Harris, P., 2007, e-print arXiv:0709.3100.
Hart, J. A., T. M. Antonsen, Jr., and E. Ott, 2009, Phys. Rev. E **79**, 016208.
Hauser, W., and H. Feshbach, 1952, Phys. Rev. **87**, 366.
Henley, E. M., and B. A. Jacobsohn, 1959, Phys. Rev. **113**, 225.
Heusler, S., S. Müller, A. Altland, P. Braun, and F. Haake, 2007, Phys. Rev. Lett. **98**, 044103.
Hodgson, P. E., 1963, *The Optical Model of Elastic Scattering* (Clarendon, Gloucestershire).
Hofferbert, R., H. Alt, C. Dembowski, H.-D. Gräf, H. L. Harney, A. Heine, H. Rehfeld, and A. Richter, 2005, Phys. Rev. E **71**, 046201.
Hofmann, H. M., J. Richert, and W. Tepel, 1975, Ann. Phys. (N.Y.) **90**, 391.
Hofmann, H. M., J. Richert, W. Tepel, and H. A. Weidenmüller, 1975, Ann. Phys. (N.Y.) **90**, 403.
Holbrow, C. H., and H. H. Barschall, 1963, Nucl. Phys. **42**, 264.
Huffmann, P. R., N. R. Roberson, W. S. Wilburn, C. R. Gould, D. G. Haase, C. D. Keith, B. W. Raichle, M. L. Seely, and J. R. Walston, 1997, Phys. Rev. C **55**, 2684.
Hüfner, J., C. Mahaux, and H. A. Weidenmüller, 1967, Nucl. Phys. A **105**, 489.
Humblet, J., and L. Rosenfeld, 1961, Nucl. Phys. **26**, 529.
Imry, J., 2002, *Introduction to Mesoscopic Physics*, 2nd ed. (Oxford University Press, Oxford).
Jänecke, J., 1969, in *Isospin in Nuclear Physics*, edited by D. H. Wilkinson (North-Holland, Amsterdam), p. 297.
Kawai, M., A. K. Kerman, and K. W. McVoy, 1973, Ann. Phys. (N.Y.) **75**, 156.
Kerman, A. K., and A. Sevgen, 1976, Ann. Phys. (N.Y.) **102**, 570.
Keyworth, G. A., G. C. Kyker, Jr., E. G. Bilpuch, and H. W. Newson, 1966, Nucl. Phys. **89**, 590.

Kicińska-Habior, M., 2005, Acta Phys. Pol. B **36**, 1133.
Kicińska-Habior, M., K. A. Snover, J. A. Behr, C. A. Gossett, J. H. Gundlach, Z. M. Drebi, M. S. Kaplan, and D. P. Wells, 1994, Nucl. Phys. A **569**, 17.
Kleinwächter, P., and I. Rotter, 1985, Phys. Rev. C **32**, 1742.
Koning, A. J., and J. M. Akkermans, 1991, Ann. Phys. (N.Y.) **208**, 216.
Koning, A. J., and J. P. Delaroche, 2003, Nucl. Phys. A **713**, 231.
Kötzle, A., P. Jesinger, F. Gönnenwein, G. A. Petrov, V. I. Petrova, A. M. Gagarski, G. Danilyan, O. Zimmer, and V. Nesvizhevsky, 2000, Nucl. Instrum. Methods Phys. Res. A **440**, 750.
Kretschmer, W., and M. Wangler, 1978, Phys. Rev. Lett. **41**, 1224.
Kuhl, U., R Höhmann, J. Main, and H.-J. Stöckmann, 2008, Phys. Rev. Lett. **100**, 254101.
Lane, A. M., 1969, in *Isospin in Nuclear Physics*, edited by D. H. Wilkinson (North-Holland, Amsterdam), p. 509.
Lane, A. M., 1971, Ann. Phys. (N.Y.) **63**, 171.
Lane, A. M., and J. E. Lynn, 1957, Proc. R. Soc. (London), Sect. A **70**, 557.
Lane, A. M., J. E. Lynn, and J. D. Moses, 1974, Nucl. Phys. A **232**, 189.
Lane, A. M., and R. G. Thomas, 1958, Rev. Mod. Phys. **30**, 257.
Lehmann, N., D. Saher, V. V. Sokolov, and H. J. Sommers, 1995, Nucl. Phys. A **582**, 223.
Lehmann, N., D. V. Savin, V. V. Sokolov, and H. J. Sommers, 1995, Physica D **86**, 572.
Lemmer, R. H., and C. M. Shakin, 1964, Ann. Phys. (N.Y.) **27**, 13.
Lewenkopf, C. H., A. Müller, and E. Doron, 1992, Phys. Rev. A **45**, 2635.
Lewenkopf, C. H., and H. A. Weidenmüller, 1991, Ann. Phys. (N.Y.) **212**, 53.
Londergan, J. T., J. C. Peng, and A. W. Thomas, 2010, Rev. Mod. Phys. **82**, 2009.
Lynn, J. E., 1968, *The Theory of Neutron Resonance Reactions* (Clarendon, Oxford).
Lynn, J. E., 1969, *Report of Second IAEA Symposium of Physics and Chemistry of Fission* (IAEA, Vienna), p. 249.
Lyuboshitz, V. L., 1978a, Sov. Phys. JETP **28**, 30.
Lyuboshitz, V. L., 1978b, Sov. J. Nucl. Phys. **27**, 502.
Madroñero, J., and A. Buchleitner, 2005, Phys. Rev. Lett. **95**, 263601.
Mahaux, C., and H. A. Weidenmüller, 1969, *Shell-Model Approach to Nuclear Reactions* (North-Holland, Amsterdam).
Mahaux, C., and H. A. Weidenmüller, 1979, Annu. Rev. Nucl. Part. Sci. **29**, 1.
Main, J., and G. Wunner, 1992, Phys. Rev. Lett. **69**, 586.
Mello, P. A., P. Pereyra, and T. H. Seligman, 1985, Ann. Phys. (N.Y.) **161**, 254.
Michel, N., W. Nazarewicz, and M. Ploszajczak, 2004, Phys. Rev. C **70**, 064313.
Miller, G., A. K. Opper, and E. J. Stephenson, 2006, Annu. Rev. Nucl. Part. Sci. **56**, 253.
Mitchell, G. E., E. G. Bilpuch, C. R. Bybee, J. M. Drake, and J. F. Shriner, Jr., 1993, Nucl. Phys. A **560**, 483.
Mitchell, G. E., E. G. Bilpuch, J. F. Shriner, Jr., and A. M. Lane, 1985, Phys. Rep. **117**, 1.
Mitchell, G. E., J. D. Bowman, S. I. Penttilä, and E. I. Sharapov, 2001, Phys. Rep. **354**, 157.
Mitchell, G. E., J. D. Bowman, and H. A. Weidenmüller, 1999, Rev. Mod. Phys. **71**, 445.
Moldauer, P. A., 1961, Phys. Rev. **123**, 968.
Moldauer, P. A., 1963, Phys. Rev. **129**, 754.
Moldauer, P. A., 1964, Phys. Rev. **135**, B642.
Moldauer, P. A., 1969, Phys. Rev. **177**, 1841.
Moldauer, P. A., 1975a, Phys. Rev. C **11**, 426.
Moldauer, P. A., 1975b, Phys. Rev. C **12**, 744.
Moldauer, P. A., 1976, Phys. Rev. C **14**, 764.
Moldauer, P. A., 1980, Nucl. Phys. A **344**, 185.
Moses, E. I., R. N. Boyd, B. A. Remington, C. J. Keane, and R. Al-Ayat, 2009, Phys. Plasmas **16**, 041006.
Mulhall, D., A. Volya, and V. Zelevinsky, 2000 Phys. Rev. Lett. **85**, 4016.
Nishioka, H., and H. A. Weidenmüller, 1985, Phys. Lett. **157B**, 101.
Nörenberg, W., and H. A. Weidenmüller, 1980, *Introduction to the Theory of Heavy-Ion Collisions*, Lecture Notes in Physics Vol. 51 (Springer-Verlag, Berlin).
Okolowicz, J., M. Ploszajczak, and I. Rotter, 2003, Phys. Rep. **374**, 271.
Ossipov, A., and Y. V. Fyodorov, 2005, Phys. Rev. B **71**, 125133.
Ott, E., 2009, private communication.
Papenbrock, T., and H. A. Weidenmüller, 2007, Rev. Mod. Phys. **79**, 997.
Papenbrock, T., and H. A. Weidenmüller, 2008, Phys. Rev. C **78**, 054305.
Pearson, J. M., and A. Richter, 1975, Phys. Lett. **56B**, 112.
Pluhar, Z., H. A. Weidenmüller, J. A. Zuk, C. H. Lewenkopf, and F. J. Wegner, 1995, Ann. Phys. (N.Y.) **243**, 1.
Porter, C. E., 1965, *Statistical Theories of Spectra: Fluctuations* (Academic, New York).
Porter, C. E., and R. G. Thomas, 1956, Phys. Rev. **104**, 483.
Primack, H., and U. Smilansky, 1994, J. Phys. A **27**, 4439.
Reffo, G., F. Fabbri, and H. Gruppelaar, 1976, Lett. Nuovo Cimento Soc. Ital. Fis. **17**, 1.
Reid, S. A., and H. Reisler, 1996, J. Chem. Phys. **100**, 474.
Richard, P., C. F. Moore, D. Robson, and J. D. Fox, 1964, Phys. Rev. Lett. **13**, 343.
Richter, A., 1974, in *Nuclear Spectroscopy and Reactions*, edited by J. Cerny and B. Part (Academic, New York), Vol. 343.
Richter, A., 1999, in *The IMA Volumes in Mathematics and its Applications*, edited by D. A. Hejhal, J. Friedmann, M. C. Gutzwiller, and A. M. Odlyzko (Springer, New York), Vol. 109, p. 479.
Robson, D., 1965, Phys. Rev. **137**, B535.
Rosenzweig, N., and C. E. Porter, 1960, Phys. Rev. **120**, 1698.
Satchler, R. G., 1963, Phys. Lett. **7**, 55.
Savin, D. V., Y. V. Fyodorov, and H. J. Sommers, 2001, Phys. Rev. E **63**, 035202(R).
Savin, D. V., Y. V. Fyodorov, and H. J. Sommers, 2006, Acta Phys. Pol. A **109**, 53.
Schäfer, F., 2009, private communication.
Schäfer, L., and F. Wegner, 1980, Z. Phys. B: Condens. Matter **38**, 113.
Schäfer, R., T. Gorin, T. H. Seligmann, and H.-J. Stöckmann, 2003, J. Phys. A: Math. Gen. **36**, 3289.
Schomerus, H., K. M. Frahm, M. Patra, and C. W. J. Beenakker, 2000, Physica A **278**, 469.
Sharapov, E. I., J. D. Bowman, B. E. Crawford, P. P. J. Delheij, C. M. Frankle, M. Inuma, J. N. Knudson, L. Y. Lowie, J. E. Lynch, A. Maisaike, Y. Matsuda, G. E. Mitchell, S. I. Penttillä, H. Postma, N. R. Roberson, S. J. Seestrom, S. L. Stephenson, Y.-F. Yen, and V. W. Yuan, 2000, Phys. Rev. C **61**,

025501.
Simonius, M., 1974, Phys. Lett. **52B**, 279.
Simpson, J. J., S. J. Wilson, W. R. Dixon, R. S. Storey, and J. A. Kuehner, 1978, Phys. Rev. Lett. **40**, 154.
Smilansky, U., 1991, in *Chaos and Quantum Physics*, edited by M. J. Giannoni *et al.*, Proceedings of the Les Houches Summer School, Session LII (North-Holland, Amsterdam), p. 372.
Smith, F. T., 1960a, Phys. Rev. **118**, 349.
Smith, F. T., 1960b, Phys. Rev. **119**, 2098.
Snover, K. A., 1984, J. Phys. (Paris) **45**, Suppl. 3, C4-337.
So, P., S. Anlage, E. Ott, and R. N. Oerter, 1995, Phys. Rev. Lett. **74**, 2662.
Sokolov, V. V., and V. G. Zelevinsky, 1988, Phys. Lett. B **202**, 10.
Sokolov, V. V., and V. G. Zelevinsky, 1989, Nucl. Phys. A **504**, 562.
Sokolov, V. V., and V. G. Zelevinsky, 1992, Ann. Phys. (N.Y.) **216**, 323.
Sokolov, V. V., and V. G. Zelevinsky, 1997, Phys. Rev. C **56**, 311.
Sommers, H. J., Y. V. Fyodorov, and M. Titov, 1999, J. Phys. A **32**, L77.
Sorathia, S., F. M. Izrailev, G. L. Celardo, V. G. Zelevinsky, and G. P. Berman, 2009, EPL **88**, 27003.
Spijkervet, A. L., 1978, Ph.D. thesis (Rijksuniversiteit Groningen, The Netherlands).
Sridhar, S., 1991, Phys. Rev. Lett. **67**, 785.
Stania, G., and H. Walther, 2005, Phys. Rev. Lett. **95**, 194101.
Steiner, A. W., M. Prakash, J. M. Lattimer, and P. J. Ellis, 2005, Phys. Rep. **411**, 325.
Stöckmann, H.-J., 2000, *Quantum Chaos: An Introduction* (Cambridge University Press, Cambridge).
Stöckmann, H.-J., and J. Stein, 1990, Phys. Rev. Lett. **64**, 2215.
Sushkov, O. P., and V. V. Flambaum, 1980, JETP Lett. **32**, 377.
Sushkov, O. P., and V. V. Flambaum, 1982, Sov. Phys. Usp. **25**, 1.
Tepel, J. W., H. M. Hofmann, and H. A. Weidenmüller, 1974, Phys. Lett. **49B**, 1.
Tilley, D. R., H. R. Weller, C. M. Cheves, and R. M. Chasteler, 1995, Nucl. Phys. A **595**, 1.
Tomsovic, S., M. B. Johnson, A. Hayes, and J. D. Bowman, 2000, Phys. Rev. C **62**, 054607.
Ullah, N., 1969, J. Math. Phys. **10**, 2099.
Vager, Z., 1971, Phys. Lett. **36B**, 269.
Verbaarschot, J. J. M., 1986, Ann. Phys. (N.Y.) **168**, 368.
Verbaarschot, J. J. M., H. A. Weidenmüller, and M. R. Zirnbauer, 1984a, Phys. Rev. Lett. **52**, 1597.
Verbaarschot, J. J. M., H. A. Weidenmüller, and M. R. Zirnbauer, 1984b, Phys. Lett. **149B**, 263.
Verbaarschot, J. J. M., H. A. Weidenmüller, and M. R. Zirnbauer, 1985, Phys. Rep. **129**, 367.
Verbaarschot, J. J. M., and M. R. Zirnbauer, 1985, J. Phys. A **17**, 1093.
Volya, A., and V. Zelevinsky, 2006, Phys. Rev. C **74**, 064314.
von Witsch, W., A. Richter, and P. von Brentano, 1968, Phys. Rev. **169**, 923.
Weidenmüller, H. A., 1964, Phys. Lett. **10**, 331.
Weidenmüller, H. A., 1967, Phys. Lett. **24B**, 441.
Weidenmüller, H. A., 1980, in *Progress in Nuclear and Particle Physics*, edited by D. H. Wilkinson (North-Holland, Amsterdam), Vol. 3, p. 49.
Weidenmüller, H. A., 1984, Ann. Phys. **158**, 120.
Weidenmüller, H. A., 1990, Nucl. Phys. A **518**, 1.
Weidenmüller, H. A., 2002, in *Scattering*, edited by R. Pike and P. Sabatier (Academic, San Diego), p. 1393.
Weidenmüller, H. A., and G. E. Mitchell, 2009, Rev. Mod. Phys. **81**, 539.
Wess, J., and B. Zumino, 1974a, Nucl. Phys. B **70**, 39.
Wess, J., and B. Zumino, 1974b, Phys. Lett. **49B**, 52.
Wigner, E. P., 1955a, Ann. Math. **62**, 548.
Wigner, E. P., 1955b, Phys. Rev. **98**, 145.
Wigner, E. P., 1957, Ann. Math. **65**, 203.
Wigner, E. P., and L. Eisenbud, 1947, Phys. Rev. **72**, 29.
Wójcik, E., M. Kicińska-Habior, O. Kijewska, M. Kowalczyk, M. Kisielinski, and J. Choiński, 2007, Acta Phys. Pol. B **38**, 1469.
Wolfenstein, L., 1951, Phys. Rev. **82**, 690.
Xu, J., A.-T. Le, T. Morishita, and C. D. Lin, 2008, Phys. Rev. A **78**, 012701.
Zelevinsky, V., B. A. Brown, N. Frazier, and M. Horoi, 1996, Phys. Rep. **276**, 85.
Zhu, S.-L., C. M. Maekawa, B. R. Holstein, M. J. Ramsey-Musolf, and U. van Kolck, 2005, Nucl. Phys. A **748**, 435.